

**INTERPLAY OF POLYMER AND OLIGONUCLEOTIDE
PROPERTIES IN THE NATURE OF ANTISENSE EFFECTS**

By

SUMATI SUNDARAM

A Dissertation submitted to the

Graduate School-New Brunswick

Rutgers, The State University of New Jersey

in partial fulfillment of the requirements

for the degree of

Doctor of Philosophy

Graduate Program in Chemical and Biochemical Engineering

written under the direction of

DR. CHARLES M. ROTH

and approved by

New Brunswick, New Jersey

January 2008

Abstract of the Dissertation

Interplay of polymer and oligonucleotide properties in the nature of antisense effects

By SUMATI SUNDARAM

Dissertation Director: Dr. CHARLES M. ROTH

Antisense oligonucleotides can be utilized to silence the expression of a target gene via sequence-specific complementary base pairing. Antisense technology is applied as a basic research tool and is being developed therapeutically for a wide range of indications including cancer, inflammatory diseases and viral diseases. Its widespread application is impeded by the poor cellular delivery of oligonucleotides (ONs). Rational design of carriers for enhanced ON delivery demands a better understanding of the role of the vector on the extent and time course of antisense effects. This work highlights the interplay of polymer and ON properties in the nature of polymer mediated antisense responses. First, we demonstrate that ON structure exerts a significant influence on the strength of ON binding to, and dissociation from, the cationic polymer, poly-L-lysine. The finding implicates secondary structure as a relevant design parameter for antisense ONs and stresses the need for a comprehensive evaluation of ON-polymer structure-activity effects. Next, using well-characterized cationic polymer polyethyleneimine (PEI), we focus on understanding the effects of polymer molecular weight (MW) and ON backbone chemistry on antisense activity. We measure physico-chemical properties of complexes between PEI and phosphodiester and phosphorothioate backbone ONs, and

evaluate their ability to deliver ONs to cells, leading to an antisense response. Our key finding is that the antisense activity is not determined solely by PEI MW or by ON chemistry, but rather by the interplay of both factors. Of particular importance is the strength of interactions between the carrier and the ON, which determines the rate at which the ONs are delivered intracellularly. Finally, we utilize the chemistry of the ONs as a means to influence the strength of interactions between PEI and ONs, and hence control the final antisense response. We show that it is possible to improve dramatically the efficiency of lower PEI MWs as ON carriers by manipulating the degree of phosphorothioate substitution in the ON chemistry. By correlating the PEI MW & ON chemistry with the observed antisense effects, we draw insightful structure-property relationships that will aid the rational design of ON carriers.

Table of Contents

INTERPLAY OF POLYMER AND OLIGONUCLEOTIDE PROPERTIES IN THE NATURE OF ANTISENSE EFFECTS	i
Abstract of the Dissertation	ii
Table of Contents	iv
Table of Figures	vii
List of Tables	ix
Chapter 1: Introduction	1
1.1 Background: Antisense - Principles & Current status.....	1
1.2 Factors involved in effective antisense inhibition	2
1.3 Cellular delivery of antisense oligonucleotides - Need for a carrier	3
1.4 Properties and components of synthetic carriers.....	4
1.5 Design properties of vectors – lessons from viral vectors	5
1.6 Intracellular processing of synthetic vectors.....	7
1.7 Rational design of synthetic vectors.....	9
1.7.1 Structure-activity relationships	10
1.7.2 Mathematical modeling	11
1.7.3 Can we create virus-like multifunctional vectors?	13
1.8 Perspectives - Importance of being an oligo.....	14
Chapter 2: Oligonucleotide structure influences the interactions between cationic polymers and oligonucleotides.....	18
2.1 Abstract.....	18
2.2 Introduction.....	19
2.3 Materials and Methods.....	21
2.3.1 Materials	21
2.3.2 Preparation of oligoplexes	22
2.3.3 Detection of free ON using OliGreen®	22
2.3.4 ON release studies	22
2.3.5 Modeling Polymer-ON complexation	23
2.4 Results	26
2.5 Discussion	31

Chapter 3: Interplay of polyethyleneimine molecular weight and oligonucleotide backbone chemistry in the dynamics of antisense activity.....	38
3.1 Abstract.....	38
3.2 Introduction.....	39
3.3 Materials & Methods.....	42
3.3.1 Materials	42
3.3.2 PEI/ON complex formation	42
3.3.3 Detection of free ON using OliGreen	43
3.3.4 Determination of particle size using dynamic light scattering	43
3.3.5 PEI/ON dissociation studies	43
3.3.6 Cell culture.....	44
3.3.7 Antisense experiments	45
3.3.8 Flow cytometry	45
3.3.9 Mathematical model	46
3.4 Results	49
3.5 Discussion	56
Appendix.....	64
Chapter 4: Design of mixed backbone oligonucleotides for effective polymer mediated cellular delivery of antisense oligonucleotides.....	67
4.1 Abstract.....	67
4.2 Introduction.....	69
4.3 Material and methods.....	72
4.3.1 Materials	72
4.3.2 PEI/ON complex formation	72
4.3.3 Detection of free ON using OliGreen	73
4.3.4 Cell culture.....	74
4.3.5 Antisense experiments	74
4.3.6 Flow cytometry	75
4.3.7 PEI/ON dissociation studies	75
4.3.8 Confocal microscopy	76
4.4 Results	78
4.5 Discussion	85
Chapter 5: Summary & Future Directions	90
5.1 Summary.....	90
5.2 Future Directions	95
5.2.1 Characterization of the molecular interactions between polymers and ONs.....	95
5.2.2 Role of excess polymer in PEI-ON complexes	96

5.2.3 Improvement in the mechanistic picture of intracellular trafficking of polymer-ON particles	97
5.2.4 Metric to describe the variations in responses within cell populations	97
5.2.5 Rational approaches to improve polymer-mediated delivery	98
5.2.6 Generalization of results & extension to other systems.....	98
5.3 Conclusions.....	99
FIGURES.....	100
References.....	129
CURRICULUM VITAE.....	138

Table of Figures

Figure 1.1 Principle of antisense.....	100
Figure 1.2 Factors involved in effective AS inhibition.....	101
Figure 1.3 Various AS mechanisms	102
Figure 1.4 Various backbone chemistries of AS oligonucleotides	103
Figure 1.5 Common polymer chemistries used for DNA delivery.....	104
Figure 1.6 Intracellular processing of AS ON delivery	105
Figure 1.7 Proposed flip-flop mechanism for release of ONs from lipids.....	106
Figure 2.1 Structure of hairpin ONs	107
Figure 2.2 Effect of ON structure on complex formation	108
Figure 2.3 Effect of pLL molecular weight on complex formation	109
Figure 2.4 Model predictions of pLL-ON complexation behavior	110
Figure 2.5 ON release kinetics from pLL-ON complexes	111
Figure 2.6 Heparin dose response curves of the release of unstructured and hairpin structured ONs from pLL-ON complexes	112
Figure 3.1 Effect of PEI molecular weight on complex formation of PEI with PO and PS ONs.....	113
Figure 3.2 Mean hydrodynamic diameter (nm) of PEI-ON complexes	114
Figure 3.3 Heparin dose response of the release of PO and PS ONs from PEI/ON complexes	115
Figure 3.4 Dynamics of GFP down-regulation.....	116
Figure 3.5 Controls for antisense experiment	117
Figure 3.6 Dynamics of intracellular ON levels	118
Figure 3.7 Model predictions	119
Figure 3.8 Relationship between antisense inhibition and intracellular ON levels	120
Figure 4.1 Effect of PEI molecular weight on complex formation of PEI with ONs of various chemistries (mod2, mod4, mod5, modALT)	121
Figure 4.2 Dynamics of GFP down-regulation.....	122
Figure 4.3 Antisense response plot indicating correlations between PEI MWs and ON chemistries	124

Figure 4.4 Heparin induced ON release from PEI/ON complexes.....	125
Figure 4.5 Effects of chloroquine and ammonium chloride on antisense down- regulation and intracellular ON levels.....	126
Figure 4.6 Confocal microscopy of d1EGFP cells treated with PEI/ON complexes	127
Figure 5.1 Heterogeneity in GFP down-regulation in cell populations.....	128

List of Tables

Table 1.1 Components of a non-viral vector	17
Table 2.1 Free energy of unfolding of hairpin-structured and unstructured ONs...	21
Table 2.2 Ratio of molecular charges of pLL to ON.....	28
Table 3.1 Maximum intracellular ON release rates from PEI/ON complexes, computed using the fit model parameters	55
Table 4.1 Backbone chemistry of sequences utilized in the study	73

Chapter 1: Introduction

1.1 Background: Antisense - Principles & Current status

The ability to alter cellular behavior through genetic modifications has great potential as a therapeutic strategy, as well as a tool for elucidating gene function. With the advances in molecular biology and genetics, several well-developed methodologies to modify gene expression are available today, each with its own mechanism of where and how the flow of genetic information is perturbed(1). Antisense technology is one such anti-mRNA based method. The underlying concept is simple. It involves the use of short strands of nucleotides that have sequence complementary to an mRNA target of interest. These oligonucleotides, also called antisense oligonucleotides, hybridize to the target mRNA by Watson-Crick base pairing and inhibit the expression of the mRNA into protein. Theoretically, only the sequence of the target mRNA is required to design an antisense oligonucleotide that inhibits the translation of a disease-encoded protein (Figure 1.1).

The original idea that gene expression can be altered using exogenous or synthetic nucleic acids was first demonstrated in the late 1970s(2). Discovery of the existence of naturally occurring antisense RNAs and their role in regulating gene expression, in the mid 1980s, lent further credibility to the idea. Since then, promising results from several proof-of-principle studies in vitro and in animal models have fueled the rapid development of this field. This has lead to high expectations for the practical implementation of this technology in the clinic. To date, more than 600 clinical trials have been initiated, comprising 3500 patients worldwide. Several products are in Phase II

and Phase III stages (3, 4), and there already exists one commercial antisense product, Vitravene, a phosphorothioate oligodeoxynucleotide (PS ON) for the treatment of an inflammatory viral infection of the eye caused by cytomegalovirus(5). Besides having therapeutic potential, antisense is also being routinely used as a tool in cellular and molecular bioengineering(6). Several factors -- such as simplicity of principle, possibility of rational design, the ability to obtain large amounts of synthetic oligonucleotides at low costs, the promise of high specificity and low toxicity -- have contributed to the anticipation that antisense technology will have a lasting impact on medicine and biotechnology.

1.2 Factors involved in effective antisense inhibition

Practical implementation of antisense technology involves several factors that require particular attention, such as (1) target selection, (2) oligonucleotide synthesis, (3) target validation, (4) cellular delivery, and (5) ON stability, activity and toxicity (Figure 1.2). Although theoretically straightforward, choosing an effective ON sequence complementary to 15-25 bases of a large mRNA molecule with a complex secondary or tertiary structure is quite a challenge. Selection has largely been by trial and error, and the lack of efficacy is largely due to targeting inaccessible sites on the RNA molecule. Most recently, researchers have provided innovative approaches such as computer aided target selection taking into account the RNA structure or combinatorial experimental approaches (7), such as those involving huge scanning arrays that test DNA-RNA binding strength. Significant insights have also been obtained from studying the thermodynamics and kinetics of the DNA-RNA binding(8). The chosen sequence would then be targeted to a certain cell type(s), so it can bind to the target mRNA and exert its

biological activity through an antisense mechanism. There are several mechanisms of action for antisense ODNs, such as the activation of endogenous ribonuclease H, which cleaves mRNA at the hetero duplex site, or physical blockage of transcriptional machinery (Figure 1.3). Literature reports several such antisense and non-antisense mechanisms through which ON sequences are found to inhibit gene expression(9), depending on properties such as the specific ON sequence, length of the ON, and its chemistry.

ON backbone chemistry also plays a role in antisense effectiveness. Natural oligonucleotides have a phosphodiester backbone, which is degraded rapidly in cellular milieu. Several modifications have been made to the ON backbone in order to improve its nuclease resistance(10). Some of the more widely used ones include phosphorothioate, methylphosphonate and mixed backbones (Figure 1.4). Recent advances in DNA synthesis and sequencing made available large amounts of high quality, synthetic oligonucleotides of various chemistries at low costs.

1.3 Cellular delivery of antisense oligonucleotides - Need for a carrier

Despite a growing body of knowledge regarding the chemistry, biology, and pharmacology of oligonucleotides, the widespread application of antisense technology remains a daunting challenge(11). Simplicity of principle belies its practical implementation. Efficient delivery of nucleic acids to specific sites of action remains a major obstacle. In culture, when naked ODNs are delivered to cells, almost no ODNs enter the cell due to minimal interactions between the highly anionic ODNs and the negatively charged plasma membrane. Attempts have been made to chemically modify

ODNs in order to improve their cellular adsorption rates. However, the ODNs must still evade biochemical degradation and several intracellular barriers before they can have the desired effect in the cell. Accomplishing this task calls for the use of a carrier molecule, and the resulting package---ON plus carrier(s)---is termed a vector. In general, an ideal vector should be able to enhance its entry into the specific target cell, assist in overcoming several intracellular barriers, confer resistance to nuclease attack, and display minimum toxicity. Surprisingly, in vivo, ODNs are delivered relatively efficiently in the absence of any carrier molecules, and a large number of clinical trials performed to date have been with naked ODNs(12). It is proposed that certain endogenous molecules assist the in vivo transport of the ODNs. However, in vitro, the use of a delivery agent reduces the concentration of ODNs required by more than 200 fold.

1.4 Properties and components of synthetic carriers

The core components of synthetic vectors are usually carrier molecules, which can form complexes with ODNs or assemble into vesicles that can encapsulate ODNs. There are numerous elegant chemistries and ingenious designs developed for this purpose (Figure 1.5). Currently, most synthetic vectors are based on polymers or lipids, which on interaction with DNA form polymer/DNA complexes called polyplexes and lipid/DNA complexes called lipoplexes(13). A range of synthetic and natural polymers has been incorporated into vectors for DNA delivery. Naturally occurring proteins, such as histones and albumin, and polysaccharides, such as chitosan, have also been incorporated into vectors for DNA delivery(14, 15). Liposomes represent a large class of DNA delivery agents. Cationic lipids possess a hydrophobic moiety; a positively charged head group; and a linker functional group, such as ester, amide, or carbamate, to bind these

molecules together covalently. Various helper lipids, such as dioleoylphosphatidylethanolamine (DOPE), and neutral lipids, such as cholesterol and its derivatives, are used in many formulations for improving efficiencies (16). DNA has been successfully delivered to cells with cationic, neutral and anionic lipids, and mixtures thereof. In addition to polymers and lipids, delivery systems that incorporate proteins, peptides, and other biological molecules to penetrate cellular membranes are being explored. Peptides are also widely used as targeting moieties or as auxiliary molecules attached to the polymer/DNA complex for a specific purpose. Many peptides and other biological ligands have been used as cell-targeting carrier molecules, including glycoproteins, mannose, insulin, antibodies, lectins, and folic acid. The pH sensitivity of fusogenic peptides is also being exploited to penetrate cellular membranes and deliver a cargo of DNA (17). Several features such as flexibility in design, ability to be chemically or biochemically functionalized and tunable toxicity properties render synthetic vectors very attractive with which to work. However, they remain very inefficient.

1.5 Design properties of vectors – lessons from viral vectors

Despite intensive research over the past decade, non-viral vectors for gene delivery still do not compare with viral vectors in terms of efficiency. Thus, the development of non-viral vectors borrows from viruses many of their design features and properties. Viruses used for gene transfer are self-assembled biological particles on the order of 100 nm in diameter and comprised of lipids, proteins, and nucleic acids that include the gene of interest (18). For retroviruses, lipids form a bilayer and separate the viral contents from the environment. In contrast, this function is accomplished in adenovirus by a set of tightly assembled coat proteins. Several types of proteins exist in

viruses including capsid proteins, which condense the nucleic acids, envelope proteins, which bind to receptors on cellular membranes, and enzymes that aid in unpackaging and integration of the genetic material in the host cell. The genetic material may be either DNA or RNA. In the latter case, a reverse transcriptase is part of the viral vector to generate DNA inside the target cell.

Due to their multiple components and evolutionarily optimized properties, viruses are able to achieve the multi-pronged task of infection. Despite the negative charge existing on both viruses and cell membranes, viruses are able to adsorb to cells, even without envelope protein binding to cellular receptors (19). Envelope-receptor interactions appear to prevent detachment and to anchor the virus to the cell membrane. Fusion with the cell membrane then occurs, for some viruses mediated by environmentally sensitive, amphipathic peptides. The nucleic acid is released into the cell; reverse transcribed if necessary, then enters into the nucleus where it is integrated into the genome. Retroviruses do not enter the nucleus until its host cell enters mitosis, thus restricting the application of retroviruses to dividing cells. Other viruses, such as adenovirus, are able to transduce non-dividing cells through the presence of nuclear localization sequences (NLS) on capsid proteins, which mediate extrusion of the nucleic acids via the nuclear pore complex (NPC) (20).

Thus, viruses provide a set of design features that are mimicked in the development of non-viral vectors. Their capabilities include condensation of DNA into nanoparticles, protection from nuclease degradation, adsorption to cells, delivery into the cytoplasm and (for non-dividing cells) the nucleus, and unpackaging to release the nucleic acids. By nature, viruses are inherently biocompatible as they are comprised of

wholly biological entities. However, biocompatibility is a consideration for non-viral vectors. The problems encountered in viral gene delivery, such as immunogenicity and the possibility of oncogenesis, also serve as lessons for the design and development of non-viral vectors.

1.6 Intracellular processing of synthetic vectors

DNA is generally maintained in the nuclei of cells, which do not have mechanisms for importing DNA from their surroundings. Efforts to do so artificially must overcome a set of cellular barriers present as part of the cell's internal organization and protection from its environment. Thus, a detailed understanding of the interactions of non-viral vectors with the components of cellular uptake and intracellular processing pathways is necessary for improving the design of vectors (see Figure 1.6).

Detailed investigations of the intracellular processing of vectors have uncovered the complexity and multitude of events that are associated with nonviral DNA delivery.(21-23) Dissection of the processing of the carrier mediated ON delivery reveals the following steps: (a) physical and biochemical degradation in the extracellular space, (b) the extracellular matrix and cell surface interactions, (c) internalization, (d) trafficking from endosomes to lysosomes and subsequent degradation, (e) escape from endosomes into the cytoplasm, (f) dissociation of DNA from its carrier, (g) transfer into the nucleus, and (h) hybridization. The intracellular pathway of non-vector mediated delivery of ODNs is shown in figure 1.6. Complexes that are generally internalized by endocytosis are exposed to continuous acidification in the endosomal compartments ultimately leading to degradation in the lysosomes. For effective delivery, the complex and/or ON

must exit the pathway before it is degraded in the lysosomes. Exit from the endo-lysolytic pathway however does not ensure high transfection efficiency. For the delivered ON to be effective, the carrier/ON complex must dissociate, causing release of the ON, preferably close to the site of mRNA binding. ODNs, in the cellular milieu are highly susceptible to nuclease attack. DNA that remains associated with the vector even after exit from the endocytic pathway will be less susceptible to nuclease attack as association with the carrier molecule greatly reduces the possibility of DNA degradation due to nucleases. For example, when complexed with SuperFect™, the half-life of a linear ON in HeLa cell lysate increases from less than 30 min to over 16 h. The relative importance of DNA stability in the cytoplasm will depend on the vector dissociation mechanism.

Numerous studies have focused on elucidating the mechanism of escape of vectors from the endosomal pathway. Early observations of the interaction of cationic and anionic bilayers supported the flip-flop model in which lipid mixing between endosomal and cationic lipid membranes eventually leads to membrane disruption and release of ON into the cytoplasm (Figure 1.7). Unlike liposomal vectors, polymer/DNA complexes have been detected in the cytoplasm as well as in the nucleus, suggesting that not free DNA but carrier-associated DNA is probably released from the endocytic pathway(24). The higher transfection efficiencies generally observed with polyamines, such as PEI, have been attributed to its buffering capacity within the physiological pH range. This can be explained by an effect called the proton sponge hypothesis in which protonation of ionizable amine groups leads to chloride ion accumulation, with consequent osmotic endosome swelling causing rupture and enhanced escape of the polyplex (25). Vector

properties influence the relative importance of various processing steps in the pathway and consequently determine the cellular itinerary of the ODNs.

1.7 Rational design of synthetic vectors

Early approaches toward synthetic vector design involved synthesis of carrier molecules with elegant chemistries, which provided for efficient condensation and protection of DNA. More recently, efforts have been directed towards incorporation of the existing mechanistic understanding of vector-cell interactions into vector design. With the identification of several barriers to effective DNA delivery, the properties of carriers can be altered by strategic structural modifications to overcome one or more of these individual barriers. Despite the progress made so far, the field of synthetic vector development is still faced with two very important challenges: first, the best synthetic vectors available today still remain many orders of magnitude less efficient than the corresponding viral vectors; second, cell type differences are significant. In light of these challenges, it is likely that vectors will have to be optimized for each application.

Detailed investigations of the intracellular processing of vectors have revealed the complexity and multitude of events that are associated with non-viral DNA delivery. Each of the steps detailed in the earlier sections has been shown to be a limiting barrier to transfection under some circumstances. Furthermore, vector design variables may affect different steps to varying extents. A vector that is “rationally designed” to overcome one barrier may alter the cellular processing of the carrier, dramatically increasing the importance of other barriers. Therefore, systematic variation of one physical or chemical property is not likely to lead directly to a completely optimized vector, although it is

evident that the efficiency of the DNA delivery process can be modulated by the properties of the delivery system. A more integrative approach that accounts for the interdependence of individual intracellular barriers and the effects of vector properties on the barriers seems essential. This will accelerate the process of optimization of various vector design variables for a range of cell types.

1.7.1 Structure-activity relationships

In the quest for elucidating rational design principles, several researchers have attempted to draw structure-activity relationships for various vector systems. These studies generally involve determination of several biophysical properties of the carrier/DNA complexes such as size, shape, zeta-potential, and DNA condensation as well as biological properties such as transfection efficiency and cytotoxicity. A correlation between these properties is proposed to serve as a basis for the future design of vectors.

Studies with series of structurally related polymers generally do not reveal significant correlations between the physical parameters and the biological activity (27), however strong correlations have been observed between the structure of the polymers and the physicochemical properties of their complexes with DNA. Small sizes of the order of 100 nm are often required for entry through the endocytic pathway. However, larger aggregates of even up to 500 nm sediment onto cells, especially *in vitro*, thereby providing high transfection efficiencies. In the case of cationic liposome/micelle-based systems, lipoplex size has been found to be a major determinant of lipofection efficiency *in vitro*, with larger lipoplex particles showing higher efficiency than smaller ones (29).

Alternatively, researchers have varied functional attributes of the carrier to affect various steps in the intracellular processing of vectors and have obtained interesting relationships. For example, balancing the relative contribution of cationic groups and endosomal escape moieties (pH sensitive groups) resulted in lower cytotoxicity, and modifying the protonatable nitrogens in PEI highlighted the importance of amines in endosomal escape (26). Even a polymer such as PLL, which is notorious for its high cytotoxicity, has been found to exhibit much higher transfection efficiency when side chains of lower pKa, such as histidine, are attached to it (30). In the case of liposomes, studies have found transfection efficiency to be dependent on the membrane fluidity of the lipoplex membrane (16, 31). Combinatorial approaches to screen hundreds of structurally related polymers or lipids may prove useful in the identification of chemical structures that have enhanced DNA delivery properties. Such chemical structure-activity relationships provide additional insight into functionality that can then be engineered into vectors for higher efficiencies.

The utility of such structure-activity relationships will be judged by the success of their application to the rational design of future vectors. The fact that no useful correlations have been observed between the physical parameters and the biological activity of the complexes seems to suggest that such an approach oversimplifies the complexity of DNA delivery. One issue is the heterogeneity of the vectors, with the resulting concern that only a small fraction of the population may display the desired effect (32). Nonetheless, attempting to optimize the biological functionality of the complex via “one-dimensional” structure-activity relationships may not be sufficient.

1.7.2 Mathematical modeling

How is one to interpret the accumulated set of structure-activity relationships derived for disparate conditions? Mathematical modeling of the DNA delivery pathway can provide a framework for quantifying the interplay among various design variables, consequently reducing the amount of experimentation required for optimizing vectors for various cell types. In addition, combined with quantitative experimentation, it can provide insight into the molecular mechanisms and rate limiting steps for effective delivery.

Relatively few mathematical models exist for the analysis of non-viral DNA delivery, and to date there are essentially none characterizing the antisense ON delivery pathway. Mathematical representations of plasmid delivery have been based on a compartmental model, with mass action kinetics representing the various steps involved in the DNA delivery process. Data from previous experimental literature is generally used to obtain parameter values. Model outputs can be utilized to identify rate-limiting barriers and to make testable predictions. The values of some parameters, such as ligand-receptor binding and trafficking rates (for targeted delivery), may be known quite accurately, whereas others, such as rates of intracellular trafficking and degradation, are likely to be known to a much lesser degree of accuracy. Parameter sensitivity analysis provides useful insights into the importance of model parameters in determining the gene delivery efficiency. Vectors with hypothetical (rationally designed) attributes could then be tested for their effectiveness, by measuring several key parameters and relating the resulting model predictions to experimental observables.

Complete characterization of a mathematical model would require quantitative experimental data to be obtained under a consistent set of conditions (e.g., cell type, cell density, plasmid type, duration of exposure to vector). Commonly observed differences in

cell type and heterogeneity in experimental conditions make predictions more difficult to assess. There is a clear need to develop assays for the accurate, quantitative determination of absolute numbers as well as the state of both the DNA and carrier molecules in various subcellular compartments. Recent advances in fluorescent technology have led to the development of several analytical methods for the characterization and quantitation of various vector-cell interactions (34). By a combination of subcellular fractionation and flow cytometry, it is possible to obtain quantitative estimates of fluorescently labeled plasmids in various cellular compartments (35). However, care must be taken to ensure that measured levels represent intact DNA rather than degradation products. Techniques such as real-time PCR and Southern analysis, as well as in vitro transcription assays that do not require DNA labeling, might prove to be useful complements (36). Such quantitative evaluations are more challenging for systems involving ODNs, as many of the techniques applied to plasmids are not applicable to ODNs (37).

1.7.3 Can we create virus-like multifunctional vectors?

Integrating design solutions to the often conflicting demands of DNA delivery necessitates the development of multifunctional vectors. As viruses are naturally occurring biological systems that have evolved to achieve high efficiency of transduction (see Section 2.2), attempts to create virus-like particles for DNA delivery applications have been pursued for over a decade (38). “Artificial viruses” have been proposed to be mononuclear, stoichiometric, of viral size (<100nm) and capable of transfection. The aim of producing artificial viruses is to incorporate in a modular fashion several viral or virus-mimetic components to provide efficient cellular delivery characteristics, including DNA condensation, cell attachment, and release from the endosome.

Viral peptides, such as influenza virus hemagglutinin (HA), or synthetic peptides, such as GALA, have been utilized to impart endosomal disruptive functions to a polymer/DNA complex (38, 40). A major challenge in the incorporation of peptides into delivery vectors has been the display of the peptides in an ordered manner to optimally mimic viral functioning. Approaches to self-assembly of complete viral-mimetic particles have been based upon mixing of lipids bearing various functional head groups and DNA, leading to spontaneous compaction of DNA into lipid coated particles leaving surface molecular signals sticking out (41, 42). Studies have shown that supercoiled plasmid DNA is able to transform lipopolyamine micelles into a supramolecular organization characterized by ordered lamellar domains (43). Newer approaches involving size-controlled glycocluster nanoparticles (non amine/non cationic/non polymeric) are being explored .

Identification and incorporation of viral functionalities (e.g., endosomal escape or nuclear targeting) into synthetic vectors has already resulted in some increase in efficiency. Yet, other properties of viruses have been explored and mimicked to a much lesser extent. For example, the ability of viruses to unpackage their nucleic acid cargo aids in its ability to traverse the nuclear membrane and be expressed within the nucleus. A major challenge remains in the incorporation of multiple types of biomolecules into a vector, each still maintaining its critical functionality for the artificial virus.

1.8 Perspectives - Importance of being an oligo

Despite the increase in rational approaches to the design of DNA carriers, there is a pressing need for focusing attention specifically on carriers for ON delivery. Vectors

developed for delivering plasmid DNA for gene therapy applications are often used to deliver ODNs with little or no optimization of system parameters. Since fewer studies focus specifically on the analysis of cellular processing of ON vectors, much of the existing mechanistic understanding obtained in gene delivery studies are incorporated for the development of ON vectors. However, direct transfer of such knowledge may not always be appropriate, as the properties of the ON (for example; size, chemistry, structure) and the biology associated with the antisense mechanism widen the gamut of possible intracellular interactions, causing the system to be far more complex.

Relatively little is known concerning the effect of ON properties on the interactions between carriers and ODNs. Clearly, the structure and sequence composition are key features of the ON and have significant implications on its biological interactions, such as its ability to hybridize with a target mRNA(8) and its resistance to nuclease digestion. For example, ODNs designed to form stable structures, such as hairpins or loops, exhibit better resistance to nuclease digestion as compared to unstructured ODNs. Furthermore, certain applications call for the use of structured ODNs. For example, molecular beacons, which possess a hairpin structure, are fluorescent hybridization probes that are used for quantitation of complementary targets in samples and have been used for visualization of RNA in cells (44, 45). PS ODNs display some very interesting characteristics specific to its chemistry. It has been shown that PS ODNs localize to the nucleus and are capable of inducing the formation of nuclear bodies.(46) Further, they were found to shuttle continuously between the nucleus and the cytoplasm. Despite its relevance to these applications, relatively little attention has been paid to understanding

the molecular biophysics of ON interactions with carriers such as polymers, or on relating their biophysical characteristics to the biological activity of the vectors(47).

Detailed analysis of the cellular processing of vectors has identified several barriers that need to be overcome, and hence provided cues for improvement in design. Modifications in vector design enable improvement in transfection efficiencies relative to previous designs. However, ultimately, effective antisense requires availability of functional ODNs at the location of ON-mRNA binding. Although much is known about the mechanisms of ON delivery, certain quantities still remain unknown. We still do not exactly know what the destination of the ON cargo is, or how much of the delivered ON actually enables antisense inhibition. To program intracellular ON release close to the site of action, it is imperative to know where the actual ON-mRNA binding occurs. The rational design of vectors still has much to learn from the mechanisms of antisense inhibition. The possibility of rationally engineering delivery agents for a specific application at hand is precisely what renders synthetic vectors particularly appealing.

By examining vector mediated ON delivery in direct context of the antisense mechanism, we attempt to obtain an understanding of those programmable parameters that will be desirable in the design of vectors for ON delivery. Efforts will be directed to the development of tools for the quantitative analysis of the vector mediated delivery of ODNs. This will enable progress toward the rational design of synthetic vectors by the strategic exploitation of intracellular mechanisms.

Table 1.1 Components of a non-viral vector

Component	Rationale	Examples
Carrier molecule	DNA compaction, charge reduction, protection from nucleases	PLL (48), PEI (24, 49), PAMAM (50), chitosan (15), lipids (51-53)
Hydrophilic moiety	Steric stabilization, reduction of non-specific interactions	PEG(54), HPMA polymers (55, 56)
Targeting ligand	Enhanced targeted receptor mediated cellular uptake	Asialoglycoprotein, folate, EGF
Endosome disruptive agent	Escape from endosomes - unpackaging	pH sensitive peptides (30, 57), protonable amine structures (25)
Nuclear localization signal (NLS)	Nuclear targeting	SV40 T-antigen (58, 59), hnRNP A1 protein M9 , (HIV-1) Rev and Tat protein (60)

Chapter 2: Oligonucleotide structure influences the interactions between cationic polymers and oligonucleotides

2.1 Abstract

We examined the effect of oligonucleotide (ON) structure on the interactions between cationic polymers and ONs. Unstructured and hairpin structured ONs were used to form complexes with the model polymer, poly-L-lysine, and the characteristics of these polymer-ON interactions were subsequently examined. The strength of pLL-ON interactions was tested by challenge with heparin, which induced complex disruption. Both the kinetics and heparin dose response of ON release were determined. We found that hairpin structured ONs formed complexes with pLL more readily as compared to unstructured ONs. While the tight binding of hairpins with pLL inhibited their release out of the complexes, unstructured ONs were released from the complex more easily. Our results therefore highlight the role of ON structure on the association-dissociation behavior of polymer-ON complexes. These findings have implications for the selection of ON sequences and design of polymeric carriers used for cellular delivery of ONs.

2.2 Introduction

Antisense technology employs short, single-stranded oligonucleotides (ONs), typically 12-25 bases long, to inhibit gene expression by binding to complementary mRNA via Watson-Crick base pairing. Over the last decade, antisense approaches have been developed for therapeutic purposes as well as for biotechnological applications (6). However, the widespread use of antisense ONs is still hindered by several obstacles. Prominent among them is the ineffective cellular delivery of ONs, which remains a major hurdle in the utilization of ON based technologies (21).

Numerous polymeric delivery agents have been developed to enhance cellular uptake while also protecting the ONs from degradation(61),(48),(52). Progress in vector development for ON delivery often borrows principles from those developed for the delivery of plasmid DNA for gene therapy applications. Improvements in the design of new carriers focus mainly on the polymer characteristics, attempting to improve the delivery effectiveness of the vector by modifying various polymer features such as backbone chemistry and side-chain length or, increasingly, by incorporating additional functionalities into the vector(62),(28) .

Relatively little is known concerning the effect of ON properties on the interactions between carriers and ONs. Clearly, the structure and sequence composition are key features of the ON and have significant implications on its biological interactions, such as its ability to hybridize with a target mRNA(8) and its resistance to nuclease digestion. For example, ONs designed to form stable structures, such as hairpins or loops, exhibit better resistance to nuclease digestion as compared to unstructured ONs.

Furthermore, certain applications call for the use of structured ONs. For example, molecular beacons, which possess a hairpin structure, are fluorescent hybridization probes that are used for quantitation of complementary targets in samples and have been used for visualization of RNA in cells (44, 45). In addition, circular or dumbbell shaped ONs are used as decoys for transcription factor binding in an alternative approach to inhibit gene expression at the level of transcription(63, 64). Despite its relevance to these applications, relatively little attention has been paid to understanding the molecular biophysics of ON interactions with carriers such as polymers, or on relating their biophysical characteristics to the biological activity of the vectors(47).

In this study, we tested the interactions between a cationic polymer, poly-L-lysine, and ONs of different structures (unstructured vs. hairpin). Four ONs (two unstructured and two hairpins) sequences complementary to the rabbit beta-globin mRNA were selected on the basis of thermodynamic modeling, from a dataset used in our previous work(8),(65). The structures of the hairpins are shown in Figure 2.1. For the polymer we chose poly-L-lysine (pLL) as a simple well-characterized cationic polymer, due to its ease of availability and handling and its previous use in DNA delivery studies. We probed both the association and dissociation behavior of pLL-ON complexes, and found that ON structure influences significantly its interactions with pLL.

2.3 Materials and Methods

2.3.1 Materials

Four 17-mer phosphodiester ON sequences were used in the study: two unstructured ONs and two hairpin structured ONs. The sequences and free energies of unfolding of the ONs are provided in Table 2.1. Oligonucleotides were obtained from Integrated DNA Technologies (Coralville, IA). Stock solutions were prepared by reconstituting the pellet in TE (Tris-EDTA) buffer at pH 8 to a final concentration of 1 mg/mL. Poly-L-lysine (pLL) of varying molecular weights was purchased from Sigma (St. Louis, MO). Stock solutions at a concentration of 1 mg/mL were prepared in water. All stock solutions were further diluted in TE buffer as required to prepare solutions of desired concentrations. OliGreen[®], a dye that binds strongly to single-stranded DNA, was obtained from Molecular Probes (Eugene, OR). Heparin sodium salt was obtained from Sigma (Cat# H4784).

ON name	ON sequence	ΔG unfolding (kcal/mol)
SC1	5'-ATT-GCA-AGT-AAA-CAC-AG-3'	0
SC2	5'-AGC-TTG-TCA-CAG-TGC-AG-3'	0
HP1	5'-GCA-GCC-TGC-CCA-GGG-CC-3'	2.1
HP2	5'-GCC-TGA-AGT-TCT-CAG-GA-3'	3.9

Table 2.1 Free energy of unfolding of hairpin-structured and unstructured ONs

2.3.2 Preparation of oligoplexes

Oligoplexes were prepared at desired pLL-ON charge ratios by mixing equal volumes of pLL (of varying concentrations) and ONs in TE buffer at pH 8. The samples were vortexed briefly, and the solutions were then incubated at room temperature for 10-15 minutes to ensure complex formation. The pLL-ON charge ratios were calculated on a molar basis. The complexes were prepared at a final ON concentration of 5 $\mu\text{g/mL}$ unless stated otherwise.

2.3.3 Detection of free ON using OliGreen[®]

Complexes between pLL and ON were prepared at various charge ratios as described above. One hundred microliters of each complex solution was transferred to a 96 well (black-walled, clear-bottom, non-adsorbing) plate (Corning, NY). One hundred microliters of diluted OliGreen[®] reagent (1:200 in TE buffer at pH 8) was then added to all samples for free ON detection. Fluorescence measurements were made after a 3-5 minute incubation using a Cytofluor (Applied Biosystems, CA), at excitation and emission wavelengths of 485 and 520 nm, respectively, and a voltage gain of 55. All measurements were corrected for background fluorescence from a solution containing TE buffer and diluted OliGreen[®] reagent.

2.3.4 ON release studies

Fifty microliters of heparin solution (at various concentrations prepared in TE buffer at pH 8) were added to 50 μL of complex solution (final ON concentration of 2 $\mu\text{g/mL}$) in a 96 well (black-walled, clear-bottom, non-adsorbing) plate. One hundred microliters of diluted OliGreen[®] reagent was added, and the solution was mixed manually using a

multichannel pipette. Fluorescence measurements were made immediately using the Cytofluor plate reader. The kinetics of ON release from the complexes were obtained by recording fluorescence at an interval of 1 minute for up to 30 minutes. Both the kinetics and the heparin dose response of ON release were recorded for all pLL-ON complexes at pLL-ON charge ratios of 2:1 and 5:1. The percentage of ONs released was calculated from the fluorescence (F) values as:

$$\% \text{ ODN released} = \frac{[F (\text{complex} + \text{heparin}) - F (\text{ODN} + \text{heparin})]}{[F (\text{complex}) - F (\text{ODN} + \text{heparin})]} \times 100\% \quad (1)$$

2.3.5 Modeling Polymer-ON complexation

The complexation of DNA with polymers used for delivery is typically expressed in terms of fraction DNA bound (or not bound) as a function of the charge ratio of total polymer added to DNA. We first attempted to utilize simple stoichiometric models based on charge neutralization to describe the binding curves; however, these did not accurately reproduce the correct shape of the binding curves or their lack of dependence over a large range of polymer molecular weights (not shown). Consequently, we adopted models previously used to study oligomer adsorption for this task.

First, we employed the McGhee-von Hippel isotherm for the binding of ligands that occupy multiple sites to an infinite lattice. This model has been used previously, among other applications, for the interpretation of oligocation/oligonucleotide binding(66). The McGhee-von Hippel isotherm relates via statistical thermodynamics a quantity, ν , equal to the moles bound of ligand per moles of lattice sites, to the free ligand

concentration $[L]$, the number of sites occupied per ligand n , and the equilibrium constant K for binding of a ligand to a site:

$$\frac{\nu}{[L]} = K(1 - n\nu) \left[\frac{1 - n\nu}{1 - (n-1)\nu} \right]^{n-1} \quad (2)$$

Putting this into terms of the fraction of oligonucleotide bound, f , and the pLL-ON charge ratio, r , results in the implicit expression:

$$\frac{f}{1-f} \frac{1}{nD_T r} = K \left(1 - \frac{f}{r} \right) \left[\frac{1 - f/r}{1 - \left(\frac{n-1}{n} \right) f/r} \right]^{n-1} \quad (3)$$

where D_T is the total concentration of ON in the system (bound plus free). While this cannot be solved explicitly for either f or r , it can be solved for f in terms of the ratio $\phi = f/r$. The resulting expression was used to generate plots of f vs. r by enumerating f as ϕ is increased from zero towards one, then using the solution for f to calculate the corresponding r as $r = f/\phi$:

$$f = 1 - \frac{1}{n\kappa} \frac{\phi}{1-\phi} \left[\frac{1 - \left(\frac{n-1}{n} \right) \phi}{1-\phi} \right]^{n-1} \quad (4)$$

where κ is a dimensionless parameter equal to KD_T .

We also utilized an extension to the McGhee-von Hippel isotherm in which the finite size of the receptor (taken here to be pLL) is taken into account. The key feature of this approach, originally developed by Epstein(67) and later applied for analysis of

oligocation/oligonucleotide binding(68), is the computation of the number of potential configurations, Ω_j , of j ligands each covering n sites out of a total of N total sites per receptor:

$$\Omega_j = \frac{[N - (n-1)j]!}{j!(N - nj)!} \quad (5)$$

This factor is used in the computation of a partition function, Ξ , which is summed over the possible number of ligands bound, ranging from zero to J_{max} , which is the nearest integer less than or equal to N/n :

$$\Xi = \sum_{j=0}^{J_{max}} (K[D_F])^j \Omega_j \quad (6)$$

where $[D_F]$ is the concentration of free (unbound) ON. The isotherm is then found by summation of the probabilities of all possible receptor occupancies:

$$\nu = \frac{1}{N\Xi} \sum_{j=0}^{J_{max}} j (K[D_F])^j \Omega_j \quad (7)$$

We again wished to express this in terms of fraction ON bound and pLL-ON charge ratio, which was accomplished employing the relations $[D_F] = D_T(1-f)$ and $f = nvr$, to obtain:

$$\frac{Nf}{nr} = \frac{\sum_{j=0}^{J_{max}} j [\kappa(1-f)]^j \Omega_j}{\sum_{j=0}^{J_{max}} [\kappa(1-f)]^j \Omega_j} \quad (8)$$

This equation is easily solved explicitly for r in terms of f and was used to compute the charge ratios corresponding to a range of bound ON fractions.

2.4 Results

Our primary goal was to evaluate the association-dissociation behavior of complexes containing pLL and ONs of differing structures (unstructured and hairpin structured) at varying charge ratios. First, we assessed pLL-ON binding as a function of pLL-ON charge ratio for a single pLL molecular weight. For this, we used a commercially available detection reagent, OliGreen[®], which fluoresces upon binding to single-stranded DNA. Complexation of ONs with pLL and other cationic polymers results in inaccessibility of dye binding (and/or possibly fluorescence quenching). Thus, the fluorescent signal measurement corresponds to the uncomplexed ON in solution. As expected, for all ONs, the fluorescence signal decreased, indicating that more ONs were incorporated into complexes, with increasing charge ratios (Figure 2.2). At lower charge ratios, both unstructured and hairpin ONs behave more or less similarly. However, at charge ratios of one and above, almost all the hairpins were complexed, while significant quantities of unstructured ONs remained in solution, indicating less extensive complex formation.

Since pLL-ON binding was found to depend on ON structure at a single pLL molecular weight, we tested the effect of varying pLL molecular weight on these interactions. We prepared complexes of each ON with pLL of five different molecular weights ranging from 500 Da to 574 kDa and determined the amount of free ON in solution as a function of the polymer-ON charge ratio. As shown in Figure 2.3, for each ON, the pLL-ON association did not vary significantly with pLL molecular weight except at the lowest molecular weight studied, 500 Da. At this molecular weight, complex formation was extremely inefficient. At all other pLL molecular weights, pLL-ON association depended

on ON structure. Hairpins exhibited greater association with pLL than unstructured ONs, particularly at high charge ratios.

In order to understand better the lack of molecular weight dependence on pLL-ON complexation behavior for most of the pLL range tested, we compared our results with the predictions of various theoretical models. First, several stoichiometric models, including the Scatchard and Hill isotherms as well as a formulation based on charge equivalents, were tested. All these fail to capture the lack of pLL molecular weight dependence over a wide range and in most cases do not follow very well the shape of the observed binding curve. Next, we utilized the McGhee-von Hippel isotherm, which describes the extent of binding of a “large ligand”, i.e., one that covers multiple binding sites, to an infinite lattice (receptor). Since, at all but the lowest pLL molecular weight, the number of pLL charges per molecule greatly exceeds that for the ON, we took pLL as the receptor and ON as the ligand. The charge per ON is fixed at $n = 17$ and the charge per pLL, N , is determined from its molecular weight (Table 2.2). By expressing this isotherm in terms of the variables used in analysis of polymer-DNA complexes for DNA delivery – fraction DNA complexed (f) and polymer/DNA charge ratio (r) – we obtained Eq. (3), which has no dependence on polymer molecular weight and a single parameter that is not determined from molecular structure, namely the dimensionless affinity κ . Parametric plots of this model show that binding is strongly affected by low values of the affinity, whereas the dependence is much weaker for values of $\kappa > 1$ (Figure 2.4a). The experimental data for structured ONs at all pLL molecular weights from 9,800 to 574,000 Daltons falls within the band of $1 < \kappa < 5$, but due to the insensitivity of the data in this region we did not attempt to explicitly fit the value of κ to the data.

MpLL	N	N/n
500	4	0.24
9,800	76.6	4.5
25,700	201	12
84,000	656	38
574,000	4,484	270

Table 2.2 Ratio of molecular charges of pLL to ON

Since the lack of polymer molecular weight dependence in the McGhee-von Hippel model is due to treating the polymer as an infinite array, we relaxed this approximation by implementing a finite size formulation of the isotherm(67, 68). Calculation of the number of system configurations was accomplished using Eq. (5), and the isotherms were subsequently determined by application of Eq. (8). The number of configurations rises dramatically with polymer molecular weight and proved problematic under conditions corresponding to the 574,000 MW pLL. Thus, we computed isotherms corresponding to the experimentally tested molecular weights from 9,800 to 84,000, along with a lower molecular weight of 4,000, which provides a polymer charge number of $N \sim 31$, still greater than the ON charge number of $n = 17$. The results show that the lack of pLL molecular weight dependence is maintained over the range of 9,800 to 84,000 Daltons. As N is lowered to values approaching n (such as in the 4000 Da case shown), a shift of the binding curves to the right is predicted, though the effect is not nearly as dramatic as

observed experimentally when the molecular charge ratio N/n shifts to values less than 1 (cf. Figure 2.3).

We studied further the dissociation behavior of these complexes upon exposure to heparin sulfate as a competitive binding agent. Heparin is a negatively charged polysaccharide that has been previously shown to disrupt polymer-ON complexes. Furthermore, it is a component of extracellular matrices and thus encountered by DNA delivery vectors on their route to cellular entry(69, 70). In our study, pLL-ON complexes were prepared at various conditions, and then heparin was added to dissociate the complexes, releasing ON into solution. OliGreen[®] was used to measure the amount of ON released over 30 minutes. Both the kinetics and heparin dose response of release were recorded. In each measurement, we corrected for changes in background fluorescence due to heparin addition alone. This change was found to be dependent on the heparin concentration (data not shown) and thus was measured and accounted for in each experiment.

The raw data from one such experiment with controls is shown in Figure 2.5a. For ON alone, a high and stable fluorescence signal was recorded. The addition of pLL at a 2:1 charge ratio resulted in an almost complete loss of signal, indicative of complex formation. Addition of heparin induced a gradual increase in fluorescence from the baseline, indicating release of the ON. From the heparin concentration ($5\text{ }\mu\text{g/mL} = 0.4\text{ }\mu\text{M}$) and the characteristic time of release ($\sim 1\text{ min}$), we estimate the second-order rate constant for ON release by heparin to be on the order of $1\text{ }\mu\text{M}^{-1}\text{ min}^{-1}$. This value is within the range observed for binding of antisense oligonucleotides to their structured complementary RNA targets(8) and is significantly less than that which would be

observed for the diffusion-limited binding of heparin to pLL. Thus, the process is kinetically controlled, and the pLL-ON complexes are competitively disrupted by addition of heparin.

The kinetics of ON release from complexes at 2:1 and 5:1 pLL-ON ratios (at 5 $\mu\text{g/mL}$ heparin concentration) are shown in Figures 2.5b and 2.5c, respectively. Consistent with the finding that hairpin ONs associate to a greater extent with pLL as compared to unstructured ONs, the pLL-hairpin complexes did not release ONs very easily. Nearly all of the unstructured ONs were released out of the complexes within 15-20 minutes, while up to 80% of hairpin ONs remained bound to pLL at 30 minutes. This effect was relatively insensitive to the two charge ratios used. At both charge ratios, pLL-unstructured ON complexes dissociated to a greater extent and at a faster rate, releasing more ONs.

The dose response of ON release with varying amounts of heparin was determined, using release at the end of 15 minutes as the measurement. As expected, increasing amounts of ONs were released with higher doses of heparin at a single pLL-ON charge ratio (Figure 2.6). At higher polymer-ON charge ratios, such as 5:1, greater heparin amounts were required to release similar ON amounts. This is to be expected, since a significant amount of free pLL presumably exists at a charge ratio of 5:1, which the heparin would titrate more easily than complex-bound material. In all cases, nonetheless, unstructured ONs were released from the complexes at lower heparin doses as compared to hairpins, further underlining the strength of pLL-hairpin interactions.

2.5 Discussion

Cellular delivery remains a major hurdle in the utilization of ON-based applications such as antisense technology(21). Although vector development for the efficient delivery of ONs is an active area of research, there are few systematic studies focusing on understanding carrier-ON interactions for the purpose of rational vector design. Here, we examined the influence of ON structure on its interactions with the cationic polymer, poly-L-lysine (pLL). We found that ON structure influences the association-dissociation behavior of pLL-ON complexes. Specifically, hairpin structured ONs associate with pLL and form complexes more readily than unstructured ONs. Moreover, the strength of this binding causes poor release of hairpins from the complex.

Existing studies of the interactions between oligonucleotides and cationic polymers have focused primarily on the salt dependence of binding as a probe of their electrostatic properties(66, 68). Other aspects of these interactions, such as their dependence on molecular structure, kinetics and stability in the presence of other species, are less well understood. Studies have shown that complexes between pLL and ONs are multimolecular in composition with several ONs and multiple pLL chains participating in complex formation(71). In order to enhance our understanding of these interactions, the ON structure and pLL molecular weight were varied in this study.

The study of polymer-DNA complexes for gene or oligonucleotide delivery requires a reagent to detect the DNA and a means to determine the state of the DNA (bound or free). Oligonucleotides can be synthesized with fluorescent dyes incorporated, usually at the 5'-end of the molecule, and these have been used in prior studies of ON

complexation, with the state evaluated by agarose or polyacrylamide gel electrophoresis. However, the attached dyes may affect complexation behavior. To avoid this issue, in all our assays, detection of ON was performed using OliGreen[®], a commercially available dye that binds preferentially to single-stranded DNA. Although the intensities of OliGreen[®] fluorescence depend on oligonucleotide sequence, all of our results utilize fluorescence intensities normalized to free solution values. We assessed the complexation behavior using OliGreen[®] fluorescence in microtiter plates formulated to minimize fluorescence background and non-specific adsorption. Complex formation between DNA and polymer leads to inaccessibility of the dye to ON and a resultant decrease in fluorescence intensity with increasing polymer concentration. This assay procedure is analogous to previous approaches for studying plasmid complex formation with polymers and lipids using DNA-binding dyes(72-74).

Our assays provided reproducible data probing quantitatively the complexation between the cationic polymer, pLL, and ONs, which are anionic. For plasmid DNA, electrostatic interactions with cationic polymer lead to condensation of the DNA at a critical ratio of positive to negative charges and the formation of toroidal, rod-shaped or spherical complexes(75). As a result, complex formation for plasmid DNA is assayed by exclusion of DNA binding dyes such as ethidium bromide. This type of procedure is also employed for polymer-oligonucleotide complexes, even though oligonucleotides do not possess a super-structure to condense in the manner of plasmid DNA. Previous results, as well as those presented here, support the notion that pLL resides on the outside of pLL-ON complexes since the OliGreen[®] dye was excluded. The fact that unstructured ONs exhibited an excess fluorescence even at high charge ratios suggests the possibility that a

fraction of the oligonucleotide is complexed yet remains accessible to OliGreen®. However, we have also found that unstructured ONs more effectively displace fluorescently labeled ONs from pLL-ON complexes, providing independent confirmation that the differences observed are due to binding variations (results not shown). Moreover, our heparin dissociation studies (Figure 2.6) also point to a difference in the pLL-ON interaction with ON structure.

The dependence of complex formation on ON structure observed in our work could be due to the differences in charge density distributions of the ONs. The linear charge density of pLL, which has a charge for roughly each 128 g of molecular weight, is greater than that for an ON, with a charge for roughly each 330 g of molecular weight. Thus, it is reasonable that decreasing the charge density of pLL or increasing the charge density of ON would lead to a more symmetric charge distribution and hence to more efficient complexation. Hairpin ONs provide a higher local concentration of charges as compared to unstructured ONs, which may allow for a more symmetric interaction with the charge groups in pLL. An effect of DNA charge density on complexation has been found using plasmid DNA of varying topology, where cationic copolymers were shown to bind preferentially to supercoiled DNA compared to linear DNA⁽⁷⁷⁾. Our results suggest that ON structure may similarly influence the electrostatics of complex formation.

Complex formation is highly inefficient at low pLL molecular weight, which is in agreement with observed trends for polymer-plasmid DNA binding⁽⁷⁷⁾. This molecular weight (500 Daltons by the vendor) is the only one studied for which the amount of charge per pLL molecule is less than that per ON molecule (Table 2.2). For higher

molecular weights of pLL, there was no difference in pLL-ON binding with varying pLL molecular weight. These results can be interpreted using isotherms developed for ligands that cover multiple sites upon binding(66, 67). We applied these isotherms (Eqs. (3) and (8)) assuming that the ON is the ligand binding to sites on pLL, with sites corresponding to each charge group. Thus, $n = 17$ lattice sites are covered by the ON upon binding to pLL. For the polymer molecular weights utilized in this study, these isotherms predicted either no (for an infinite lattice) or negligible (for a finite size lattice) dependence on pLL molecular weight. This result is in agreement with the experimental data and is not predicted based on stoichiometric binding between a polycationic polymer molecule and a neutralizing number of oligonucleotides. At the lowest pLL molecular weight, the number of charges per pLL becomes less than that for the ON. As a result, there is no site on the pLL large enough to accommodate the ON. The same type of isotherm could then be applied by reversing the roles of ligand and receptor. However, in doing so, it was not possible to obtain a form that was calculable for f and r as in Eq. (8). Nonetheless, we would expect that the interaction would be considerably weaker, as the fundamental adsorption event would involve four charge groups (for $N = 4$ at pLL MW 500) as opposed to seventeen for all other molecular weights. This large reduction in the affinity of a single adsorption event is likely a major reason for the shift in the binding curve when the number of pLL charges becomes less than the number of ON charges. Thus, a combination of polymer adsorption isotherms and site number considerations explain the pLL molecular weight dependence of binding. They do not, however, explain the ON structure effect; to do so would require a more structurally detailed approach.

Polyanion disruption assays, using molecules such as dextran sulfate, poly-L-aspartic acid and heparin, have been used to study the dissociation behavior of carrier-DNA complexes. Here, we used heparin to disrupt the pLL-ON complexes and found the release profiles to depend on ON structure. Heparin is a negatively charged polysaccharide, belonging to a family of glycosaminoglycans (GAGs) that are often incorporated in the extracellular matrix and are also found intracellularly. The implications of GAGs in DNA delivery have been studied by various research groups^{(78),(70),(79)}. While GAGs have been shown to inhibit DNA delivery, the mechanism is poorly understood but believed to involve disruption of complexes in the extracellular matrix. Although ease of ON release is important, the fact that hairpin structured ONs remain associated with polymer in the presence of equivalent levels of heparin may serve useful when trying to avoid GAG-induced disruption of complexes, and promoting other mechanisms of intracellular ON release. We did not find significant differences in the release profiles, upon addition of heparin, for ONs complexed with pLL of molecular weight ranging from 9,800 to 574,000 Daltons (data not shown), consistent with the complexation curve behavior. Conversely, plasmid DNA tends to exhibit differences in complexation and transfection efficiency as a function of polymer molecular weight^(77, 80). Plasmid transfection efficiency has been found to decrease for large plasmid insert sizes; however, it is not clear whether this is due to polymer-DNA delivery effects or due to a size dependence of plasmid expression in the nucleus^(81, 82).

Unpackaging of the carrier-ON complex accompanied by release of DNA poses a barrier to carrier-based cellular delivery of DNA. As such, there should be an optimum degree of association between the DNA and carrier, as accelerated dissociation of the

complex will lead to degradation of DNA by nucleases, whereas tightly bound rigid complexes may hinder the transport and functionality of DNA (e.g., hybridization to target mRNA for antisense ONs). Certain carriers, despite being effective in binding or encapsulating DNA and protecting it from degradation, have been shown to release plasmid DNA poorly, often leading to low transfection efficiencies(83). Indeed, transfection efficiency can either increase(77) or decrease with polymer molecular weight, suggesting further that there is a balance of binding strengths necessary that likely depends greatly on the local microenvironment of the target cells.

In our studies, the concentrations of heparin required to induce dissociation were quite modest, suggesting that dissociation of polymer-ON by heparin and other anionic biopolymers is likely to be a significant barrier for cellular delivery of ONs to living cells. Furthermore, the time scale (minutes) of the dissociation process that we observed is rapid enough to compete with cellular entry mechanisms. Future studies will determine the impact of the differences in complexation and dissociation behavior noted here on cellular uptake and processing. It should be noted that cellular uptake and ON release from delivery agents depend on the particular cell type as well as carrier characteristics. A study of hairpin vs. unstructured ONs found identical uptake rates in T cells(63), but these results were obtained in the absence of a polymeric carrier. In any event, our results have important implications for the design of polymer based vectors for ON delivery.

In particular, we have shown that ON structure influences the interactions between cationic polymers such as pLL, and ONs. The structure of ONs is an important parameter that also influences additional properties relevant for antisense activity, such as its interaction with the mRNA target and the rate of ON degradation by nucleases.

Selection of effective antisense sequences and their efficient cellular delivery are key factors that determine the outcome of an antisense experiment. The fact that ON structure affects its association with carriers that are used for delivery therefore highlights the importance of ON properties on vector design and provides another consideration for the rational design and control of carrier mediated ON delivery.

Chapter 3: Interplay of polyethyleneimine molecular weight and oligonucleotide backbone chemistry in the dynamics of antisense activity

3.1 Abstract

The widespread utilization of gene silencing techniques, such as antisense, is impeded by the poor cellular delivery of oligonucleotides (ONs). Rational design of carriers for enhanced ON delivery demands a better understanding of the role of the vector on the extent and time course of antisense effects. The aim of this study is to understand the effects of polymer molecular weight (MW) and ON backbone chemistry on antisense activity. Complexes were prepared between branched polyethyleneimine (PEI) of various MWs and ONs of phosphodiester and phosphorothioate chemistries. We measured their physico-chemical properties and evaluated their ability to deliver ONs to cells, leading to an antisense response. Our key finding is that the antisense activity is not determined solely by PEI MW or by ON chemistry, but rather by the interplay of both factors. While the extent of target mRNA down-regulation was determined primarily by the polymer MW, dynamics were determined principally by the ON chemistry. Of particular importance is the strength of interactions between the carrier and the ON, which determines the rate at which the ONs are delivered intracellularly. We also present a mathematical model of the antisense process to highlight the importance of ON delivery to antisense down-regulation.

3.2 Introduction

Antisense technology provides a simple and elegant means to regulate gene expression, either for therapeutic purposes or for studying gene function (3, 6, 10). With one FDA approved drug and approximately twenty candidates in various stages of clinical trials, there is growing promise for the success of this approach (84, 85). Additionally, the excitement generated by the advent of siRNA has rejuvenated interest in gene silencing technologies in general (86). Advances in oligonucleotide synthesis have now made it relatively simple to modify the chemistry of these molecules. This has enabled the creation of oligonucleotides with diverse properties and has thus greatly widened their overall utilization as specific mediators of gene silencing.

With the growing progress in functional genomics, there is an increasing need for the routine application of gene silencing tools such as antisense in basic research. Despite the conceptual simplicity, utilization of antisense as a routine tool for in vitro studies is greatly impaired by the poor cellular delivery of these molecules. Delivery of oligonucleotides (ONs) in a stable form and relevant dose to the appropriate target site of action remains a considerable challenge to date (87, 88). The reduced cellular entry and rapid degradation of these molecules in the presence of cellular nucleases calls for the utilization of carrier molecules. Various types of carriers, including polymers, lipids and peptides (89-93) of diverse chemistries, have been tested for their effectiveness as DNA delivery vectors. However, substantial optimization is generally required to make these carriers work for the particular application at hand. The large variations in vector effectiveness among cell types, as well as the relatively high cytotoxicity of the currently

available carriers, continue to fuel the demand for more rationally designed carrier systems (27).

To improve further the design of DNA carriers, extensive research is being conducted to identify cellular barriers to carrier mediated delivery of ONs (21). Efforts are directed towards determining structure-property relationships that relate carrier properties to antisense effectiveness. However, it remains somewhat unclear what factors ultimately dictate the effects observed. Of particular importance is the fact that much of the design principles developed for plasmid DNA carriers are often used interchangeably for antisense ONs or siRNA. Although this may work in certain cases, the small size of ONs (10-22 bases) and variations in their backbone chemistry and structure endow them with unique properties that alter their interactions with carriers in comparison to plasmid DNA, and hence influence the design criteria for oligonucleotide carriers. There are several examples in literature that point to such differences in terms of ON structure, ON chemistry, and sequence composition (94-97). Hence, there is a need for systematic investigations of the interactions of carriers with ONs, both at the molecular level as well as at the cellular level, to acquire a mechanistic understanding of their cellular processing.

The goal of the present study is to understand the role of the vector, i.e. the properties of both the carrier and the ON, on the extent and dynamics of the antisense effect. For our study, we chose the cationic polymer, polyethyleneimine (PEI), as the model polymer. Our rationale for doing so is two-fold. First, PEI is a well characterized carrier molecule (98). It has been utilized extensively for the delivery of plasmid DNA due to its high charge density and endosomolytic activity. Several reviews are available

detailing the effectiveness and mechanism of action of PEI and its various modifications for the delivery of DNA to a range of cell types (99-101). There are fewer studies focusing specifically on the delivery of ONs using PEI. Second, we wish to determine the optimal PEI MW for delivery of ONs of various chemistries. Specifically, we utilized five molecular weights (MWs) of the branched form of the polymer, in combination with phosphodiester (PO) and phosphorothioate (PS) ON backbone chemistries. While a range of alternative chemistries is now available, PO and PS ONs are still utilized most often for in vitro work. We studied the polymer-ON interactions and further evaluated their efficacy in delivering active antisense ONs to cells. We demonstrate that the observed antisense effect is not determined solely by the carrier properties, but by the particular combination of polymer and ON properties. Of particular importance is the strength of interactions between the carrier and the ON, which determines the rate at which the ONs are delivered intracellularly.

3.3 Materials & Methods

3.3.1 Materials

A 20-mer anti-GFP sequence identified previously (102, 103) as an effective inhibitor of pd1EGFP expression (5'-TTG TGG CCG TTT ACG TCG CC -3') and a scrambled control (5'- TTG CTT GTA CCG TGC GTG CC -3') were utilized in the study. The phosphodiester, phosphorothioate and fluorescently tagged (5' Cy5 end modified) forms of these sequences were obtained from Integrated DNA Technologies (Coralville, IA). Stock solutions were prepared by reconstituting each pellet in water to a final concentration of 100 μ M. Branched polyethylenimine (PEI) of molecular weights 1.2 kDa (Cat# 6088), 10 kDa (Cat# 19850) and 70 kDa (Cat# 00618) was purchased from Polysciences, Inc. (Warrington, PA). Additionally, PEI of molecular weight 25 kDa (Cat# 408727) and 600-1000 kDa (Cat# 3880) was purchased from Sigma. Stock solutions at a concentration of 10 residue mM (0.43 mg/mL) were prepared in water and the pH adjusted to 7.0 using HCl. OliGreen, a fluorescent dye that binds strongly to single-stranded DNA, was obtained from Molecular Probes (Eugene, OR). Heparin sodium salt was obtained from Sigma (Cat# H4784). Unless stated otherwise, all cell culture products were obtained from Invitrogen (Carlsbad, CA).

3.3.2 PEI/ON complex formation

PEI/ON complexes were prepared at desired PEI/ON charge ratios by mixing equal volumes of PEI (of varying concentrations) and ONs in PBS. The samples were vortexed briefly, and the solutions were then incubated at room temperature for 10-15 min to ensure complex formation. Experimental evidence (stabilization of fluorescence

corresponding to free ON) confirmed that this time was sufficient for complex formation. The PEI/ON charge ratios were calculated on a molar basis. The complexes were prepared at a final ON concentration of 10 µg/mL (approximately 1.64 µM) unless stated otherwise.

3.3.3 Detection of free ON using OliGreen

Complexes between PEI and ONs were prepared at various charge ratios as described above. One hundred microliters of each complex solution was transferred to a 96 well (black-walled, clear-bottom, nonadsorbing) plate (Corning, NY, USA). A total of 100 µL of diluted OliGreen reagent (1:100 in TE buffer at pH 8) was then added to all samples for free ON detection. Fluorescence measurements were made after a 3-5 min incubation using a Cytofluor (Applied Biosystems, CA, USA), at excitation and emission wavelengths of 485 and 520 nm, respectively, and a voltage gain of 55. All measurements were corrected for background fluorescence from a solution containing TE buffer and diluted OliGreen reagent.

3.3.4 Determination of particle size using dynamic light scattering

Complexes were prepared by mixing PEI and ON solutions (final ON concentration of 50 µg/mL, charge ratio of 10:1 in PBS), and immediately analyzed using a Brookhaven Particle Size Analyzer (Holtsville, NY) for 15 minutes with readings taken at an interval of every 3 minutes. Measurements were performed in triplicate.

3.3.5 PEI/ON dissociation studies

PEI/ON complexes (charge ratio 10:1, final ON concentration of 5 µg/mL ~ 0.8 µM, volume 50 µL) were prepared as described previously and transferred to a 96 well (black walled, clear bottom, nonadsorbing) plate. One hundred microliters of diluted OliGreen reagent were added to each well and mixed manually with a multichannel pipet. Fifty microliters of heparin solution (at various concentrations prepared in TE buffer at pH 8) were then added to the wells, and the plate was maintained at 37°C. Fluorescence measurements were made at the end of one hour from the time of heparin addition using the Cytofluor plate reader. The percentage of ONs released was calculated from the fluorescence (F) values as

$$\% \text{ ODN released} = \frac{[F (\text{complex} + \text{heparin}) - F (\text{ODN} + \text{heparin})]}{[F (\text{complex}) - F (\text{ODN} + \text{heparin})]} \times 100$$

In each measurement, we corrected for changes in background fluorescence due to heparin addition alone. This change was found to be dependent on the heparin concentration (data not shown), and thus was measured and accounted for in each experiment.

3.3.6 Cell culture

Chinese hamster ovary (CHO-K1) cells (ATCC, Manassas, VA) were maintained in F-12K medium (Kaighn's modification of Ham's F-12; ATCC, Manassas, VA) supplemented with 10% fetal bovine serum and penicillin-streptomycin solution. CHO-d1EGFP cells (CHO-K1 cells stably expressing a destabilized green fluorescent protein transgene) were previously produced by transfecting CHO-K1 cells with the 4.9 kb d1EGFP-N1 plasmid (BD Biosciences Clontech, Palo Alto, CA, USA), and maintained

under constant selective pressure by G418 (500 $\mu\text{g/ml}$). All cell lines were cultivated in a humidified atmosphere containing 5% CO_2 at 37°C.

3.3.7 Antisense experiments

CHO or CHO-d1EGFP cells were plated at a density of 1.5×10^5 cells/well in 12 well plates 18 h prior to transfection. Prior to introduction of ONs, cell culture medium in each well was replaced with 800 μL of OptiMEM^(R) (reduced serum medium). Further, 200 μL of PEI/ON complex solution prepared in PBS was added to each well so the final ON concentration in each well (1 mL) was 300 nM. To measure the intracellular levels of ONs released from the complexes, cells were treated with complexes prepared with Cy5-ONs. At the end of the incubation period of 4 h, the transfection mixture was replaced with serum containing growth medium and maintained under normal growth conditions (5% CO_2 , humidified atmosphere, 37°C). Medium in the wells was replaced with fresh serum containing medium every 24 h. At various times, cells were assayed for antisense activity (GFP fluorescence) and/or ON levels (Cy5-ON fluorescence) by flow cytometry. As controls, cells were also exposed to only PEI (in the absence of ONs), only ONs (in the absence of PEI) as well as complexes prepared with scrambled ON sequences to check for sequence specificity. All times indicated are relative to when complexes were first introduced to the cells, which represents $t=0$.

3.3.8 Flow cytometry

Replicate wells of cells were washed in PBS, detached with trypsin-EDTA, washed with serum-containing medium, pelleted by centrifugation for 5 min at 200 g, washed with PBS, resuspended in 500 μL of PBS and maintained on ice before being subjected to

flow cytometry analysis. 10,000 cells were analyzed on a FACSCalibur two-laser, four-color flow cytometer (BD Biosciences) for GFP fluorescence in FL1 (green) channel and Cy5-ON fluorescence in FL4 (far-red) channel. CellQuest software was used to acquire and analyze the results. Viable cells were gated according to their typical forward/side scatter characteristics. The flow cytometer was calibrated with fluorescent beads (CaliBRITE Beads, BD Biosciences) prior to each use to ensure comparable readings over the period of the study.

3.3.9 Mathematical model

We previously developed a detailed mathematical model describing the cellular events that an antisense ON undergoes in its attempt to reach and block its target in the cell (104). The model was based on mass action kinetic equations on the ON and took into account a set of compartments based on cellular location (e.g., cell membrane, endosome, cytoplasm) and molecular state (e.g., free, hybridized or degraded). Here, we present a simplified version that describes the intracellular delivery of ONs and the subsequent antisense response. The model highlights the significance of ON release from polymer/ON complexes to the overall nature of antisense down-regulation.

Transfer of ONs from outside the cell to the intracellular space is described as a single process. For the sake of simplicity, all intermediate steps such as cellular uptake, endosomal escape, and release from PEI/ON complexes are lumped into this single process. Antisense ONs outside the cell and inside the cell are each assumed to degrade by a first order process.

By solution of the governing mass-action kinetic equations (see Appendix), the dynamics of intracellular ON levels (A_i) can be represented by

$$A_i(t) = \gamma(e^{-\alpha t} - e^{-\beta t}) \quad (2)$$

Experimental results (Cy5-ON fluorescence) were fit to Equation (1) using a non-linear equation solver, and the parameters α, β and γ were estimated. A combination of these parameters, $\gamma(\beta - \alpha)$, is equal to the initial rate of intracellular uptake/release of ONs (Appendix, Equation A4).

Antisense ONs released from PEI/ON complexes intracellularly are then capable of binding to the target mRNA to elicit an antisense response. We neglect all other events such as non-target interactions or protein binding. Further, we assume the ON-mRNA hybridization to be in rapid equilibrium, denoted by the equilibrium constant K . The total mRNA from the target gene can therefore be present in the unbound or hybridized form. It can be shown (Appendix) that, following perturbation of the steady-state with an antisense oligonucleotide, the amounts of mRNA and protein, relative to steady-state, μ and π respectively, are given by

$$\frac{d\mu}{dt} = \lambda \left(1 - \frac{\mu}{1 + KA_i(t)}\right) \quad (3)$$

$$\frac{d\pi}{dt} = \delta \left(\frac{\mu}{1 + KA_i(t)} - \pi\right) \quad (4)$$

In these equations, the GFP mRNA and protein degradation rates (λ and δ respectively) utilized in the model were 0.069 and 0.69 h⁻¹ respectively. Given the $A_i(t)$ profiles

separately measured and fit to Equation 1, only the equilibrium constant K remains as an adjustable parameter. Equations (2) and (3) were solved simultaneously for the objective of minimizing the error associated with K . A more detailed explanation of the methods employed to solve the model and fit its parameters is provided in the Appendix.

3.4 Results

First, we tested the ability of PEI of molecular weights ranging from 1.2K to 600K to form complexes with ONs, as a function of the PEI/ON charge ratio. We measured the amounts of free (unbound) DNA in solution using a dye, OliGreen, which fluoresces upon binding to single-stranded DNA (89, 94). As shown in Figure 3.1, the fluorescence levels decrease with increasing PEI/ON charge ratios. At higher charge ratios ($\geq 5:1$ for PO ONs or $\geq 2:1$ for PS ONs), only residual amounts of free (unbound) ONs are detected in solution, indicating complex formation. All PEI MWs behave similarly in their ability to bind with ONs, except that complex formation is highly inefficient for PEI/PO complexes at the lowest MW PEI (1.2K). In fact, even at the highest charge ratio (20:1), there is no significant binding between PEI (MW 1.2K) and PO ONs. Therefore, PEI MW 1.2K was excluded from all further studies. For all PEI MWs, the complexation curve is shifted to lower charge ratios for PS ONs relative to PO ONs, indicating a greater affinity for the PEI-PS ON interaction.

In order to characterize further the PEI/ON complexes, particle sizes were estimated in the form of mean hydrodynamic diameter using dynamic light scattering. Complexes prepared at various PEI/ON charge ratios in PBS were subjected to particle size measurements for 15 minutes at a regular interval of 3 minutes. For charge ratios below 10:1, complexes were found to aggregate, as indicated by the rapid increase in particle size (data not shown). Although the OliGreen binding assay indicated PEI-ON association at these charge ratios, stable, sub-micron sized complexes were formed only at a charge ratio of 10:1 or above. At a charge ratio of 10:1, only 10K/PO complexes

displayed particle aggregation, with the particle diameter increasing from 200 to 450 nm within 15 minutes. Irrespective of the PEI MW and ON chemistry, all other particles were stable in the presence of salt and maintained a mean diameter of approximately 200 nm (Figure 3.2). All further studies were therefore performed at a charge ratio of 10:1.

For effective cellular delivery, polycation-ON complexes should be of an appropriate strength to withstand encounters with other macromolecular species while entering the cell and during intracellular trafficking but also to dissociate (unpackage) the ON at some point to allow recognition of the target mRNA. We probed the strength of the PEI/ON interactions by studying the dissociation behavior of these complexes upon exposure to heparin sulfate as a competitive binding agent (94). Complexes were prepared at a PEI/ON charge ratio of 10:1, after which heparin was added to dissociate the complexes, releasing ONs into solution. OliGreen was used to measure the amount of ONs released, following subtraction due to the minor effect of heparin on OliGreen fluorescence. The dose response of ON release with varying amounts of heparin was determined, using release at the end of one hour as the measurement. Increasing amounts of ONs were released with higher doses of heparin for PEI/ON complexes of both ON chemistries, with several notable characteristics (Figure 3.3). For PEI/PO complexes, the data revealed a threshold heparin concentration above which most of the ONs were released from the complexes. There was no significant effect of the PEI molecular weight on the release of PO ONs from PEI. On the other hand, PEI MW plays a more definitive role on PEI/PS interactions. Higher amounts of PS ONs were released with increasing PEI MW (Single factor ANOVA test, $p=0.0005$, for PEI/PS complexes challenged with heparin at 20 $\mu\text{g/mL}$), indicating reduced strength of binding between PEI of higher MW

and PS ONs. Furthermore, a comparison of the release profiles for the two ON chemistries indicates enhanced strength of binding (lesser release) between PEI and PS ONs as compared to PO ONs.

Having studied the physico-chemical properties of PEI/ON complexes, we tested the effectiveness of these polymers in delivering anti-d1EGFP ONs to CHO cells stably expressing the d1EGFP transgene (89). Cells were treated with complexes of PEI (various MWs) and ONs (PS and PO backbone chemistries) for 4 hours, and subjected to flow cytometry at each of several times over a 72 h time period. Under all conditions, more than 90% of the cells were gated as live. The fluorescence levels indicated in Figure 3.4 are normalized to the green fluorescence of time-matched, untreated CHO cells that stably express the d1EGFP transgene.

Antisense ONs delivered with PEI produced transient reductions in average GFP levels, with as much as 80% reduction observed 8 hours from when cells are treated with PEI/ON complexes under the best conditions. The time scale over which antisense effects were observed varied distinctly with the ON chemistry. As shown in Figure 3.4a, PO ONs delivered with PEI produced a rapid and brief response. GFP levels declined steeply, with as much as 60% of the fluorescence lost in the first 4 hours, when ONs are delivered with PEI MW 25K. The maximum down-regulation was observed close to the 8 h time point, shortly after which the GFP levels rise swiftly and return to base level by 48 hours from administration. In comparison, PS ONs delivered with PEI exhibited a more gradual antisense response that was sustained for a longer duration (Figure 3.4b). The antisense effects were maximal between 8 and 24 h, and only gradually returned to base

level over a 72 h time period. These differences in the onset of down-regulation between PO & PS ONs are more distinct at the earlier time points such as 4 h.

Whereas ON chemistry determined primarily the dynamics of antisense effects, the molecular weight of PEI used to deliver the ONs influenced strongly the extent of down-regulation observed over the same time scale. PO ONs delivered with intermediate MW PEI (25K) produced the highest levels of GFP down-regulation, while lower levels of down-regulation were recorded when PO ONs were delivered with all other MWs (10K, 70K and 600K). Interestingly, for PS ONs, the effect of the carrier MW was more pronounced and quite different from that of PO. Almost no down-regulation was observed when PS ONs were delivered with the PEI of MW 10 or 25K. In contrast, almost 80% inhibition was obtained when PS ONs were delivered with higher MW PEI (70 & 600K).

A number of controls were utilized to evaluate the contribution of ON labeling dye, free polymer, and ON sequence on GFP down-regulation (Figure 3.5). When cells were treated with ONs in the absence of PEI, no antisense effects (i.e., decrease in GFP expression) were observed, highlighting the need for a carrier. The carrier itself exhibited minimal nonspecific effects. We also exposed cells to complexes of PEI and scrambled anti-GFP sequences to verify the specificity of the anti-GFP sequences. In order to segregate any false effects due to inefficient/incomplete ON delivery, we used the particular PEI MW that provided maximum intracellular ON levels for each of the backbone chemistries, i.e., MW 25K for PO ONs and MW 70K for PS ONs. In all cases, the anti-GFP sequences exhibited significantly greater down-regulation than the

scrambled ones (Single factor ANOVA test, $p < 0.01$ for complexes of PEI with PO and PS ONs), providing evidence for reasonable sequence specificity of antisense inhibition.

In general, utilization of the d1EGFP transgene as the antisense target provides a simple means to capture the antisense down-regulation by measurement of GFP fluorescence (89, 102, 103). To detect simultaneously the presence of delivered, intracellular ONs, fluorescently (Cy5) end-tagged ONs were utilized in our experiments. Statistically indistinguishable levels of antisense inhibition were observed with dye-labeled vs. unlabeled ONs (Single factor ANOVA test, $p > 0.05$, for complexes of PEI with anti-GFP PO ONs, and for PEI with anti-GFP PS ONs), indicating that the label did not appreciably alter delivery or antisense behavior (Figure 3.5). Because Cy5 tagged ONs complexed to PEI do not fluoresce (data not shown), the ON fluorescence measured by flow cytometry corresponds to ONs released from PEI within cells. Absolute fluorescence levels are indicated in Figure 3.6 and are representative of data from several runs. The levels of intracellular PO ONs increase rapidly to a maximum at around 4 h after exposure (Figure 3.6a). PO ONs also disappear quickly from cells with negligible amounts detected after 48 h. Maximum levels of intracellular PO ONs are detected when delivered using the intermediate PEI MW of 25K. In contrast, the levels of intracellular PS ONs delivered with PEI increase slowly, reaching a maximum between 8 and 24 h after treatment (Figure 3.6b). PS ONs are retained within cells for a longer duration, being cleared only after 72 h. It was interesting to note that very little ON was detected intracellularly when PEI of lower MW such as 10K and 25K were used as carriers for PS ONs. Higher MW PEI (70K, 600K) delivered the highest amounts of intracellular PS ONs.

To quantify the relationship implied by Figures 3.4 and 3.6 between intracellular ON release and antisense inhibition, we integrated these measurements using a mathematical model based on mass-action kinetics. By fitting the results from the ON uptake experiments to a simple lumped uptake/release process with intracellular and extracellular degradation (Appendix, Figure A1(a) and Equation A3), we simulated the dynamics of intracellular ON levels shown in Figures 3.7a and 3.7b. A comparison of the model fit to the experimental results in Figures 3.6a and 3.6b shows that this model captures the dynamics observed in the intracellular release levels. Using a combination of parameters obtained from the model fit, we calculated the initial intracellular ON release rates ($k_1 A_{e0}$) for various PEI/ON complexes (Table 3.1). This one parameter captures the observed PEI MW and ON backbone dependences. Maximum ON release rates were obtained with intermediate PEI MW (25K) for PO ONs, while the higher PEI MW (70K & 600K) release more PS ONs. This parameter also shows quantitatively that the initial uptake and release of PO ONs exceeds that of PS ONs.

Using a mass action kinetic description of ON-mRNA hybridization (Appendix, Figure A1(b)) and coupling it to a description of translation (Appendix, Figure A1(c)), we also modeled the overall antisense dynamics. Estimates of GFP mRNA half-life from literature vary from 3-12 hours (105-108), from which we utilized a half-life of 10 hours for our calculations. The protein half-life was estimated as 1 hour, which is the nominal value for the destabilized version of the enhanced green fluorescent protein (d1EGFP). By incorporating these half-life estimates and the parameters from the ON uptake model, a single value of the ON-mRNA equilibrium constant (0.004 and 0.0084 for PO and PS ONs respectively) was fit for each ON chemistry across all PEI MWs. As shown in

Figures 3.7c & 3.7d, the GFP down-regulation data (Figures 3.4a & 3.4b) were captured reasonably well by the model. Although the maximum down-regulation is somewhat under-predicted, the model predicts accurately the trends with respect to PEI MW and the overall time scale of effects for each of the ON chemistries, in particular the delayed onset and sustained activities of PS vs. PO backbones ONs.

PEI MW	ON chemistry	
	PO	PS
10K	111.6	15.1
25K	365.9	20.6
70K	273.7	59.4
600K	33.3	86.8

Table 3.1 Maximum intracellular ON release rates from PEI/ON complexes, computed using the fit model parameters

3.5 Discussion

PEI has garnered significant attention in recent times as a building block for creating effective DNA carriers and has been tested both in vitro and in vivo to target a large number of cell types (27, 99, 109-113). Several modifications have been proposed to take advantage of the unique buffering capabilities of this molecule while reducing the toxicity associated with its use (114, 115). However, most of these reports focus on delivering plasmid DNA for gene therapy applications. There are strikingly fewer systematic studies on the utilization of PEI for single-stranded DNA molecules. Insights obtained from PEI mediated plasmid DNA studies are generally extended for the application of delivering small DNA such as antisense oligonucleotides. However, as noted by us and other researchers (96, 109, 116), these generalizations may not hold, especially given the considerable differences in the size, structure and chemistry between oligonucleotides and plasmid DNA. In fact, these small DNA molecules (10-20 bases) are often observed to exhibit weaker electrostatic complexation with polycations due to the small number of charged units per ON molecules. While the linear form of PEI of MW 25K is often touted as the most effective carrier for delivering plasmid DNA, we found it ineffective for both PO and PS ONs (data not shown). Hence, to specifically identify issues related to PEI mediated ON delivery, we performed a systematic study with a set of branched PEI MWs and ON chemistries.

Using the d1EGFP gene as an easily quantifiable antisense target, we screened various combinations of PEI MWs (1.2K, 10K, 25K, 70K, 600K) and ON chemistries (PO and PS) for their ability to elicit an effective antisense response. For PO ONs, maximum antisense response was observed with intermediate MW PEI (25K) as the

carrier, while complexes of PS ONs with higher MW PEI such as 70K and 600K produced comparable levels of d1EGFP down-regulation. These particular PEI/ON combinations that achieved highest antisense response were also the ones that delivered the most ONs, i.e., maximum intracellular ON levels were recorded for these cases. Indeed, a monotonic relationship is apparent when the maximum antisense inhibition is plotted against the maximum ONs delivered for each combination of PEI MW and ON chemistry (Figure 3.8). Conditions under which no antisense inhibition was observed occurred because no ONs were delivered using those particular PEI/ON combinations. A correlation between intracellular levels of short interfering RNA and gene silencing has also been reported (117).

Why do different combinations of PEI MW and ON chemistry deliver different ON levels? Studies of various PEI MWs for delivery of plasmid DNA do not provide a clear view, as they have produced conflicting trends. In some cases, transfection efficiency was found to increase with PEI MW (77), while in others low MW PEI was effective as a gene delivery agent (113). The toxicity associated with very high MW PEI offsets its use as DNA carrier (118), making the less toxic low MW PEI a more attractive candidate for further improvement despite its lower net charge density. To date, very little mechanistic explanation for the differences in behavior of various MWs has been provided. Previous investigations of the cellular processing of PEI/DNA complexes suggests that complexes are taken up by binding with proteoglycans, such as syndecan, and further trafficked through the endocytic pathway (112, 119). The similar size of all our complexes (200 nm) suggests a low probability of differences in the rate of internalization of the complexes. PEI is believed to enable escape of polyplexes from the

endo-lysosomal pathway by a "proton-sponge" effect, by which complexes and/or DNA are released into the cytoplasm (100, 120). It is not clear where or how the DNA is ultimately released from the complex. Previous studies demonstrate no significant differences in the buffering capacity of PEI of various MWs in the relevant pH range of 5-7 (98). Some studies suggest the involvement of cytoplasmic proteins and other charged molecules in the competitive release of DNA from PEI/DNA complexes (121). Therefore, we hypothesize that at least part of the MW backbone effects could be due to the kinetics of complex dissociation (unpackaging) and that these could be evaluated in vitro using the heparin competition assay.

Indeed, the differences in PEI-ON interactions are reflected in the heparin competition assay, where we observe a MW dependence on the amount of ONs released from PEI/PS ON complexes. Specifically, in the presence of heparin, complexes made with higher MW release more PS ONs than complexes made with lower MW PEI. However, when we tested the strength of the PEI-PO ON interactions by competition with heparin, we did not find any significant differences among the various PEI MWs. As such, it appears that the MW influences delivery of PO ONs in a manner not captured by the heparin competition assay, perhaps determining where in the cell (e.g., endosome vs. cytoplasm) the DNA gets released. Competition with heparin has been used in previous studies as a measure of the stability of carrier/DNA complexes. Our studies suggest that higher stability may correspond to very tight binding that inhibits the release of DNA from the complexes. There are several such examples in the literature, wherein polymers that bind DNA effectively do not release them intracellularly despite their buffering capabilities (114, 122). Our results provide some insights for such observations and

additionally suggest an interplay of polymer architecture and ON chemistry in complex stability vs. dissociation. Such differences in carrier performance based on ON chemistry have been observed by others (97). Similar to Dheur et al. (83), we found PEI 25K ineffective for PS ONs, but in addition, we find MWs higher than 25K (such as 70K and 600K) to be efficient in delivering PS ONs.

Apart from identifying higher PEI MWs as effective carriers for PS ONs, our results more significantly highlight the importance of the strength of the electrostatic interactions between the PEI and ONs, which ultimately dominates the rate and extent of DNA release. Both the PEI architecture and ON chemistry play a role in these interactions. The degree of protonation and the flexibility of the polymer chains are speculated to be significant. For example, fractured dendrimers that have more flexible chains are better at delivering plasmid DNA as compared to intact dendrimers (123). In our system, higher MW PEI probably possesses more flexible chains, which are able to interact with the heparin (in our non-cellular assay) and with unspecified species in cells, leading to release of ONs. The role of the ON backbone is somewhat less clear. Both ON chemistries are known to have similar charge densities due to the phosphate groups; however, phosphorothioates are known to be more hydrophobic than phosphodiesteres. The PO and PS backbones differ only by a single atom: the non-bridging oxygen is replaced by sulfur in the PS backbone. Compared to oxygen, the sulfur atom has less electronegativity. Studies report that the lower charge density of the sulfur atom increases its polarizability, strengthening the interaction with lower charge density groups in proteins (124). This was reflected in our PEI-ON binding assay, in which PS ONs were found to bind to even the lowest MW of PEI (1.2K). In contrast, 1.2K PEI and PO ONs

did not bind even at very high charge ratios. Furthermore, PEI-PS ONs displayed higher strength of interactions in the heparin competition assay. The manifestation of these molecular interactions on the cellular processing of the vectors is indeed quite dramatic, in that some complexes are apparently so tightly bound that they are incapable of releasing the ONs. As these interactions can be modulated by appropriate modifications to carrier and ON properties, they present a design opportunity for producing an effective antisense response.

We also observed distinctly different antisense dynamics dependent on ON chemistry. The overall antisense dynamics consists of two phases: (1) the initial onset of gene inhibition leading to maximum down-regulation and (2) the duration for which the antisense effects last. The latter can be easily explained based on the known differences in the resistance of PO and PS ONs to nucleases. The rapid disappearance of PO effects is consistent with the susceptibility of PO ONs to intracellular nucleases. PS ONs are known to be more nuclease resistant and to survive in the cell for longer (125), leading to sustained antisense effects, which lasted for up to 72 hours in our studies.

Based on our previous detailed kinetic modeling (104), we would expect, for equivalent delivery characteristics, substantially less silencing of gene expression for PO vs. PS ONs based on the higher nuclease degradation rate of the former. The fact that we observed significant, albeit short-lived, silencing with some PO ONs suggests that they are being delivered to the cytoplasm at a faster rate than their PS counterparts. The dynamics of intracellular release and gene silencing support this view. For PO ONs, the onset of gene inhibition was more rapid with maximum inhibition observed at 8 h (Figure 3.4a). For PS ONs, the onset was somewhat slower, and antisense activity was greatest between 8 to 24

hours from when cells were first exposed to PEI/ON complexes (Figure 3.4b). A more rapid intracellular release was also observed with the PO ONs (Figure 3.6), although the intracellular release measurements should be considered under the caveat that the measured intracellular fluorescence may include contributions from partially degraded ONs and free fluorescent tag in addition to delivered, fully intact ON. Overall, the results suggest that PEI/PS complexes take longer to release ONs. Our in vitro heparin competition assay results highlight these differences in strengths between PEI and the ONs of PO and PS chemistries (Figure 3.3). These results suggest the possibility that a mixture of PO & PS chemistries would possibly demonstrate both early and sustained antisense activity (126). We are currently testing this hypothesis by using PO backbones with varying degree of PS substitution.

Because of the rapidly changing levels of intracellular Cy5-ON fluorescence and d1EGFP fluorescence at early times and the discrete time points at which fluorescence is measured, it can be difficult to discern the differences in dynamics among some of the samples. Our mathematical model of the overall antisense process provides a useful framework for interpreting these measurements. By fitting experimental results to a relatively simple function, we were able to simulate the intracellular ON levels and calculate intracellular ON release rates from various PEI/ON complexes. The release rates account quantitatively for the variation in activity as a function of PEI MW and also demonstrate a markedly increased release rate for PO vs. PS ONs (Table 3.1). To capture the antisense dynamics, we simplified the overall antisense process by incorporating only critical features such as equilibrium ON-mRNA hybridization. The fact that, with the parameters calculated from the intracellular ON function and a single globally optimized

parameter (ON-mRNA binding constant), we can fit all of the activity data with fidelity of the trends, is a further indication that intracellular release governs the activity to a considerable extent. Mechanistically this implies that downstream barriers such as trafficking, nucleo-cytoplasmic shuttling, association with proteins, and binding to non-target mRNA do not seem to be as significant in governing the dynamics and MW effects, though they could still be important in a manner that is not dependent on PEI MW. A similar approach has been used to identify rate-limiting steps in siRNA gene silencing in vitro and in vivo (127).

Overall, the results presented here have important implications for the rational design of polymeric carriers and ON backbones used for antisense applications. We have demonstrated that the final antisense activity observed is determined not solely by either carrier or ON chemistry, but rather by the interplay of both factors. While the extent of down-regulation was determined primarily by the polymer MW, the dynamics were determined chiefly by the ON chemistry. Of particular importance is the strength of interaction between the carrier and the ON, which determines the rate at which the ONs are released intracellularly. From a practical standpoint, our results identify PEI MWs that are effective for delivering ONs of PO and PS chemistries. This approach should be useful in predicting and interpreting results for ONs of other chemistries as well, though it will be interesting to see to what extent the observed trends and correlations hold in other cell types. While PEI MW 25K is generally considered the golden standard for plasmid DNA delivery, this is not true for the delivery of ONs. More strikingly, we find that the performance of a particular PEI MW is determined by the chemistry of the ON it is used to deliver. For example, PEI 25K was most effective in delivering PO ONs, but

no PS ONs could be delivered with the same carrier. Modifications of polymers with targeting molecules such as ligands or PEG could affect the interactions with the ONs and hence influence the overall ON release dynamics. Thus, one should be able to control the onset and duration of antisense activity via biophysically guided selection of ONs and carriers.

Appendix

Details of and solutions to the mathematical model

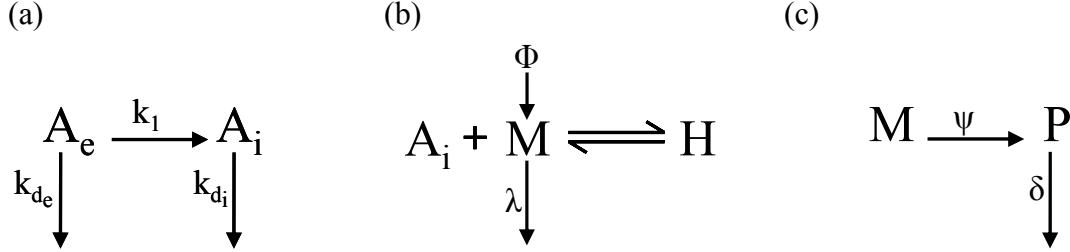


Figure A1. Schematic representing processes taken into consideration for modeling (a) intracellular antisense ON levels, A_i , (b) mRNA levels, M , and (c) protein levels, P

Modeling of intracellular ON levels

Transfer of ONs from outside the cell (A_e) to the intracellular space (A_i) is described as a single process, represented by the first order kinetic rate constant k_1 . For the sake of simplicity, all intermediate steps such as cellular uptake, endosomal escape, and release from PEI/ON complexes are lumped into this single process. Extracellular and intracellular ONs are assumed to each degrade by a first order process represented by the kinetic rate constants, k_{de} and k_{di} respectively.

The differential equations describing the mass balances of extracellular and intracellular ONs are as follows:

$$\frac{dA_e}{dt} = -(k_{de} + k_1)A_e \quad (A1)$$

$$\frac{dA_i}{dt} = k_1A_e - k_{di}A_i \quad (A2)$$

Solving these differential equations subject to the initial conditions $A_e(0) = A_{e0}$ and $A_i(0) = 0$, we obtain

$$A_i = \gamma(e^{-\alpha t} - e^{-\beta t}) \quad (A3)$$

where

$$\alpha = k_{de} + k_1, \beta = k_{di}, \gamma = \frac{k_1 A_{e0}}{\beta - \alpha} \quad (A4)$$

The combination of parameters $\gamma(\beta - \alpha) = k_1 A_{e0}$ therefore represents the maximum rate of ONs released intracellularly. We fit our experimental data to equation (A3) using the *fsolve* function in MATLAB, and thus obtain best-fit estimates for α , β and γ for each combination of PEI MW and ON chemistry used.

Modeling of antisense activity

Antisense ONs released from PEI/ON complexes intracellularly, (A_i), are then capable of binding to the mRNA (M) to elicit an antisense response. We neglect all other events

such as non-target interactions or protein binding. Further, we assume the ON-mRNA hybridization to be in rapid equilibrium, denoted by the equilibrium constant K . The total mRNA (M_T) from the target gene can therefore be present in the unbound form (M) or hybridized form (H). The constant Φ represents the rate of synthesis of mRNA, while the degradation of mRNA is described by a first order kinetic constant, λ . We assume that only unbound mRNA can be degraded. Similarly the synthesis and degradation of the protein (P) are represented by the first order kinetic rate constants ψ and δ respectively.

The differential equations describing the mRNA and protein levels are:

$$\frac{dM_T}{dt} = \Phi - \lambda M \quad (\text{A5})$$

$$\frac{dP}{dt} = \psi M - \delta P \quad (\text{A6})$$

The mass balance on the mRNA is:

$$M_T = M + H \quad (\text{A7})$$

Definition of the equilibrium constant K gives

$$K = \frac{H}{MA_i} \quad (\text{A8})$$

Using (A7) and (A8), we obtain an expression for the fraction of unbound mRNA capable of translation into protein as,

$$\frac{M}{M_T} = \frac{1}{1 + KA_i} \quad (\text{A9})$$

Solving equations (A5) and (A6) under steady-state conditions, we obtain the steady-state mRNA and protein levels:

$$M_{ss} = \frac{\Phi}{\lambda}, P_{ss} = \frac{\psi M_{ss}}{\delta} \quad (\text{A10})$$

Using these steady-state values, we can non-dimensionalize the equations as follows:

$$\mu = \frac{M_T}{M_{ss}}, \pi = \frac{P}{P_{ss}} \quad (\text{A11})$$

Combining with equation (A9), equations (A5) and (A6) can be represented in dimensionless form as:

$$\frac{d\mu}{dt} = \lambda \left(1 - \frac{\mu}{1 + KA_i(t)} \right) \quad (\text{A12})$$

$$\frac{d\pi}{dt} = \delta \left(\frac{\mu}{1 + KA_i(t)} - \pi \right) \quad (\text{A13})$$

Incorporating equation (A3) into equations (A12) and (A13) reduces these equations to a three parameter form. Estimates for λ (0.069 h^{-1}) and δ (0.69 h^{-1}), which denote the degradation rates of d1EGFP mRNA and protein respectively, were obtained from the literature. Our strategy for obtaining the dynamics of antisense activity was as follows:

using a guess value for K , we simulated the dynamics of μ and π by solving the differential equations (A12) and (A13) simultaneously using an ODE solver (*ode15s*) in MATLAB. By comparing these simulated dynamics to the experimental results, we computed the error at each data point. The overall error was calculated as the SSE (sum of squares of error) over all experimental time-points for all PEI MW for each of the ON chemistries separately. A new K value was guessed, and the procedure was repeated until a minimum was achieved for the global error.

Chapter 4: Design of mixed backbone oligonucleotides for effective polymer mediated cellular delivery of antisense oligonucleotides

4.1 Abstract

Polyethyleneimine (PEI) is a cationic polymer that has been widely utilized as a DNA delivery carrier for gene and oligonucleotide based therapies. In our previous work, we found that while lower PEI MWs (10K, 25K) are ineffective in delivering phosphorothioate (PS) oligonucleotides, complexes of higher MW PEI (70K, 600K) and PS ONs were very efficient in eliciting an antisense response. Particularly, the strength of the interactions between the PEI and oligonucleotides seemed to play a critical role in the overall antisense response observed. Here, we show that it is possible to tune the effectiveness of the vector in eliciting an antisense response by varying the degree of phosphorothioate substitution in a phosphodiester oligonucleotide sequence. We designed a panel of phosphodiester sequences with increasing number of end capped phosphorothioate bonds. We studied the ability of these oligonucleotides to form complexes with a panel of molecular weights of branched PEI. Further, we evaluated their levels of intracellular delivery and elicitation of an antisense response in a stably pd1EGFP expressing CHO cell line. To provide a mechanistic understanding for our results, we draw explanations from various assays that mimic key intracellular processing steps. We measure the levels of cellular internalization and release of complexes, assess the influence of adding endocytic pH buffering reagents such as chloroquine and ammonium chloride, and determine the ability of the complexes to release DNA by

measuring the in vitro rates of dissociation of complexes in the presence of a competing anionic entity. We find that by altering the degree and pattern of phosphorothioate substitution in a phosphodiester oligonucleotide, we are able to modulate the efficiency of lower PEI MWs as oligonucleotide carriers and the dynamics of gene silencing. By correlating the PEI MW & oligonucleotide chemistry with the observed antisense effects, we are able to draw insightful structure-property relationships that will aid the rational design of oligonucleotide carriers.

4.2 Introduction

Gene silencing methods such as antisense and RNA interference have gained extensive popularity in recent times due to exponential increases in our acquisition of genome sequences coupled with rapid advances in our understanding of gene functions individually and in disease pathways. However, delivery of these silencing molecules to their target site of action in a therapeutically relevant dosage and stable form remains the key obstacle hindering their widespread usage. While viruses have evolved mechanisms to perform this task with high efficiency, synthetic DNA carriers continue to be popular alternatives to their viral counterparts due to their ease of production, tunable properties and low immunogenicity. Although a wide range of polymer and lipid based carriers of varying architectures and chemistries have been designed based on guiding biomimetic principles, their functionalities still remain orders of magnitude lower than viral carriers. Hence, there is a pressing need for the rational design of improved carriers that will aid the safe and effective delivery of these oligonucleotides.

In general, synthetic carriers comprise polymer or lipid molecules that either bind to or encapsulate the DNA material. Additional ligands and other functional entities are often incorporated into the structure to enhance the functionality of the carrier. How these various components organize themselves clearly plays a role in the observed functionality of the vector. Several studies already exist that attempt to correlate the physico-chemical properties of these carrier/DNA particles with the observed delivery efficiency. However, the ability to predict, manipulate and control the organization of several synthetic entities into a highly efficient, non-immunogenic delivery vector calls for a detailed understanding of the interactions between the various components of the vector, as well

as the interactions of the vector with cellular and subcellular entities during the process of delivering the cargo DNA.

The delivery process itself involves multiple steps such as cellular internalization, trafficking through the endocytic or other pathways, escape from the endosomes and finally release of the cargo DNA at the site of action. Studies focusing on the cellular processing of vectors have identified several rate-limiting steps that severely affect the delivery efficiency. Particularly, the ability to escape the endo-lysolytic pathway and the unpackaging of the vector have gained much attention. Mechanistic understanding of the ability of the vectors in dealing with these barriers has further aided vector design. In fact, several strategies have been developed to overcome one or more of these barriers.

One polymeric carrier that has garnered much attention due to its ability to buffer endosomal pH is polyethyleneimine (PEI). It has been widely studied in vitro and has been tested in the clinic. The molecular weight of PEI is known to affect the delivery efficiency. Higher PEI MWs are generally more efficient as DNA carriers; however, they display excessive toxicity. Lower PEI MWs are less toxic, but are not as efficient. Although PEI has been studied widely for delivery of plasmid DNA, fewer studies focus specifically on its interactions with ssDNA for antisense use. The differences in the size and structure of the DNA greatly influence these interactions, and even 25 kDa PEI, which is considered the golden standard for plasmid DNA delivery, does not work efficiently for delivering phosphorothioate ONs.

Previously, we found that a strong interplay of PEI MW and ON chemistry governs the extent and dynamics of antisense silencing. The strength of PEI-ON

interactions was found to be particularly important, as those PEI-ON combinations that did not work effectively also did not release ON intracellularly. In the current work, we utilize the chemistry of the ONs as a means to influence the strength of interactions between PEI and ONs, and hence control the antisense response. This approach was adopted towards two outcomes. First, the ability to utilize low molecular weight to deliver ONs effectively is attractive. Second, analyzing the interactions of several ONs varying in the number of PS bonds with several PEI MWs will enhance our understanding of the factors influencing the delivery efficiency. For these purposes, we designed a panel of phosphodiester sequences with increasing number of end capped phosphorothioate bonds. We tested the effectiveness of complexes prepared between these ONs and a series of PEI MWs in delivering ONs to cells and eliciting an antisense response. We demonstrate that by altering the degree of phosphorothioate substitution in a phosphodiester ON, we can improve dramatically the efficiency of lower PEI MWs as ON carriers. Further, we are able to draw insightful structure-property relationships that will aid the rational design of ON carriers by correlating the PEI MW & ON chemistry with the observed antisense effects.

4.3 Material and methods

4.3.1 Materials

A 20-mer anti-GFP sequence identified previously as an effective inhibitor of pd1EGFP expression (5'-TTG TGG CCG TTT ACG TCG CC -3') and a scrambled control (5'- TTG CTT GTA CCG TGC GTG CC -3') were utilized in the study. A panel of phosphodiester sequences with increasing number of end capped phosphorothioate bonds (shown in Table 4.I) and fluorescently tagged (5' Cy5 end modified) forms of these sequences were obtained from Integrated DNA Technologies (Coralville, IA). Stock solutions were prepared by reconstituting each pellet in water to a final concentration of 100 μ M. Branched polyethylenimine (PEI) of molecular weights 1.2 kDa (Cat# 6088), 10 kDa (Cat# 19850) and 70 kDa (Cat# 00618) was purchased from Polysciences, Inc. (Warrington, PA). Additionally, PEI of molecular weight 25 kDa (Cat# 408727) and 600-1000 kDa (Cat# 3880) was purchased from Sigma. Stock solutions at a concentration of 10 residue mM (0.43 mg/mL) were prepared in water and the pH adjusted to 7.0 using HCl. OliGreen, a fluorescent dye that binds strongly to single-stranded DNA, was obtained from Molecular Probes (Eugene, OR). Heparin sodium salt was obtained from Sigma (Cat# H4784). Unless stated otherwise, all cell culture products were obtained from Invitrogen (Carlsbad, CA).

4.3.2 PEI/ON complex formation

PEI/ON complexes were prepared at desired PEI/ON charge ratios by mixing equal volumes of PEI (of varying concentrations) and ONs in PBS. The samples were vortexed briefly, and the solutions were then incubated at room temperature for 10-15 min to

ensure complex formation. Experimental evidence (stabilization of fluorescence corresponding to free ON) confirmed that this time was sufficient for complex formation. The PEI/ON charge ratios were calculated on a molar basis. The complexes were prepared at a final ON concentration of 10 µg/mL (approximately 1.64 µM) unless stated otherwise.

Name	Sequence ("*" denotes phosphorothioate bond)
MOD2	5'-T*T*G T G G C C G T T T A C G T C G*C*C-3'
MOD4	5'-T*T*G*T*G G C C G T T T A C G T*C*G*C*C-3'
MOD5	5'-T*T*G*T*G*G C C G T T T A C G*T*C*G*C*C-3'
MODALT	5'-T*T G*T G*G C*C G*T T*T A*C G*T C*G C*C-3'

Table 4.1 Backbone chemistry of sequences utilized in the study

(* denotes phosphorothioate bonds)

4.3.3 Detection of free ON using OliGreen

Complexes between PEI and ONs were prepared at various charge ratios as described above. One hundred microliters of each complex solution was transferred to a 96 well (black-walled, clear-bottom, nonadsorbing) plate (Corning, NY, USA). A total of 100 µL of diluted OliGreen reagent (1:100 in TE buffer at pH 8) was then added to all samples for free ON detection. Fluorescence measurements were made after a 3-5 min incubation using a Cytofluor (Applied Biosystems, CA, USA), at excitation and emission wavelengths of 485 and 520 nm, respectively, and a voltage gain of 55. All

measurements were corrected for background fluorescence from a solution containing TE buffer and diluted OliGreen reagent.

4.3.4 Cell culture

Chinese hamster ovary (CHO-K1) cells (ATCC, Manassas, VA) were maintained in F-12K medium (Kaighn's modification of Ham's F-12; ATCC, Manassas, VA) supplemented with 10% fetal bovine serum and penicillin-streptomycin solution. CHO-d1EGFP cells (CHO-K1 cells stably expressing a destabilized green fluorescent protein transgene) were previously produced by transfecting CHO-K1 cells with the 4.9 kb d1EGFP-N1 plasmid (BD Biosciences Clontech, Palo Alto, CA, USA), and maintained under constant selective pressure by G418 (500 $\mu\text{g/ml}$). All cell lines were cultivated in a humidified atmosphere containing 5% CO_2 at 37°C.

4.3.5 Antisense experiments

CHO or CHO-d1EGFP cells were plated at a density of 1.5×10^5 cells/well in 12 well plates 18 h prior to transfection. Prior to introduction of ONs, cell culture medium in each well was replaced with 800 μL of OptiMEM^(R) (reduced serum medium). Next, 200 μL of PEI/ON complex solution prepared in PBS was added to each well so the final ON concentration in each well (1 mL) was 300 nM. To measure the intracellular levels of ONs released from the complexes, cells were treated with complexes prepared with Cy5-ONs. At the end of the incubation period of 4 h, the transfection mixture was replaced with serum containing growth medium and maintained under normal growth conditions (5% CO_2 , humidified atmosphere, 37°C). Medium in the wells was replaced with fresh serum containing medium every 24 h. At various times, cells were assayed for antisense

activity (GFP fluorescence) and/or ON levels (Cy5-ON fluorescence) by flow cytometry. As controls, cells were also exposed to only PEI (in the absence of ONs), only ONs (in the absence of PEI) as well as complexes prepared with scrambled ON sequences to check for sequence specificity. All times indicated are relative to when complexes were first introduced to the cells, which represents $t=0$. For investigation of the effects of chloroquine and ammonium chloride, cells were treated with the desired PEI/ON complexes for 4 h in the presence of 100 μ M chloroquine or 10 mM ammonium chloride in OptiMEM and assayed at the desired time point.

4.3.6 Flow cytometry

Replicate wells of cells were washed in PBS, detached with trypsin-EDTA, washed with serum-containing medium, pelleted by centrifugation for 5 min at 200 g, washed with PBS, resuspended in 500 μ L of PBS and maintained on ice before being subjected to flow cytometry analysis. 10,000 cells were analyzed on a FACSCalibur two-laser, four-color flow cytometer (BD Biosciences) for GFP fluorescence in FL1 (green) channel and Cy5-ON fluorescence in FL4 (far-red) channel. CellQuest software was used to acquire and analyze the results. Viable cells were gated according to their typical forward/side scatter characteristics. The flow cytometer was calibrated with fluorescent beads (CaliBRITE Beads, BD Biosciences) prior to each use to ensure comparable readings over the period of the study.

4.3.7 PEI/ON dissociation studies

PEI/ON complexes (charge ratio 10:1, final ON concentration of 5 μ g/mL \sim 0.8 μ M, volume 50 μ L) were prepared as described previously and transferred to a 96 well (black

walled, clear bottom, nonadsorbing) plate. One hundred microliters of diluted OliGreen reagent were added to each well and mixed manually with a multichannel pipet. Fifty microliters of heparin solution (at various concentrations prepared in TE buffer at pH 8) were then added to the wells, and the plate was maintained at 37°C. Fluorescence measurements were made at the end of one hour from the time of heparin addition using the Cytofluor plate reader. The percentage of ONs released was calculated from the fluorescence (F) values as

$$\% \text{ ODN released} = \frac{[F (\text{complex \& heparin}) - F (\text{ODN \& heparin})]}{[F (\text{complex}) - F (\text{ODN \& heparin})]} \times 100$$

In each measurement, we corrected for changes in background fluorescence due to heparin addition alone. This change was found to be dependent on the heparin concentration (data not shown), and thus was measured and accounted for in each experiment.

4.3.8 Confocal microscopy

CHO-d1EGFP cells were seeded onto 8 well, cover glass chambers (Labtek Corporation) in 200 μ L of complete growth medium (containing 500 μ g/mL G418) and grown overnight. Complexes of Lipofectamine/Cy-PS ONs (weight ratio 2.5:1), 25K PEI/Cy5-PS (10:1) and 25K PEI/Cy5-PS (20:1) were prepared and introduced to the cells at 300 nM ON concentration in Opti-MEM. For testing the effects of chloroquine, the complexes were first incubated in 100 μ M chloroquine supplemented OptiMEM. After 4 h incubation, the cells were washed twice with PBS and cultured in complete growth medium for another 20 h. GFP fluorescent cells were then visualized at 63X

magnification, 488 nm excitation, and 500-555 nm emission using a Leica TCS SP2 microscope (Leica Microsystems, Inc., Exton, PA). Cy5 fluorescence was excited at 633 nm, and light emission was collected at 650-750 nm.

4.4 Results

First, we tested the ability of the various ONs to form complexes with branched PEI of molecular weights ranging from 1.2K to 600K, as a function of the PEI/ON charge ratio. We measured the amounts of free (unbound) DNA in solution using a dye, OliGreen, which fluoresces upon binding to single-stranded DNA. As shown in Figure 4.1(a), the fluorescence levels decrease with increasing PEI/ON charge ratios. At higher charge ratios, only residual amounts of free (unbound) ONs are detected in solution, indicating complex formation. All ONs displayed similar abilities in binding with PEI MW 70K (Fig 1A). Similar trends were observed for the interactions of these ONs with PEI MWs spanning the range of 10K to 600K (Data not shown). In contrast, clear differences in the ability to form complexes with PEI were evident among the various ONs at the lowest PEI MW 1.2K. At this MW, there is no significant binding between PEI and ONs with low phosphorothioate (PS) content, such as mod2 and mod4, even at the highest charge ratios (20:1). However, mod5 and modALT ONs bind more effectively with PEI, with over 60% of ONs in the complexed form.

We then tested the effectiveness of these polymers in delivering anti-d1EGFP ONs to CHO cells stably expressing the d1EGFP transgene. Cells were treated with complexes of PEI (various MWs) and ONs (all backbone chemistries) for 4 hours, and subjected to flow cytometry at each of several times over a 48 h time period. Under all conditions, more than 90% of the cells were gated as live. The fluorescence levels indicated in Figure 4.2 are normalized to the green fluorescence of time-matched, untreated CHO cells that stably express the d1EGFP transgene. We observed as much as 80% reduction in GFP levels 8 hours from when cells are treated with PEI/ON complexes

under the best conditions. The time scale over which antisense effects were observed was similar for mod2, mod4 and mod5 ONs delivered using PEI, with GFP levels returning to base levels by 48 hours from administration. In comparison, antisense effects were sustained for a longer duration for modALT ONs delivered with PEI, with as much as 40% of GFP fluorescence remaining inhibited at 48 h. Whereas ON chemistry determined the dynamics of antisense effects, the molecular weight of PEI used to deliver the ONs influenced the extent of down-regulation observed over the same time scale. This is similar to what we observed in our previous work where various PEI MWs were used to deliver pure PO and PS ONs. When PEI MWs greater than 10K such as 25K, 70K or 600K were utilized as delivery carriers, the highest levels of down-regulation (up to 80%) were observed irrespective of the ON chemistry. In contrast, when ONs were delivered with PEI 10K, the GFP levels were not inhibited to a great extent. A maximum of 60% down-regulation was observed for mod2 ONs, while even lower levels of 20-30% inhibition were recorded for mod4, mod5, mod ALT ONs delivered with PEI 10K.

In order to understand the overall dependence of antisense response on PEI MW and ON chemistry, we plotted the maximum down-regulation recorded for each of the PEI/ON combinations against both PEI MW and ON chemistry (Figure 4.3). For each of the ON chemistries other than PO we observed a threshold PEI MW beyond which maximum down-regulation was recorded. ONs delivered with PEI MWs 1.2K or 10K elicited very little antisense response, except for pure PO ON with 10K PEI. However, when PEI MW higher than 10K (25K, 70K or 600K Da) were utilized as carriers, a dramatic increase in activity (maximum down-regulation) was observed. For PS ONs, this threshold was shifted to still higher PEI MW. PEI MWs 1.2K, 10K and 25K did not

elicit a significant antisense down-regulation, while MWs greater than 25K imparted maximum activity. Such cooperative dependence on PEI MW was observed for ONs with any extent of PS substitution. For PO ONs, as noted by us previously, an optimum performance was observed at intermediate PEI MW, while higher or lower PEI MW did not perform as well. For each of the PEI MWs greater than 25K, maximum down-regulation was observed irrespective of the ON chemistry. 25K PEI did not deliver any PS ONs leading to no antisense response. However, its functionality as ON carrier soared to maximum with a decrease in the PS substitution in the chemistry of the ON to be delivered. For lower PEI MW such as 10K, we observed similar increase in delivery potential with decrease in PS substitution in the ON chemistry. However, here the decrease in GFP levels was more gradual rather than a threshold as observed by varying the PEI MW. Similar trends were observed for the lower PEI MW 1.2K which displayed the lowest levels of GFP down-regulation for mod4, mod5, modALT and PS ONs. Complexes of PEI 1.2K/PO and PEI 1.2K/mod2 were excluded from the analysis due to the very poor complex formation observed at the conditions studied.

We sought to understand the nature of the observed dependence of antisense down-regulation on PEI MW and ON chemistry. Since antisense down-regulation levels correspond to levels of ONs delivered intracellularly, we wanted to determine if certain combinations of PEI/ON complexes were limited in their ability to release ONs due to enhanced PEI-ON binding. Hence, we probed the strength of PEI/ON interactions by studying the dissociation behavior of these complexes upon exposure to heparin sulfate as a competitive binding agent. Complexes were prepared at a PEI/ON charge ratio of 10:1, after which heparin was added to dissociate the complexes, releasing ONs into solution.

OliGreen was used to measure the amount of ONs released at the end of one hour of exposure to heparin. For all PEI/ON complexes, almost 100% of the ONs were released (Figure 4.4), indicating that these complexes were not limited in their ability to release ONs. There was no significant effect of the PEI molecular weight on the release of the ONs from PEI.

Since treatment with heparin may not be completely representative of the actual cellular events leading to the release of ONs from PEI-ON complexes intracellularly, we performed a cellular assay to obtain further insight into the observed behavior. We hypothesized that by perturbing the intracellular release process of ONs, it may be possible to get a better understanding of the factors involved in the poor performance of certain PEI/ON combinations. We chose 3 means to do this - (1) increase the PEI/ON charge ratio from 10: 1 to 20:1 (2) treatment with 100 μ M chloroquine (3) treatment with 10 mM ammonium chloride. We selected those combinations of PEI MWs and ON chemistries that performed poorly in eliciting an antisense response (mainly all 10K/ON combinations as well as 25K/PS complexes) and recorded the antisense performance on perturbation of intracellular release by the treatment mentioned above. Cells were treated with various PEI/ON complexes in the presence of 100 μ M chloroquine or 10 mM ammonium chloride for 4 hours, after which the transfection medium was replaced with regular growth medium. At either 8 hours (for 10K/ON complexes) or 24 hours (for 25K/ON complexes) after the introduction of the antisense treatment, cells were analyzed for GFP fluorescence (as a measure of antisense effects) and Cy-5 fluorescence (as an estimate of the levels of ONs released intracellularly).

When cells were exposed to PEI 10K/ON complexes at a higher charge ratio of 20:1, GFP down-regulation increased by around 20% in comparison to treatments with complexes at a 10:1 charge ratio (Figure 4.5(a)). Treatment of cells with 10:1 or 20:1 10K/ON complexes in the presence of chloroquine improved antisense performance by around 20 % compared to the treatments with the corresponding complexes in the absence of chloroquine. These effects were generally additive, i. e., the antisense response could be improved by up to 40% by treating cells with 20:1 charge ratio complexes in the presence of chloroquine when comparing the levels to the original treatment of 10:1 10K/ON complexes in the absence of chloroquine. In contrast, when cells were exposed to complexes at charge ratios of 10:1 or 20:1 in the presence of 10mM ammonium chloride, the enhanced antisense response was lost. There was little or no change in GFP down-regulation levels in comparison to treatments with the corresponding charge ratio complexes in the absence of ammonium chloride. The trends were similar for all ON chemistries delivered using 10K PEI.

We performed similar analyses on complexes of 25K PEI with PS ONs. Complexes of 25K PEI with all other ON chemistries were excluded from the study as they all (except PS ONs) elicited maximum GFP down-regulation levels. At this PEI MW, we found dramatic increases in antisense response upon treatments with higher PEI:ON charge ratios and/or chloroquine. As noted previously by us and others, 25K/PS ONs (10:1 charge ratio) do not elicit any antisense response. However, when a higher PEI:ON charge ratio such as 20:1 is utilized to deliver PS ONs, GFP levels decrease by around 40 %. When complexes are introduced in the presence of chloroquine, a further 20% decrease in GFP fluorescence is observed in comparison to the corresponding

treatments in the absence of chloroquine. Thus, when higher charge ratio PEI:ON complexes are employed in the presence of chloroquine, the PEI/ON combination that was previously unable to elicit an antisense response, now exhibits around 60-70% GFP down-regulation. However, the effects were lost once again when the complexes were introduced in the presence of ammonium chloride. This was similar to what we observed when cells were exposed to complexes of 10K PEI in the presence of ammonium chloride.

In order to ensure that the increase in antisense down-regulation observed upon these treatments was due to enhanced intracellular ON release, we additionally measured the levels of Cy5 fluorescence. As mentioned above, complexes were prepared with PEI and Cy tagged ONs and then introduced on the cells. These complexes do not fluoresce (data not shown) when the ON is bound to the PEI. Hence, increase in the Cy5 levels corresponds to ONs that have been released intracellularly. When cells were treated with complexes in the presence of chloroquine, significant increases in Cy5 fluorescence levels were observed (Figure 4.5(b)). Similar increases were observed when higher charge ratio PEI:ON complexes were utilized in the study. However, little or no increases were recorded when complexes were introduced onto the cells in the presence of ammonium chloride. These trends with respect to charge ratio and treatments in the presence of chloroquine or ammonium chloride were similar to those observed in the GFP levels.

In order to provide more direct evidence for the increased intracellular release, we visualized the cells using a confocal microscope. Cells were treated with complexes prepared with Cy5 tagged ONs and the appropriate carrier for 4 hours and visualized 24h

after the introduction of the complexes. In comparison to untreated cells (Figure 4.6(a)) and cells treated with lipofectamine/CyPS ONs (Figure 4.6(b)), we observed very little Cy5 fluorescence in punctate form in cells treated with complexes made of 25K PEI and Cy-PS ONs (Figure 4.6(c)). When the complexes were introduced in the presence of chloroquine, there was some increase in the fluorescence (Figure 4.6(d)), but the fluorescence was still observed in the punctate manner within the cells. In striking contrast, visibly significant increases in Cy5 levels and enhanced GFP silencing are observed when cells are treated with 25K PEI complexes at a higher charge ratio of 20:1 in the presence of chloroquine (Figure 4.6(e)). Furthermore, the Cy5 fluorescence distribution in these cells is considerably more uniform, encompassing the cytoplasm and the nucleus similar to that seen for ONs delivered using Lipofectamine (Figure 4.6(b)), indicative of release of the Cy5-ON from the PEI and the endosomes. These results substantiate the trends observed in the previous flow cytometric analyses and thus provide a mechanistic basis for the observed trends in the presence of chloroquine and higher PEI/ON charge ratios.

4.5 Discussion

Cellular delivery of ONs remains a major obstacle in the widespread utilization of ON based technologies. Hence, there is a pressing need for the rational design of carriers for effective ON delivery. Studies on the cellular processing of carrier-ON complexes have greatly increased our understanding of the intracellular barriers to efficient ON delivery. Chief among them is the ability to escape the endocytic pathway. Carriers such as PEI that provide a means to buffer the endosomal pH and hence improve ON delivery have garnered great attention. Several carriers that mimic such pH buffering capabilities have been designed to provide non-toxic, more efficient alternatives to delivery carriers such as PEI. However, in many cases, little or no ON delivery was observed despite the endosomal buffering capabilities, and it was found that carrier-ON complexes are unable to dissociate intracellularly. Increasingly it is becoming clear that engineering pH buffering capacities might be required but is not the only necessary design criterion.

In our previous work, when we utilized PEI to deliver PS ONs, we found that higher PEI MW are very efficient in delivering ONs, but complexes of lower PEI-ON complexes are incapable of eliciting an antisense response. The strength of the PEI-ON interactions was found to be particularly important. We attempted to solve this problem in the current work by altering the strength of PEI-ON interactions. To achieve this, we modified the chemistry of the ONs. By altering the extent of PS substitution in a PO backbone, we showed that it was indeed possible to induce release of ONs from the PEI-ON complexes. We further extended this analysis to a series of ONs with increasing degrees of PS substitution in the backbone chemistry. By studying a panel of complexes made with various PEI MWs and various ON chemistries, we obtained interesting

structure-property relationships. Mainly we noted that the ability to modulate the release of ONs from the complexes was dependent on the PEI MW. While we are able to improve delivery using 25K PEI, the improvement in function with the various ONs was limited when 10K PEI was used, and almost unaffected when 1.2K PEI was utilized. These results therefore point to an interesting interplay of polymer-ON interactions on antisense effects.

To alter the extent of PS substitution in the PO backbone, we designed PS end-capped sequences, and progressively increased the extent of end capped PS bonds. While mod2, mod4 and mod5 have 2, 4 and 5 PS bonds at each end (for totals of 4, 8 and 10, respectively), modALT has 10 PS bonds that alternate through the length of the sequence. End-capped chemistries are often used in antisense studies as alternatives to pure PS sequences for several reasons. They enable retention of the nuclease resistant properties of PS ONs while also reducing the non-specific effects that are detrimental to obtaining an antisense response. In fact, when we delivered these ONs with Lipofectamine2000, we noticed subsequent increase in the durations for which the effects lasted. Antisense effects were maintained for the longest durations for modALT in comparison to other ONs possibly due to the presence of PS bonds at both the exterior and interior of the sequence leading to protection from both exo and endonucleases. When modALT ONs were delivered with PEIs, the duration of action was also extended although not quite as dramatically as with Lipofectamine2000. This is possibly due to the incomplete release of ONs from PEI-ON complexes.

The variations in the antisense down-regulation levels for the various combinations of PEI MWs and ON chemistries were due to differences in the amounts of

ONs delivered, as the extent of down-regulation was directly correlated with the levels of ONs delivered. Competitive dissociation of complexes is often used as an indicator of the nature of interactions between polymers and ONs. In order to explain the observed trends we measured the strength of interactions by competition with an anionic molecule heparin. In our previous work, heparin dissociation provided distinct molecular weight based effects for the strength of PEI-PS ON interactions. In contrast, for this series of mixed backbone ONs, we did not find a clear dependence of the PEI MW on the amounts of ONs released. In fact, almost all ONs were released from the complexes at the heparin concentration used. When PEI-ON complexes were treated with heparin at lower concentrations (data not shown), we recorded lower levels of released ONs in line with a heparin dose response. Nevertheless, no trends were observed with respect to the PEI MW. This suggests either that the heparin competitive dissociation assay may not always reflect events in the intracellular environment or that events other than vector dissociation are governing the PEI MW-ON backbone effects.

In our antisense experiments, we noticed that PEI:ON complexes at a higher charge ratio of 20:1 were much more efficient in eliciting an antisense response than complexes at a 10:1 charge ratio. While we were able to determine that the higher charge ratio complexes delivered more ONs, we were unable to determine the reasons for this. Since PEI functions in a concentration dependent manner, it is not surprising that additional PEI aids the release of ONs. However, determination of the nature of this excess PEI would be highly essential to resolve what role the excess polymer plays. We attempted to separate the excess polymer by centrifugal filtration. Interestingly there are two reports in literature that describe purification of PEI-plasmid DNA complexes by

different methods in order to determine the role of free PEI. In both studies, 50-60% of PEI was found to be free, and removal of this excess PEI reduced the overall toxicity associated with the use of PEI-plasmid DNA complexes. However, when we attempted to filter PEI-ON complexes, under all conditions that we tested, complexes were found to fall apart, releasing all ONs. This might be indicative of the fact that polymer-ON complex formation is an equilibrium process. Additionally we performed cellular experiments where the excess polymer was added to the cells separately after complexes at 10:1 charge ratio were introduced (data not shown). Under these conditions, we observed very high levels of toxicity not detected previously. This suggests that the excess polymer at a 20:1 charge ratio is associated to the ONs to some degree and is not completely free in solution. Further experimentation involving measurement of the rates of cellular internalization of complexes may provide more insights into the effects observed.

Additional testing in the presence of chloroquine and ammonium chloride seemed to suggest that indeed PEI-ON complexes are limited in their ability to dissociate and hence unable to release ONs. Chloroquine is often used in gene transfer studies as an external endosome disrupting agent. In fact, studies using chloroquine generally report improvement in DNA transfer when non-pH buffering polymers are used while little or no improvement is observed when use in conjunction with polymers such as PEI. Its exact mechanism of action is unknown, although recent studies show that it plays a role in the internalization of complexes, the escape of the endosome as well as dissociation leading to release DNA. In fact, in our experiments when cells were treated with PEI-ON complexes in the presence of chloroquine and ammonium chloride, the increase in

antisense effects was observed only with chloroquine, while treatment with ammonium chloride, which only provides a weak buffering effect, did not seem to improve the levels of ON delivery. This clearly suggests that reasons other than the ability to escape the endocytic pathway may be responsible for the intracellular delivery patterns observed as a function of PEI MW and ON backbone composition.

In summary, by varying the extent of PS substitution in the backbone chemistry we have shown that it is possible to alter the strength of interactions between PEI and ONs, and hence improve delivery efficiency. When several ONs were tested in conjunction with various PEI MWs, we found that the ability to improve the delivery by affecting the PEI-ON interactions was dependent on the PEI MW. This suggests that the nature of PEI-ON interactions is crucial to the intracellular processing of the complexes. Polymers with longer and more flexible chains are probably better at interacting with other species and leading to enhanced release. Thus, taken together, our work identifies the interplay between PEI MW and ON chemistry on the nature of antisense effects. Additionally it provides a mechanistic understanding for the observed results. Hence, these results will aid the rational design of carriers for improved ON delivery.

Chapter 5: Summary & Future Directions

5.1 Summary

Antisense technology employs short, single-stranded oligonucleotides (ONs), typically 12-25 bases long, to inhibit gene expression by binding to complementary mRNA via Watson-Crick base pairing. Over the last decade, antisense approaches have been developed for therapeutic purposes as well as for biotechnological applications. Additionally, the excitement generated by the advent of siRNA has rejuvenated interest in gene silencing technologies in general. However, the widespread use of antisense ONs is still hindered by several obstacles. Prominent among them is the ineffective cellular delivery of ONs, which remains a major hurdle in the utilization of ON based technologies.

The reduced cellular entry and rapid degradation of these molecules in the presence of cellular nucleases calls for the utilization of carrier molecules. Various types of carriers, including polymers, lipids and peptides of diverse chemistries, have been tested for their effectiveness as DNA delivery vectors. However, substantial optimization is generally required to make these carriers work for the particular application at hand. The large variations in vector effectiveness among cell types, as well as the relatively high cytotoxicity of the currently available carriers, continue to fuel the demand for more rationally designed carrier systems. Nevertheless, progress in vector development for ON delivery often borrows principles from those developed for the delivery of plasmid DNA for gene therapy applications. Improvements in the design of new carriers focus mainly on the polymer characteristics, attempting to improve the delivery effectiveness of the

vector by modifying various polymer features such as backbone chemistry and side-chain length or, increasingly, by incorporating additional functionalities into the vector.

To improve further the design of DNA carriers, extensive research is being conducted to identify cellular barriers to carrier mediated delivery of ONs. Efforts are directed towards determining structure-property relationships that relate carrier properties to antisense effectiveness. However, it remains somewhat unclear what factors ultimately dictate the effects observed. Of particular importance is the fact that much of the design principles developed for plasmid DNA carriers are often used interchangeably for antisense ONs or siRNA. Although this may work in certain cases, the small size of ONs (10-22 bases) and variations in their backbone chemistry and structure endow them with unique properties that alter their interactions with carriers in comparison to plasmid DNA, and hence influence the design criteria for oligonucleotide carriers. There are several examples in literature that point to such differences in terms of ON structure, ON chemistry, and sequence composition. Hence, there is a need for systematic investigations of the interactions of carriers with ONs, both at the molecular level as well as at the cellular level, to acquire a mechanistic understanding of their cellular processing.

This thesis deals with various aspects of polymer mediated cellular delivery of oligonucleotides for antisense therapy. Specifically, the work highlights the importance of oligonucleotide properties such as structure and backbone chemistry on the nature of interactions with the polymeric carrier, and on the subsequent cellular processing of polymer-oligonucleotide particles to ultimately achieve an antisense response.

In Chapter 2, we examined the effect of ON structure on the interactions between cationic polymers and ONs. Unstructured and hairpin structured ONs were used to form complexes with the model polymer, poly-L-lysine, and the characteristics of these polymer-ON interactions were subsequently examined. The strength of pLL-ON interactions was tested by challenge with anionic molecule heparin, which induced complex disruption. Both the kinetics and heparin dose response of ON release were determined. We found that hairpin structured ONs formed complexes with pLL more readily as compared to unstructured ONs. While the tight binding of hairpins with pLL inhibited their release out of the complexes, unstructured ONs were released from the complex more easily. Our results therefore highlight the role of ON structure on the association-dissociation behavior of polymer-ON complexes. The finding implicates secondary structure as a relevant design parameter for antisense ONs and stresses the need for a comprehensive evaluation of ON-polymer structure-activity effects.

In Chapter 3, we focus our attention on the cellular delivery of antisense ONs using another cationic polymer, polyethyleneimine (PEI). The goal of the study was to understand the role of the vector, i.e. the properties of both the carrier and the ON, on the extent and dynamics of the antisense effect. Our rationale for doing so was two-fold. First, PEI is a well characterized carrier molecule. It has been utilized extensively for the delivery of plasmid DNA due to its high charge density and endosomolytic activity. Several reviews are available detailing the effectiveness and mechanism of action of PEI and its various modifications for the delivery of DNA to a range of cell types. There are fewer studies focusing specifically on the delivery of ONs using PEI. Second, we wished to determine the optimal PEI MW for delivery of ONs of various chemistries.

Using the d1EGFP gene as an easily quantifiable antisense target, we screened various combinations of PEI MWs (1.2K, 10K, 25K, 70K, 600K) and ON chemistries (PO and PS) for their ability to elicit an effective antisense response. Complexes were prepared between branched polyethyleneimine (PEI) of various MWs and ONs of phosphodiester and phosphorothioate chemistries. We measured their physico-chemical properties and evaluated their ability to deliver ONs to cells, leading to an antisense response. We accomplished this by measuring simultaneously the dynamics of both ON uptake and antisense inhibition using a cellular assay based on single cell fluorescence measurements. Our key finding is that the antisense activity is not determined solely by PEI MW or by ON chemistry, but rather by the interplay of both factors. While the extent of target mRNA down-regulation was determined primarily by the polymer MW, dynamics were determined principally by the ON chemistry. Of particular importance is the strength of interactions between the carrier and the ON, which determines the rate at which the ONs are delivered intracellularly. We also present a mathematical model of the antisense process to highlight the importance of ON delivery to antisense down-regulation.

When utilizing various PEI MWs to deliver PS ONs, we found that while lower PEI MWs (10K, 25K) are ineffective in delivering phosphorothioate (PS) oligonucleotides, complexes of higher MW PEI (70K, 600K) and PS ONs were very efficient in eliciting an antisense response. The strength of PEI-ON interactions was found to be particularly important, as those PEI-ON combinations that did not work effectively also did not release ON intracellularly. Hence, in Chapter 4, we utilize the chemistry of the ONs as a means to influence the strength of interactions between PEI

and ONs, and hence control the antisense response. This approach was adopted towards two outcomes. First, the ability to utilize low molecular weight to deliver ONs effectively is attractive. Second, analyzing the interactions of several ONs varying in the number of PS bonds with several PEI MWs will enhance our understanding of the factors influencing the delivery efficiency. We designed a panel of phosphodiester sequences with increasing number of end capped phosphorothioate bonds. We studied the ability of these oligonucleotides to form complexes with a panel of molecular weights of branched PEI. Further, we evaluated their levels of intracellular delivery and elicitation of an antisense response in a stably pd1EGFP expressing CHO cell line. To provide a mechanistic understanding for our results, we draw explanations from various assays that mimic key intracellular processing steps. We measured the levels of cellular internalization and release of complexes, assess the influence of adding endocytic pH buffering reagents such as chloroquine and ammonium chloride, and determine the ability of the complexes to release DNA by measuring the in vitro rates of dissociation of complexes in the presence of a competing anionic entity. We find that by altering the degree and pattern of phosphorothioate substitution in a phosphodiester oligonucleotide, we are able to modulate the efficiency of lower PEI MWs as oligonucleotide carriers and the dynamics of gene silencing. By correlating the PEI MW & oligonucleotide chemistry with the observed antisense effects, we are able to draw insightful structure-property relationships that will aid the rational design of oligonucleotide carriers.

5.2 Future Directions

In this thesis, we provide evidence for the strong interplay of both polymer and ON properties on carrier-mediated cellular delivery of antisense ONs. Our results highlight several important factors that play a crucial role in obtaining effective ON delivery. While this provides a basis for the rational design of polymeric carriers for ON delivery, it also brings to light several questions that require additional investigation. Here, we provide perspectives on further improving the design of ON carriers and outline possible experimentation that might prove useful.

5.2.1 Characterization of the molecular interactions between polymers and ONs

In our studies, we characterized polymer-ON complexes by measuring the amount of ONs bound to the polymers, the size as well as the ability of the complexes to break apart leading to the release of the DNA. However, it is not clear what the molecular composition of the individual complexes is. Recent reports using fluorescence fluctuation spectroscopy (FFS) suggest that polymer-ON complexes consist of several polymer molecules bound to several ON molecules. Indeed a measure of how tightly or loosely the polymer and ON molecules are bound together in the complex would be essential in predicting the behavior of the complexes in the cellular milieu. Properties such as the degree of branching and flexibility of the polymer chains are considered to be an important aspect of the structure, enabling interactions with other charged species in the cells and hence aiding the release of the ONs. In our work, we found distinct functional responses dependent on the PEI MW. Since the degree of branching is considered to be

the same for the various branched PEI, it is possible that the higher PEI MW that are more efficient have longer and more flexible chains hanging off the complexes.

5.2.2 Role of excess polymer in PEI-ON complexes

In our antisense experiments, we noticed that PEI:ON complexes at a higher charge ratio of 20:1 were much more efficient in eliciting an antisense response than complexes at a 10:1 charge ratio. While we were able to determine that the higher charge ratio complexes delivered more ONs, we were unable to determine the reasons for this. Since PEI functions in a concentration dependent manner, it is not surprising that additional PEI aids the release of ONs. However, determination of the nature of this excess PEI would be highly essential to resolve what role the excess polymer plays. We attempted to separate the excess polymer by centrifugal filtration. However, under all conditions tested, complexes were found to fall apart releasing all ONs. This might be indicative of the fact that polymer-ON complex formation is an equilibrium process. Additionally we performed cellular experiments where the excess polymer was added to the cells separately after complexes at 10:1 charge ratio were introduced (Data not shown). Under these conditions, we observed very high levels of toxicity not detected previously. This suggests that the excess polymer at a 20:1 charge ratio is associated to the ONs to some degree and is not completely free in solution. Further experimentation involving measurement of the rates of cellular internalization of complexes may provide more insights into the effects observed.

5.2.3 Improvement in the mechanistic picture of intracellular trafficking of polymer-ON particles

In our studies, we found certain combinations of PEI-ON complexes unable to dissociate. By treatment with various endosomal-buffering agents such as chloroquine and ammonium chloride, we were able to highlight the importance of the unpackaging events over the escape from the endosomal pathway. However, more concrete evidence for these conclusions can only be obtained with more detailed intracellular studies. For example, by using appropriate fluorescent tags, it is possible to quantify the intracellular pH microenvironment of the complexes and/or the polymers and ONs. Such information will additionally aid in the mechanistic understanding of the processing of the polymer-ON complexes.

In general, more quantitative measurements of intracellular processes are required to determine the extent to which various events continue to pose barriers. With the increasing number of sophisticated techniques such as multi-particle tracking & fluorescence fluctuation spectroscopy available today, a more detailed picture of the intracellular events is bound to emerge.

5.2.4 Metric to describe the variations in responses within cell populations

Ideally, when cells are treated with carrier-ON complexes, one would expect the same levels of ONs to be delivered to the entire population of treated cells leading to a homogeneous antisense response. Nevertheless, as described in the figures below, there is a great deal of heterogeneity among the cells depending on the conditions under which they are treated. The total cell population may consist of cells with varying degrees of

down-regulation. These differences in down-regulation reflect the highly heterogeneous nature of ON delivery. To describe the extent of down-regulation, we utilized geometric mean of GFP fluorescence normalized to the control untreated GFP cells. However, mathematical characterization of cell populations using population balance models might enable us to capture these heterogeneities more precisely.

5.2.5 Rational approaches to improve polymer-mediated delivery

Our results highlighted the importance of the strength of interactions between polymers and ONs. We found that in certain cases, carrier-ON complexes were unable to dissociate intracellularly and hence ineffective in eliciting an antisense response. We utilized the extent of PS substitution in the ON backbone as one means to alter the strength of these interactions and increase functionality. Another viable approach would be to alter the structure of the polymer. Since polymer-ON interactions are electrostatic in nature, one could hypothesize that reducing the charge density on the polymer structure would loosen the interactions between the polymers and the ONs. In fact, recent reports suggest that acetylating the PEI backbone to varying degrees enables greater transfection efficiency due to increased intracellular DNA release from acetylated PEI-plasmid DNA complexes. We are currently testing this hypothesis for the delivery of ONs.

5.2.6 Generalization of results & extension to other systems

We utilized a pd1EGFP stably expressing CHO cell line for our work as it provides an easy means to detect the extent of gene silencing by direct fluorescence measurements. It is known that variability in the extent of ON delivery and hence the extent of antisense down-regulation among various cell types poses a serious barrier to the development of

efficient carriers. Hence, it would be worthwhile extending these studies to other cell types to ensure the universality of the results obtained. For this purpose, several other pd1EGFP stably expressing cell lines are being developed in our laboratory. Further testing in a more biologically relevant system involving down-regulation of oncogenes or other genes involved in various disease states will confirm the usefulness of the work and enable progress towards development of carriers to be used in clinical applications.

5.3 Conclusions

In this thesis, we provide a systematic analysis of the effects of polymer molecular weight and oligonucleotide properties such as structure and chemistry on the dynamics and extent of antisense down-regulation. Our results provide a basis for the rational design of carriers for effective ON delivery. Further improvement calls for the development of tools for the quantitative analysis of the delivery process that will further our mechanistic understanding of the vector-cell interactions. This, coupled with more detailed analysis of the biophysics of polymer-ON interactions, will aid the rational design of carriers for enhanced cellular delivery of ONs.

FIGURES

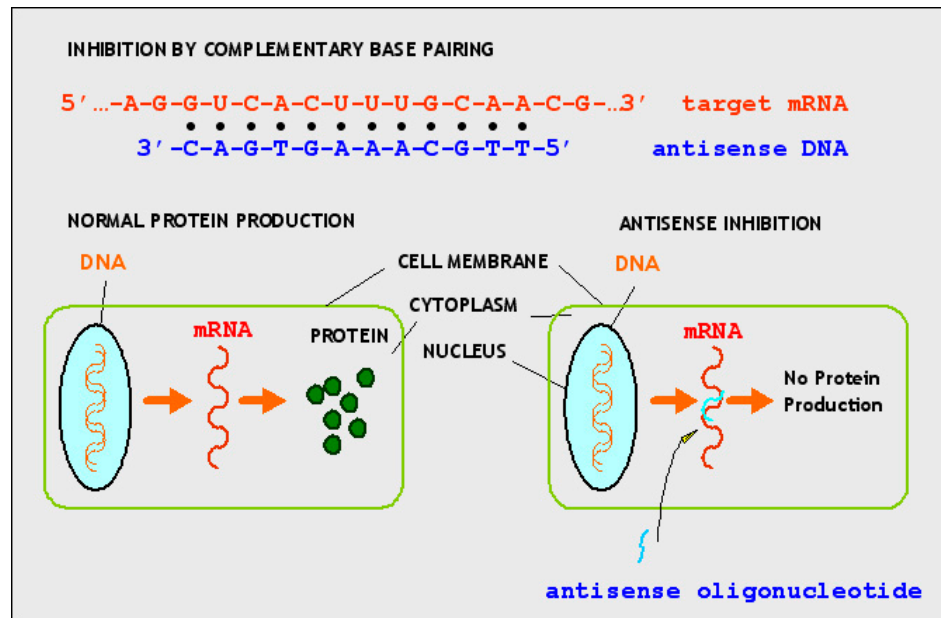


Figure 1.1 Principle of antisense.

In a normal cell, DNA is transcribed into RNA, and the RNA is translated into protein. Antisense ODNs bind the mRNA and inhibit protein production.

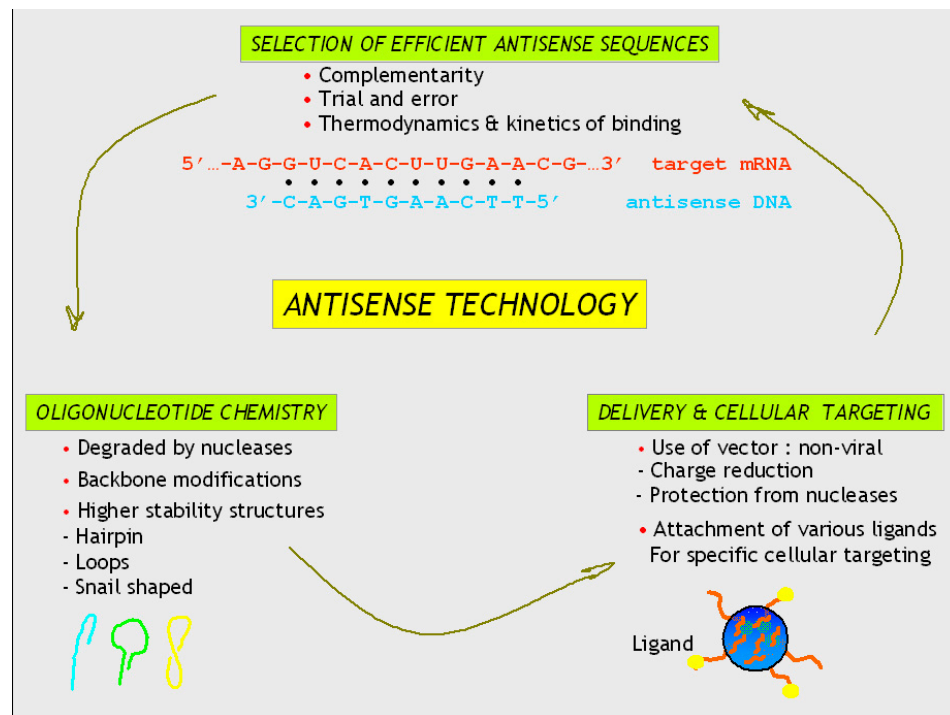


Figure 1.2 Factors involved in effective AS inhibition

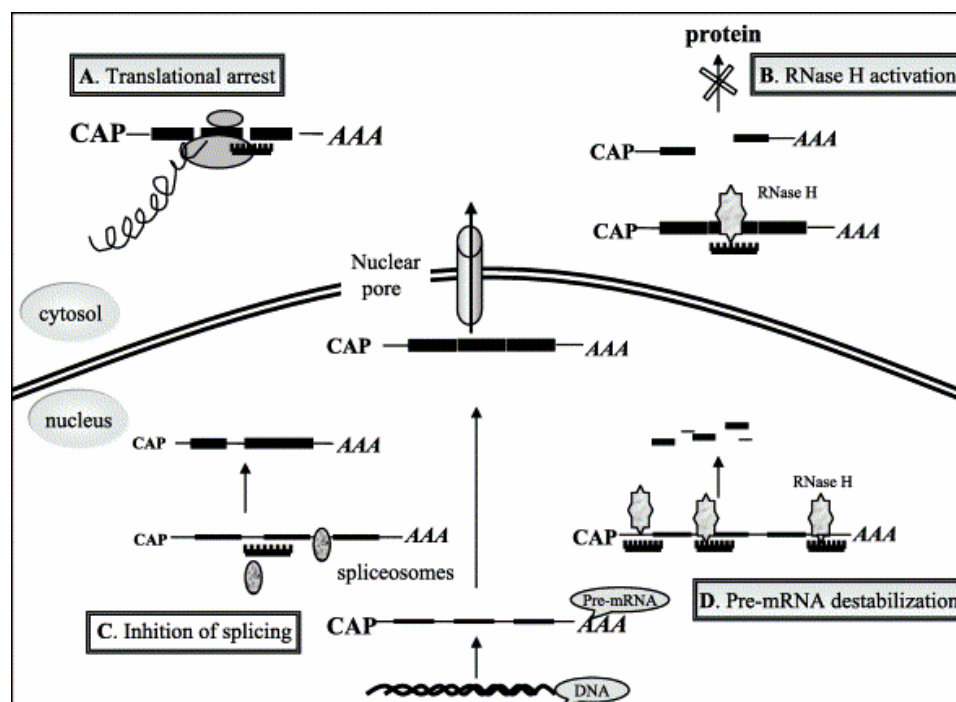


Figure 1.3 Various AS mechanisms

(Source: Shi et al, *Journal of controlled release*, 2004)(88)

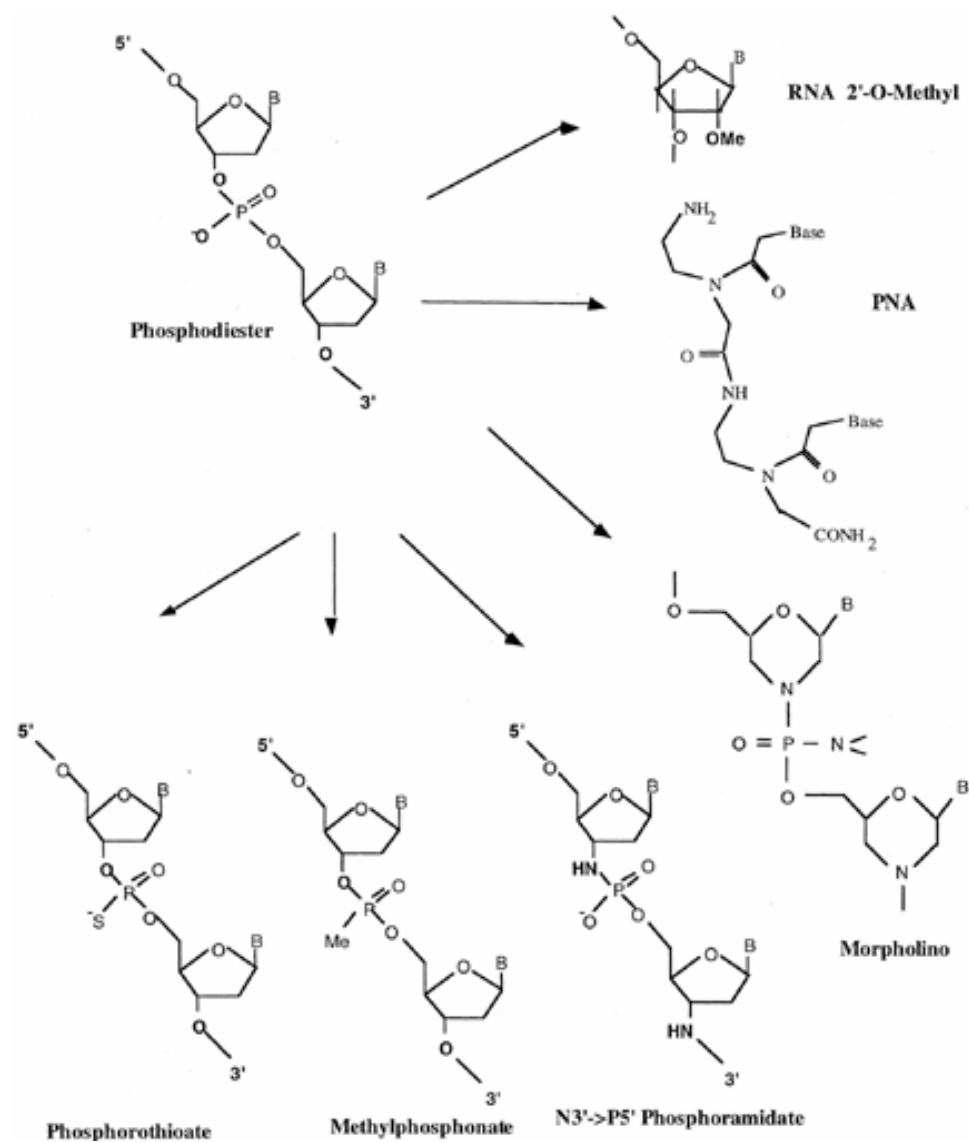


Figure 1.4 Various backbone chemistries of AS oligonucleotides

(Source: Dias et al, *Molecular cancer therapeutics*, 2002)(10)

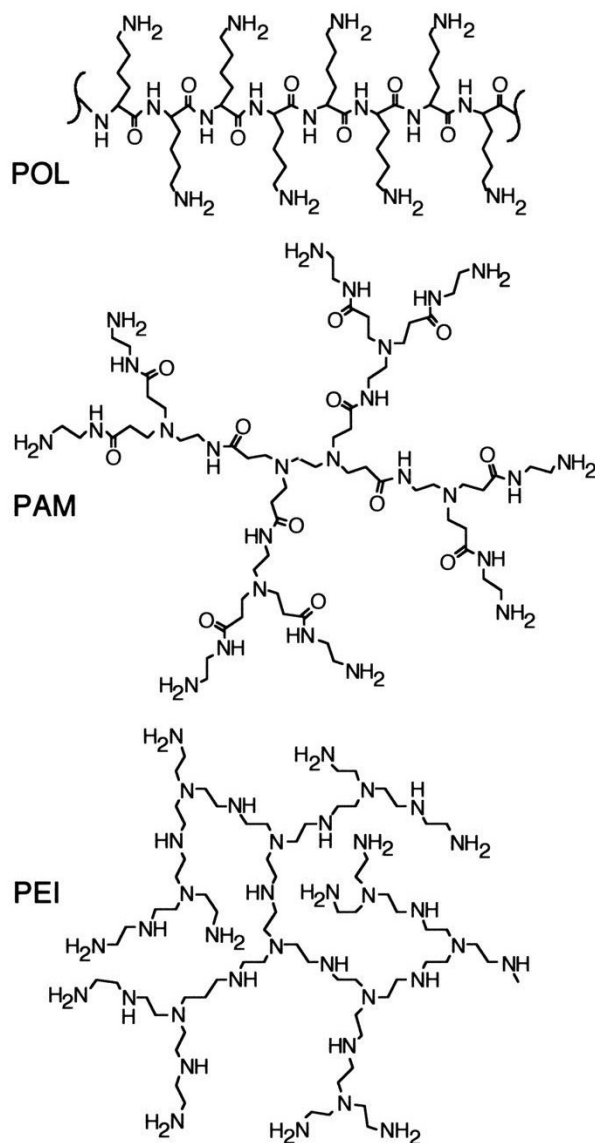


Figure 1.5 Common polymer chemistries used for DNA delivery

POL (poly-L-lysine), PAM (polyamidoamine dendrimer), PEI (polyethyleneimine).
 (Source: Sonawane et al, *Journal of biological chemistry*, 2003) (25)

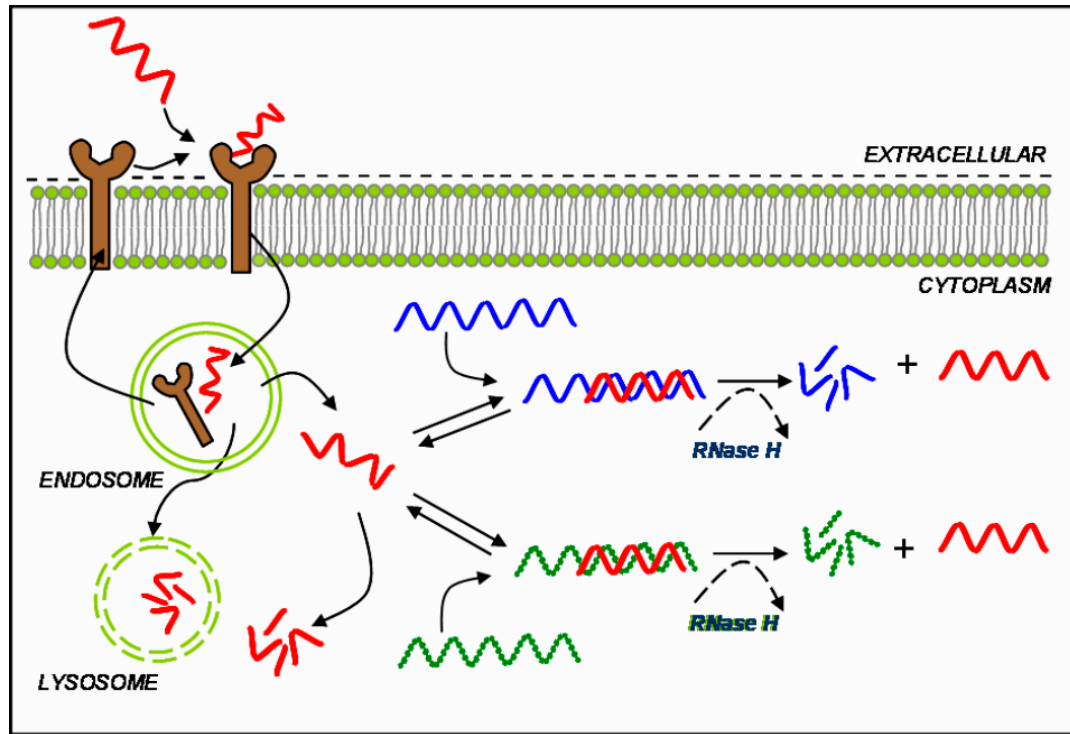


Figure 1.6 Intracellular processing of AS ON delivery (non-vector mediated)

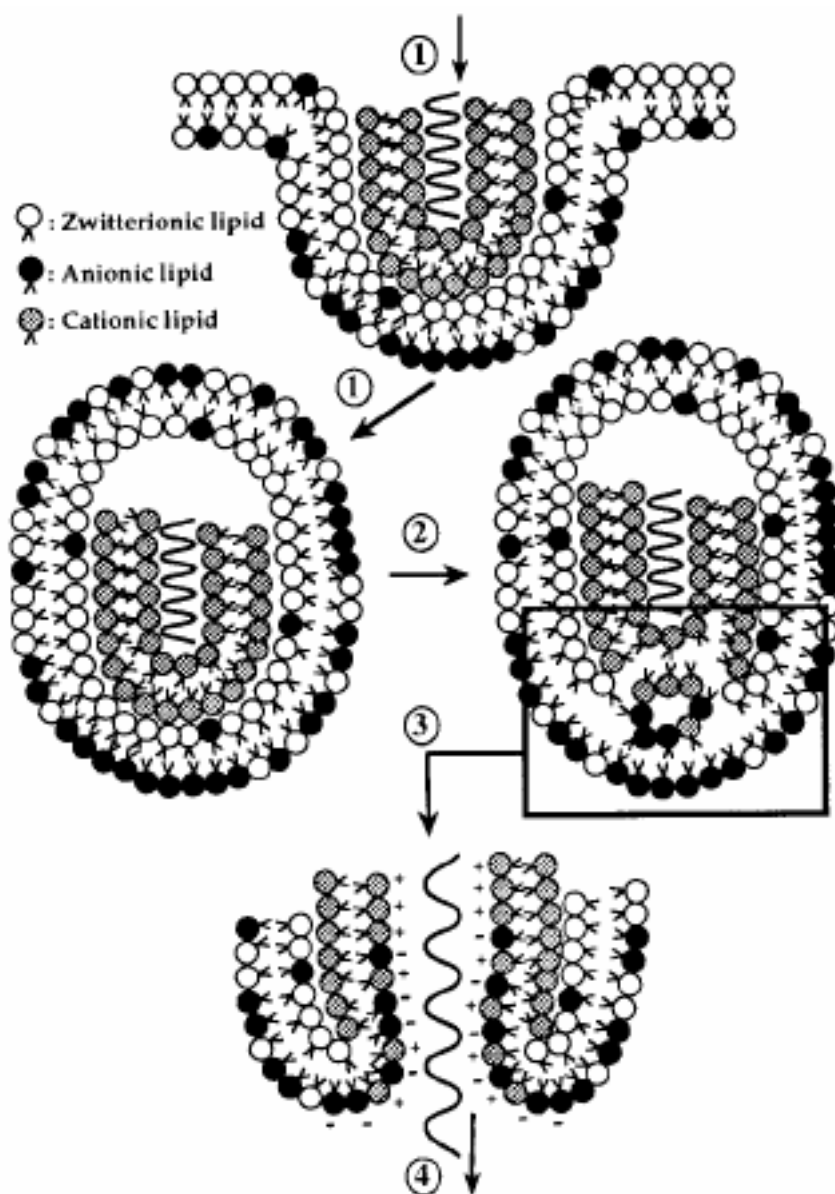
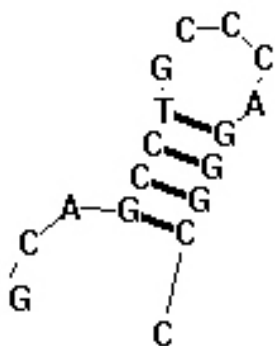


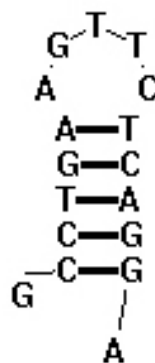
Figure 1.7 Proposed flip-flop mechanism for release of ONs from lipids

(Source: Zelphati et al, PNAS, 1996)

(a) HP1



(b) HP2

**Figure 2.1 Structure of hairpin ONs**

(a) HP1 and (b) HP2 (Generated using RNAStructure 4.1 software)(128)

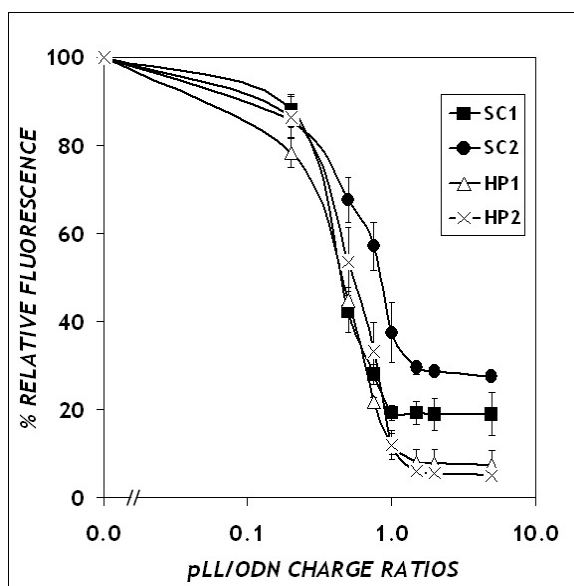


Figure 2.2 Effect of ON structure on complex formation

The OliGreen® fluorescence was measured after forming complexes between ON (in an amount corresponding to a final concentration of 5 $\mu\text{g/mL}$) and the amount of pLL necessary to attain the indicated charge ratios. Filled symbols represent the unstructured ONs, and open symbols (or X) represent hairpin structured ONs. Data represent the mean \pm standard deviation of at least 3 replicates.

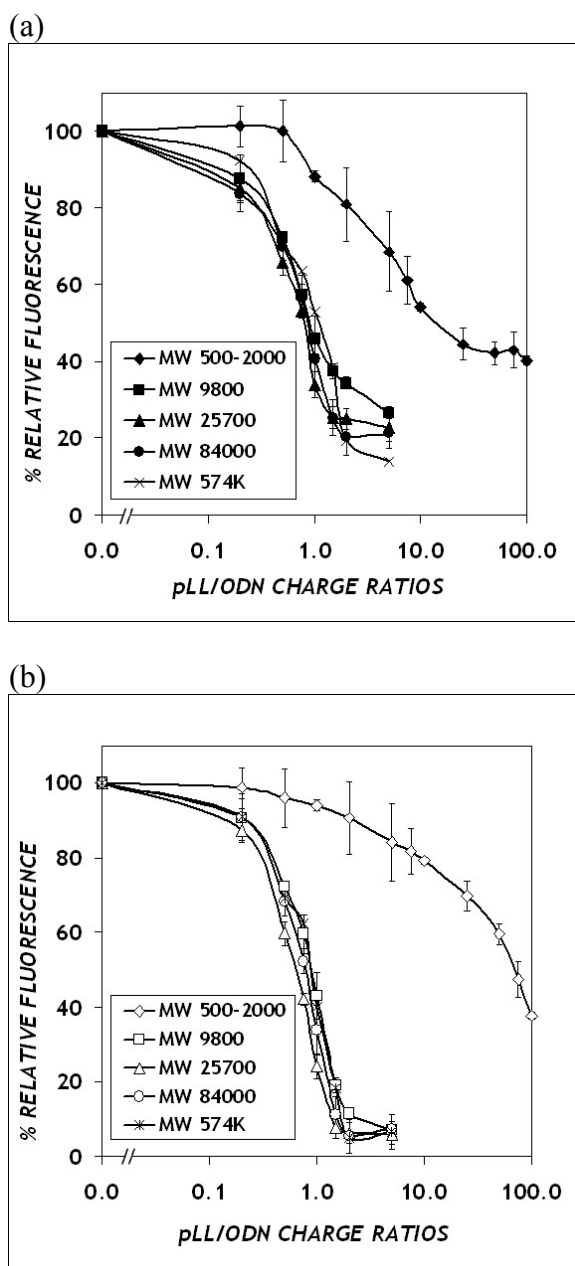


Figure 2.3 Effect of pLL molecular weight on complex formation

Determined using the OliGreen® assay for individual ONs of various structures: (a) Unstructured ONs, (b) Hairpin ONs. Data represent the mean \pm standard deviation of at least 3 replicates.

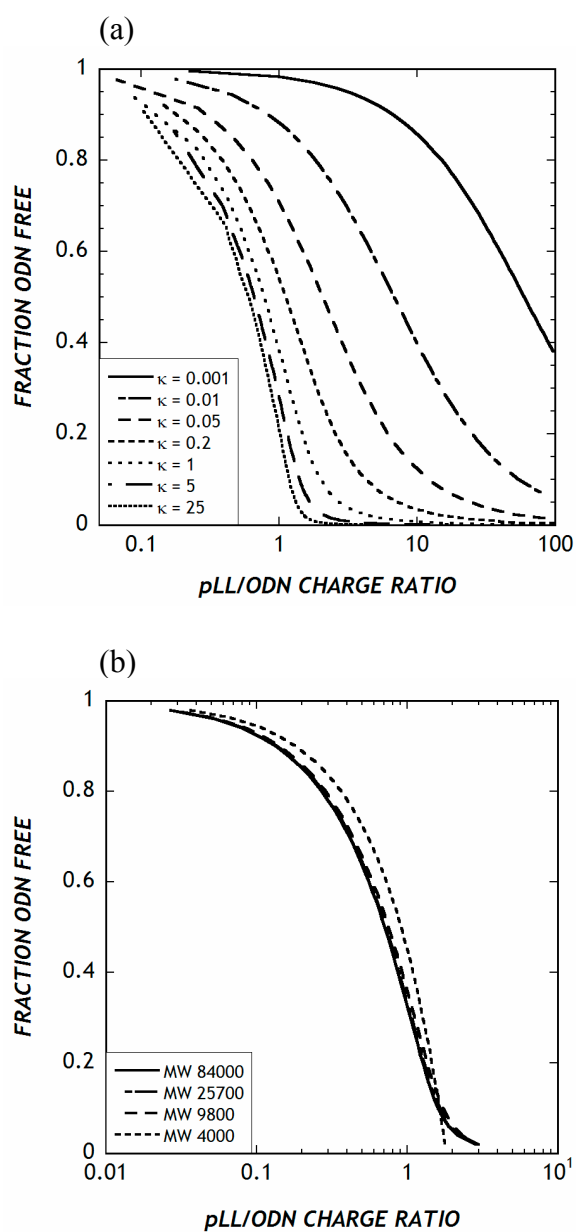


Figure 2.4 Model predictions of pLL-ON complexation behavior

(a) Predictions of the McGhee-von Hippel isotherm at varying values of dimensionless affinity, κ ; (b) Polymer molecular weight dependence, calculated using the finite size correction to the McGhee-von Hippel isotherm^(67, 68).

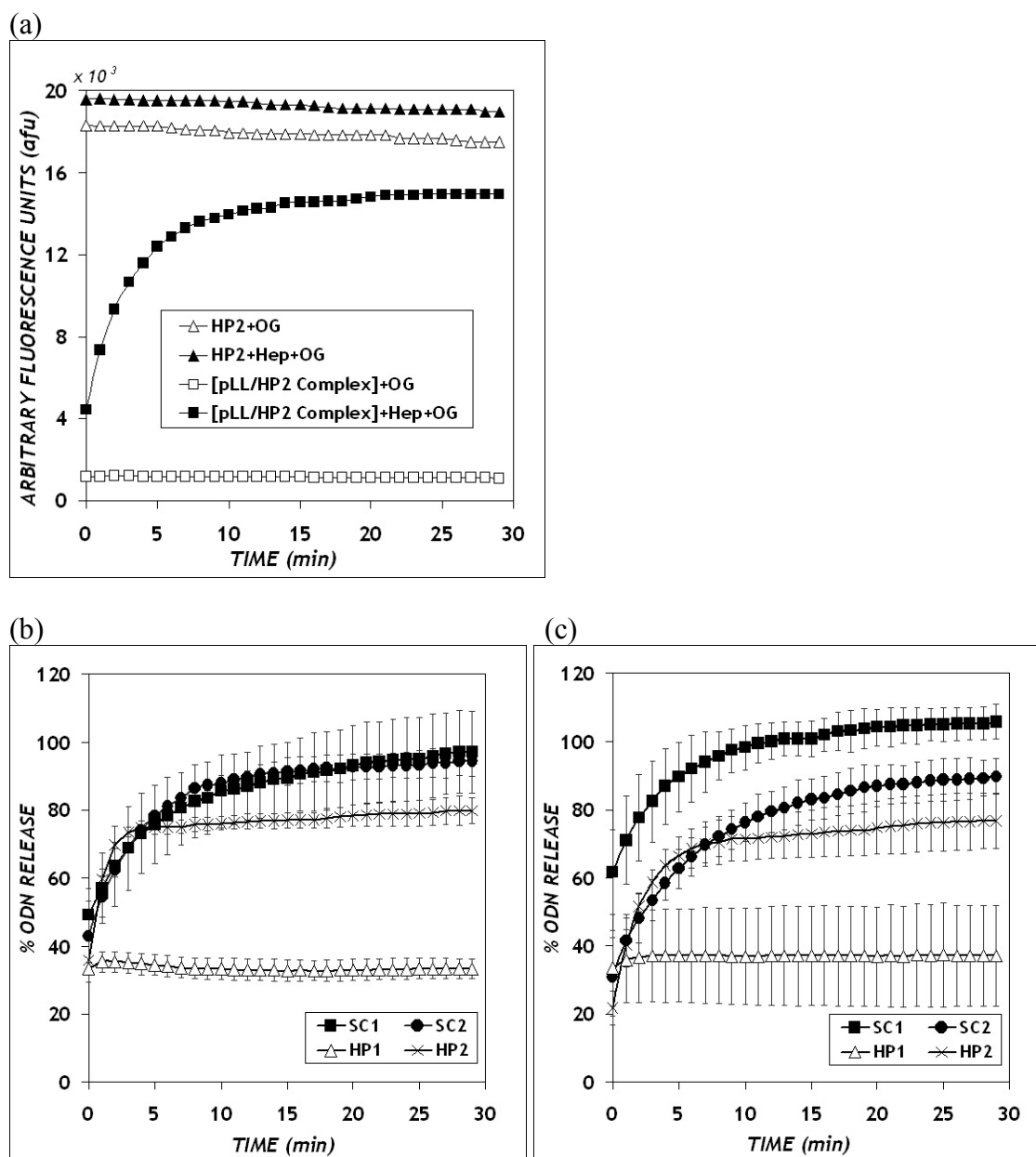


Figure 2.5 ON release kinetics from pLL-ON complexes

(a) Raw data (b) Charge ratio 2:1, heparin concentration 5 $\mu\text{g/mL}$ (c) Charge ratio 5:1, heparin concentration 10 $\mu\text{g/mL}$. Data represent the mean \pm standard deviation of at least 3 replicates.

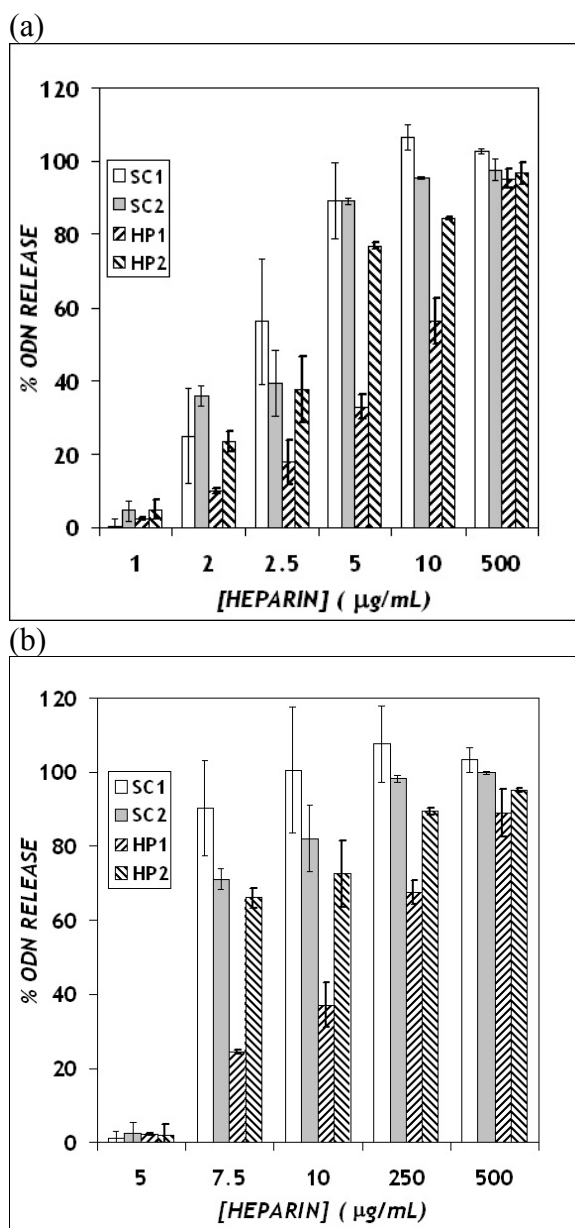


Figure 2.6 Heparin dose response curves of the release of unstructured and hairpin structured ONs from pLL-ON complexes

(a) Charge ratio 2:1, (b) Charge ratio 5:1. Data represent the mean \pm standard deviation of at least 3 replicates. (Unstructured ONs - shaded bars, hairpin ONs - hatched bars)

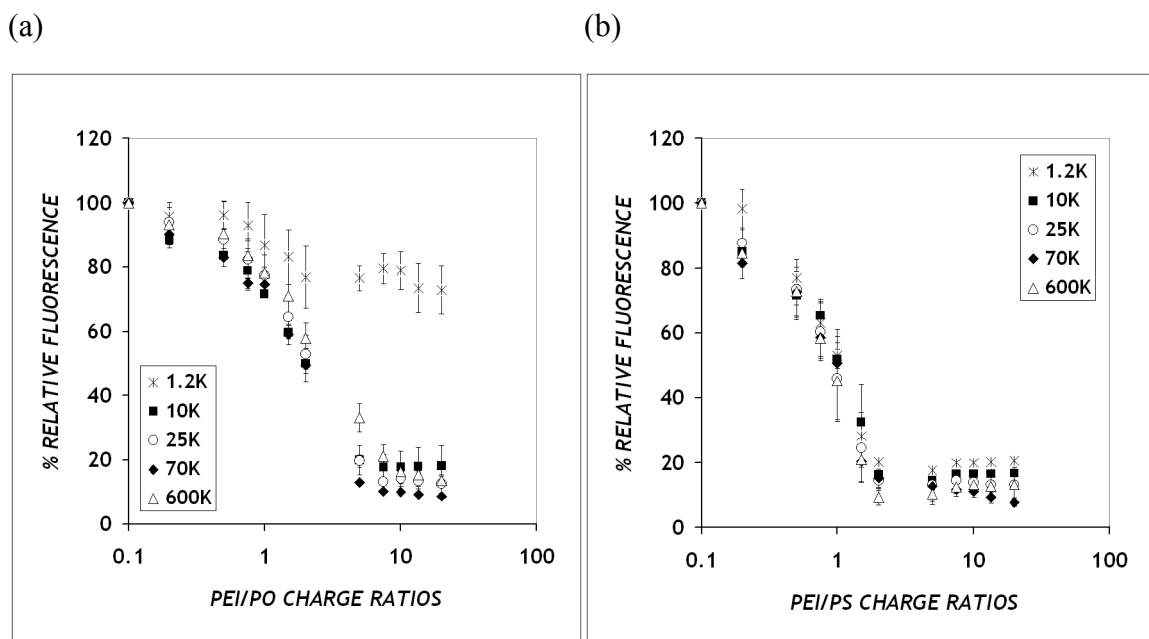


Figure 3.1 Effect of PEI molecular weight on complex formation of PEI with PO and PS ONs

(a) PO and (b) PS ONs. Complexes were prepared in PBS at a final ON concentration of 10 $\mu\text{g/mL}$. Fluorescence corresponds to free (unbound) DNA in solution, detected using a commercially available dye OliGreen that fluoresces upon binding to single-stranded DNA. Data represent mean \pm S.D. ($n=3$).

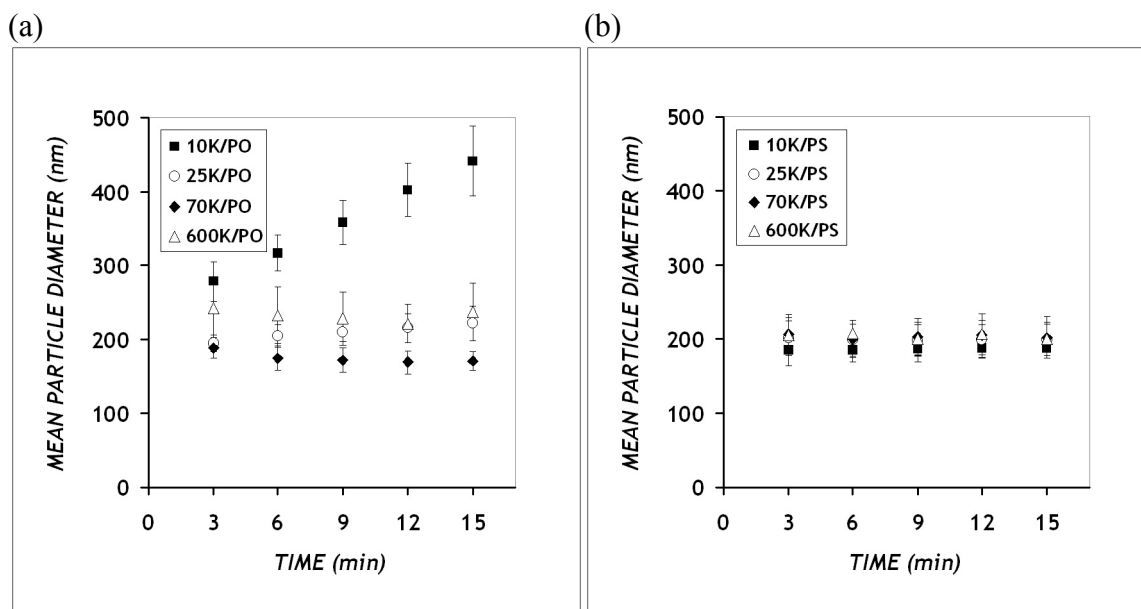


Figure 3.2 Mean hydrodynamic diameter (nm) of PEI-ON complexes

Complexes at charge ratio 10:1 and final ON concentration 50 $\mu\text{g/mL}$ were prepared in PBS between PEI with (a) PO and (b) PS ONs. Data represent mean \pm S.D. ($n \geq 3$).

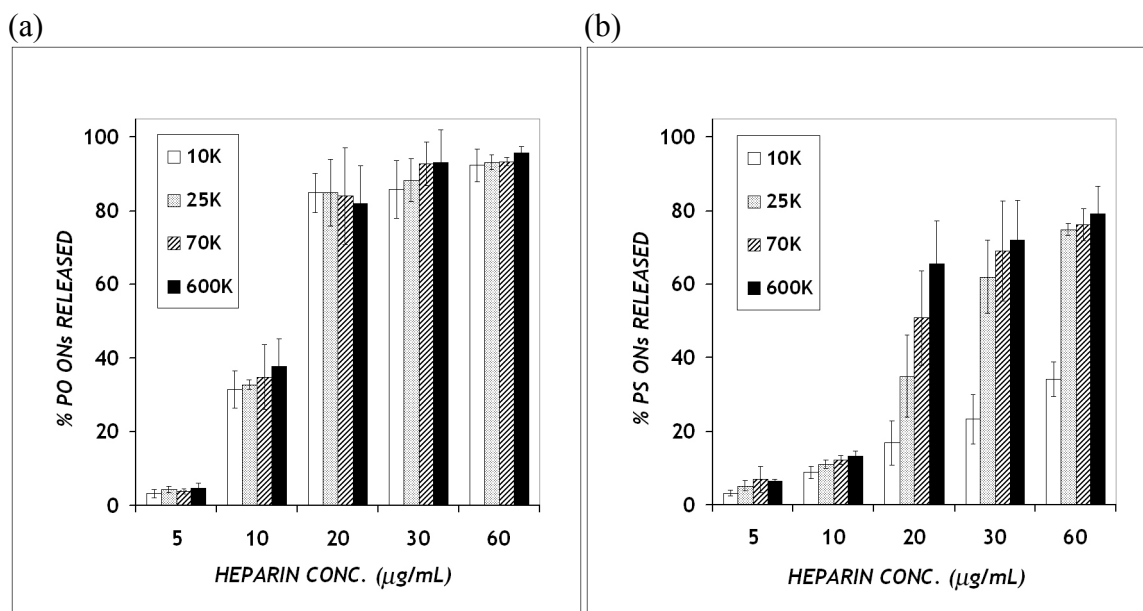


Figure 3.3 Heparin dose response of the release of PO and PS ONs from PEI/ON complexes

(a) PO and (b) PS ONs Complexes (charge ratio 10:1, final ON concentration 5 $\mu\text{g/mL}$ in PBS) were treated with heparin at various concentrations and maintained at 37°C for one hour. ONs released from the complexes were detected using OliGreen as in Figure 1. Data represent mean \pm S.D. (n=3).

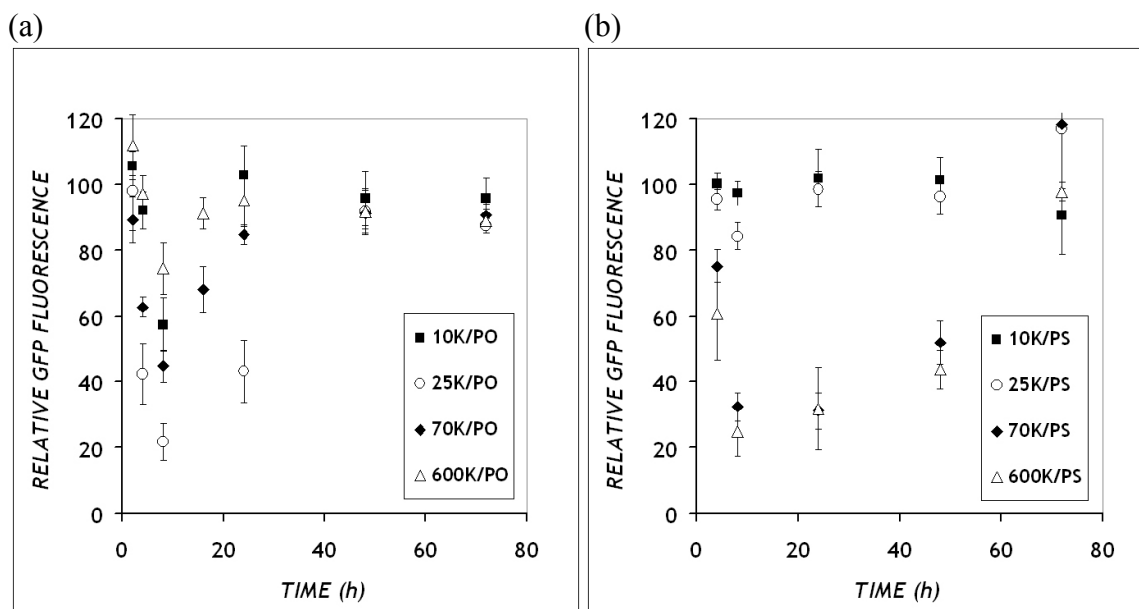


Figure 3.4 Dynamics of GFP down-regulation

CHO-d1EGFP cells were treated with PEI/Cy5-anti-GFP ON complexes prepared with (a) PO and (b) PS ONs at a final ON concentration of 300 nM for 4 hours under serum-free conditions. At various times, 10000 cells were analyzed for GFP fluorescence using flow cytometry. GFP fluorescence values are normalized to untreated control cells (100%). Data represent mean \pm S.D. (n=6)

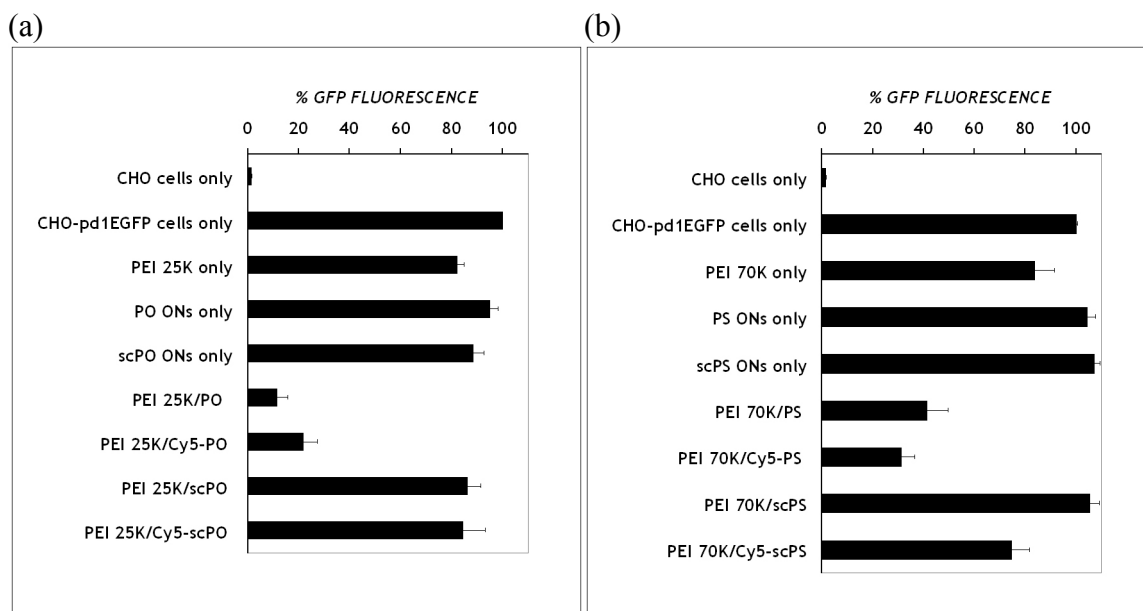


Figure 3.5 Controls for antisense experiment

Controls for antisense experiment described in Figure 3.4 are shown above. Data represent treatment with single PEI MW (that delivered maximum PO or PS ONs), and at a single time point (at which maximum antisense inhibition was detected). The abbreviation 'sc' denotes scrambled sequence control while 'Cy-' denotes ON was tagged at 5' end with Cy5 dye. Data represent mean \pm S.D. (n=3)

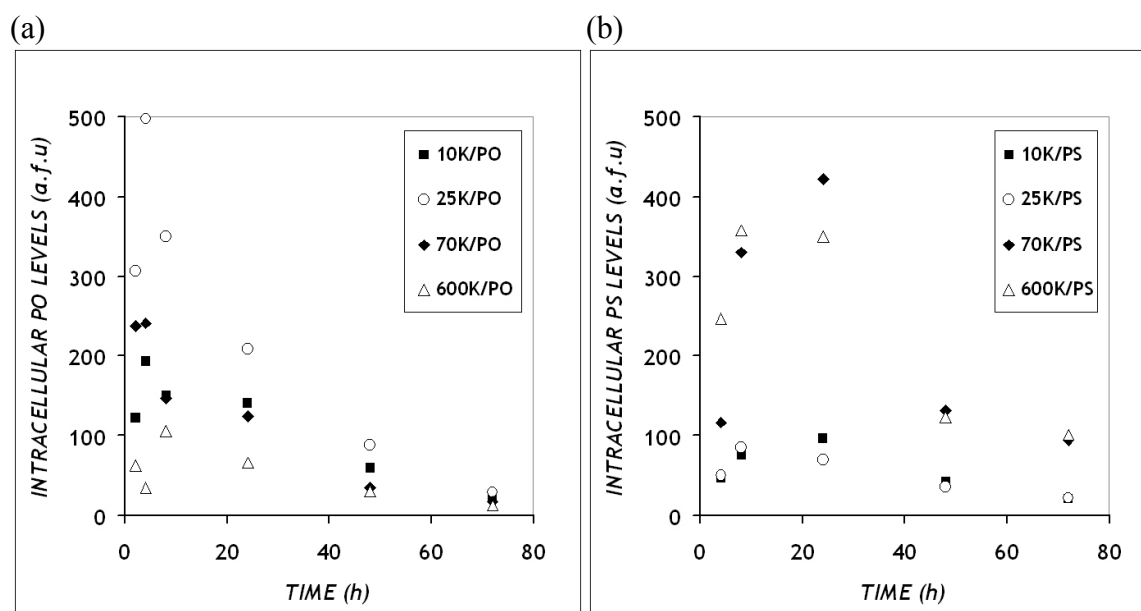


Figure 3.6 Dynamics of intracellular ON levels

CHO-d1EGFP cells were treated as described in Figure 3.4 with PEI/Cy5-anti-GFP ON complexes prepared with (a) PO and (b) PS ONs. Data represents raw geometric mean fluorescence levels of intracellular Cy5-tagged ONs captured simultaneously by flow cytometry in a separate channel, while cells are analyzed for their GFP fluorescence levels.

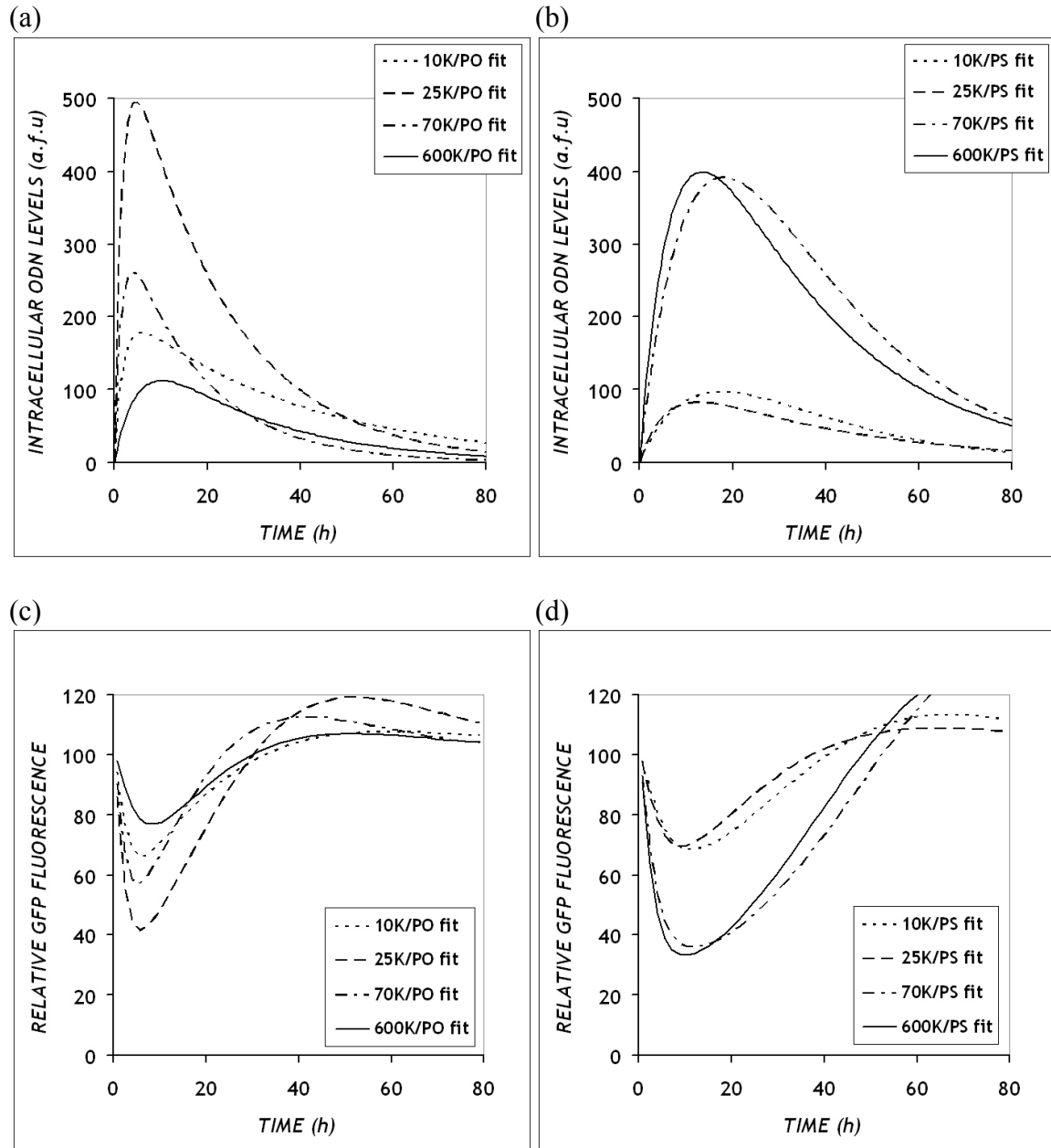


Figure 3.7 Model predictions

Model predictions of the dynamics of intracellular ON concentrations (a,b) and GFP down-regulation (c,d) in cells treated with (a,c) PEI/PO and (b,d) PEI/PS complexes, respectively.

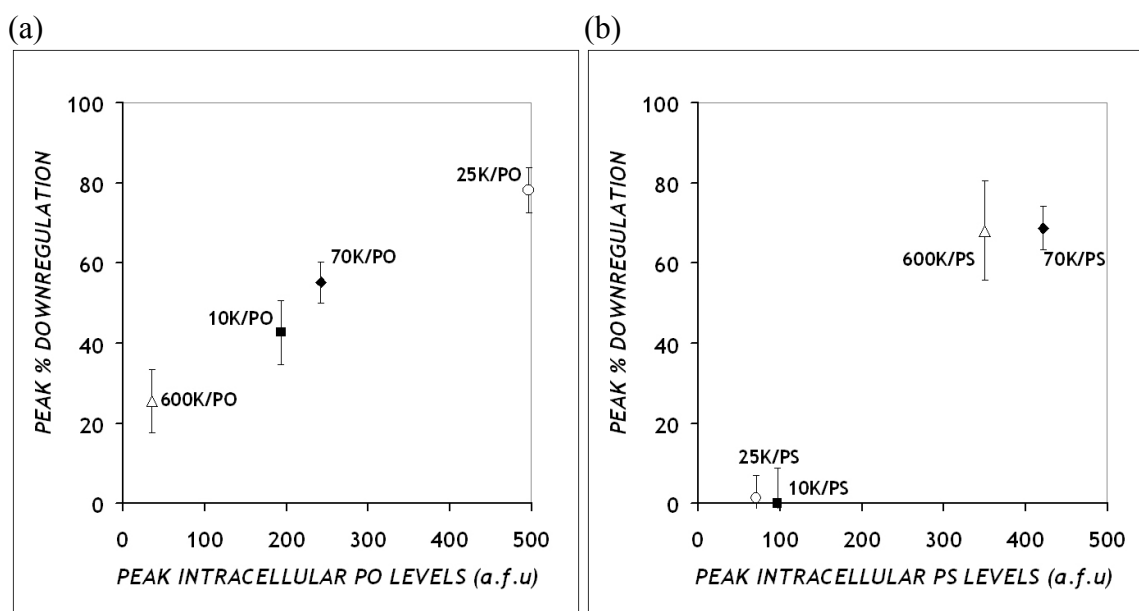


Figure 3.8 Relationship between antisense inhibition and intracellular ON levels

Each data point represents maximum down-regulation and maximum ON levels detected when the indicated PEI MW was used to deliver (a) PO and (b) PS ONs. For both sets, results correspond to data obtained 8h after PEI/ON complexes were introduced to CHO-d1EGFP cells.

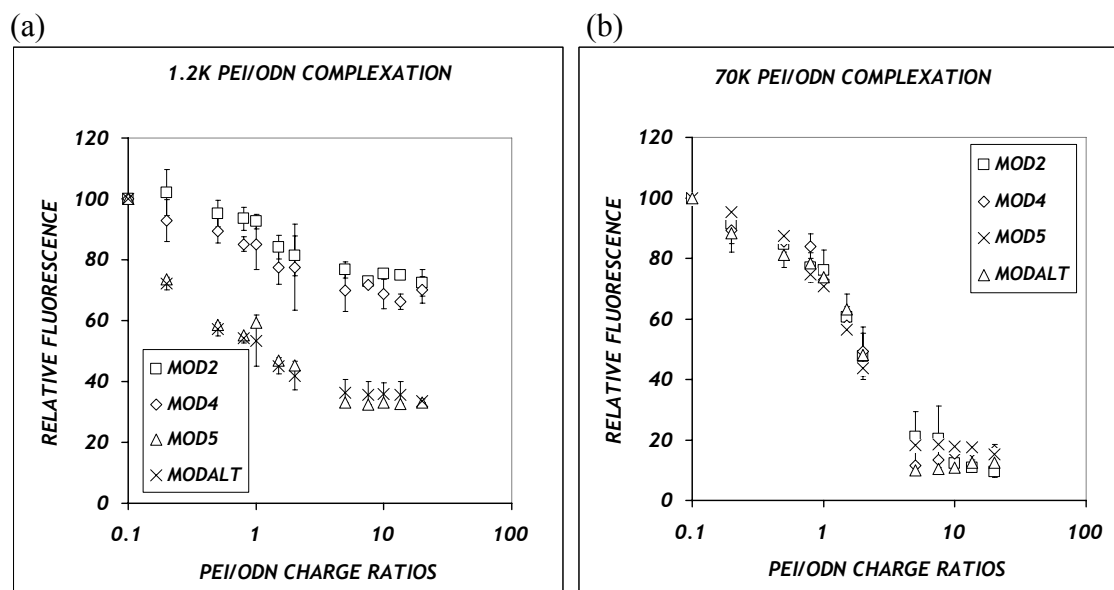
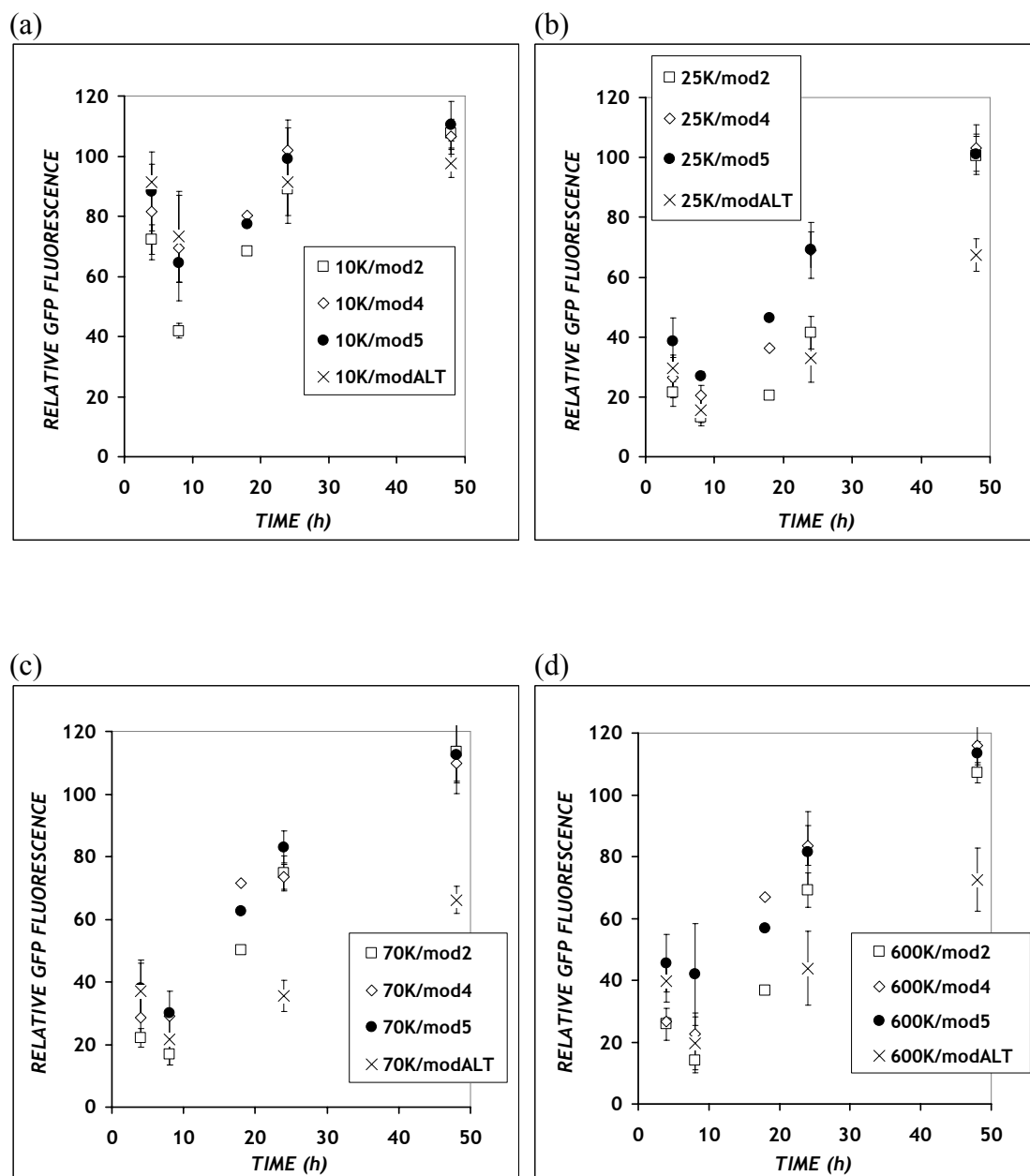


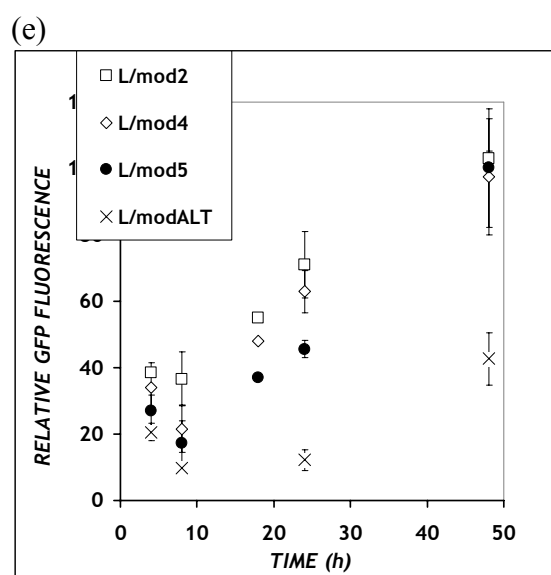
Figure 4.1 Effect of PEI molecular weight on complex formation of PEI with ONs of various chemistries (mod2, mod4, mod5, modALT)

Complexes were prepared in PBS at a final ON concentration of 10 $\mu\text{g/mL}$. Fluorescence corresponds to free (unbound) DNA in solution, detected using a commercially available dye OliGreen that fluoresces upon binding to single-stranded DNA. Data represent mean \pm S.D. (n=3).

Figure 4.2 Dynamics of GFP down-regulation

CHO-d1EGFP cells were treated with PEI/Cy5-anti-GFP ON complexes prepared with PEIs of MWs (a)10K (b) 25K (c) 70K (d) 600K (e) Lipofectamine at a final ON concentration of 300 nM for 4 hours under serum-free conditions. At various times, 10000 cells were analyzed for GFP fluorescence using flow cytometry. GFP fluorescence values are normalized to untreated control cells (100%).





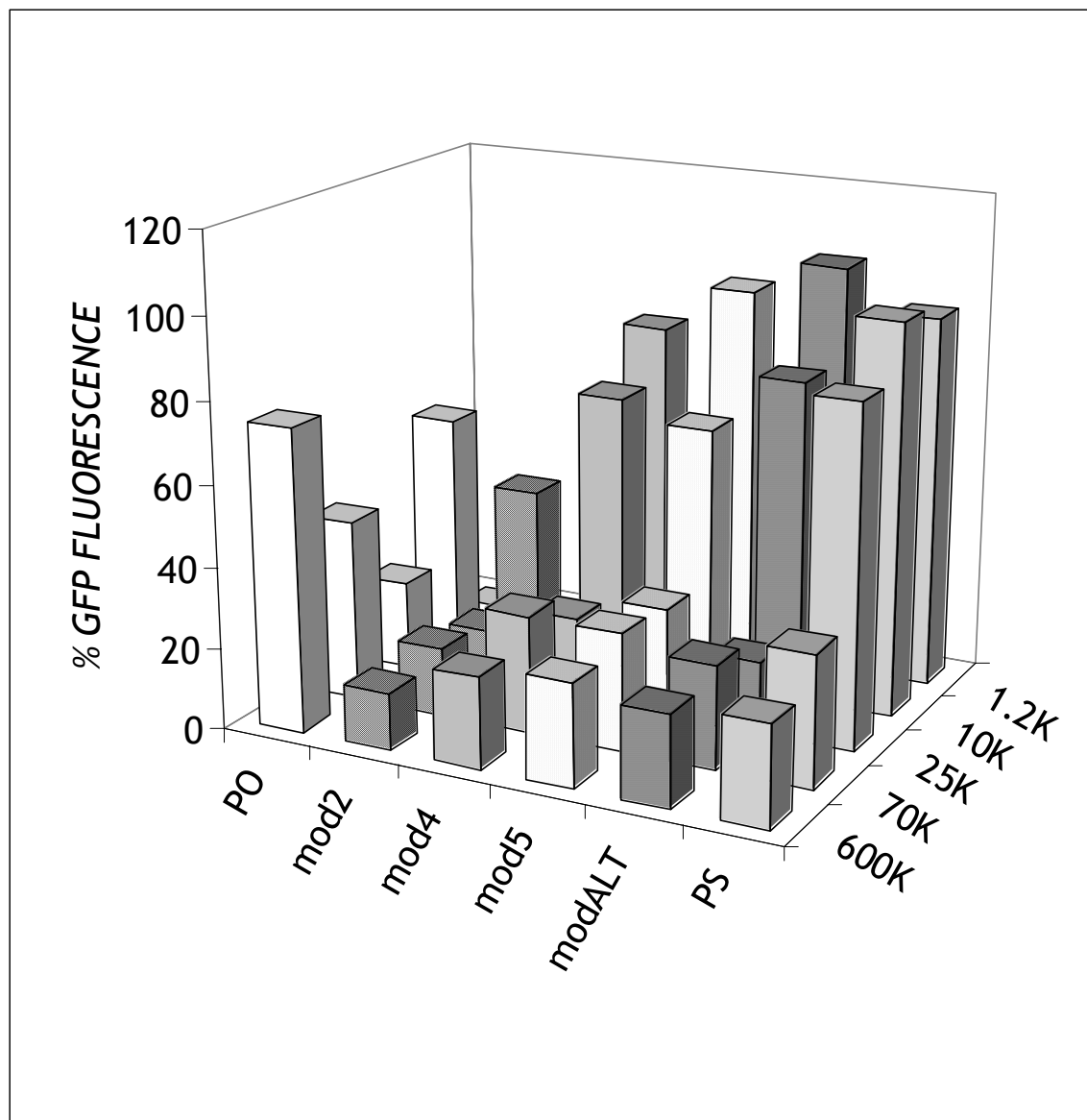


Figure 4.3 Antisense response plot indicating correlations between PEI MWs and ON chemistries

Normalized GFP fluorescence levels of d1EGFP CHO cells treated with various combinations of PEI MWs and ON chemistries for 4 hours at 300nM ON concentration recorded at time of maximum GFP down-regulation

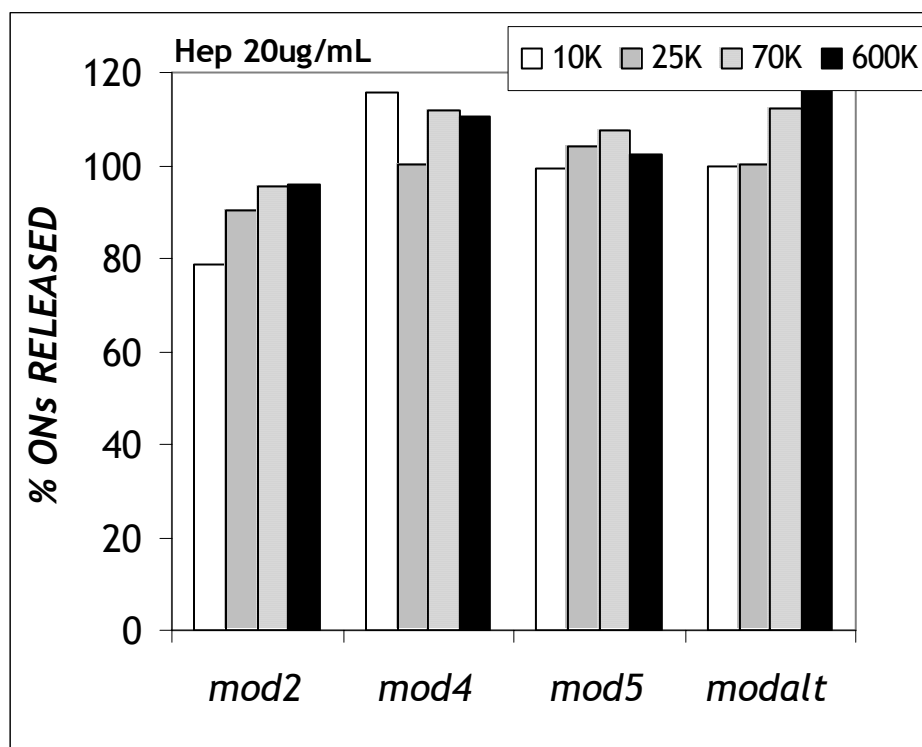


Figure 4.4 Heparin induced ON release from PEI/ON complexes

Complexes (charge ratio 10:1, final ON concentration 5 µg/mL in PBS) were treated with heparin at 20 µg/mL and maintained at 37°C for one hour. ONs released from the complexes were detected using OliGreen

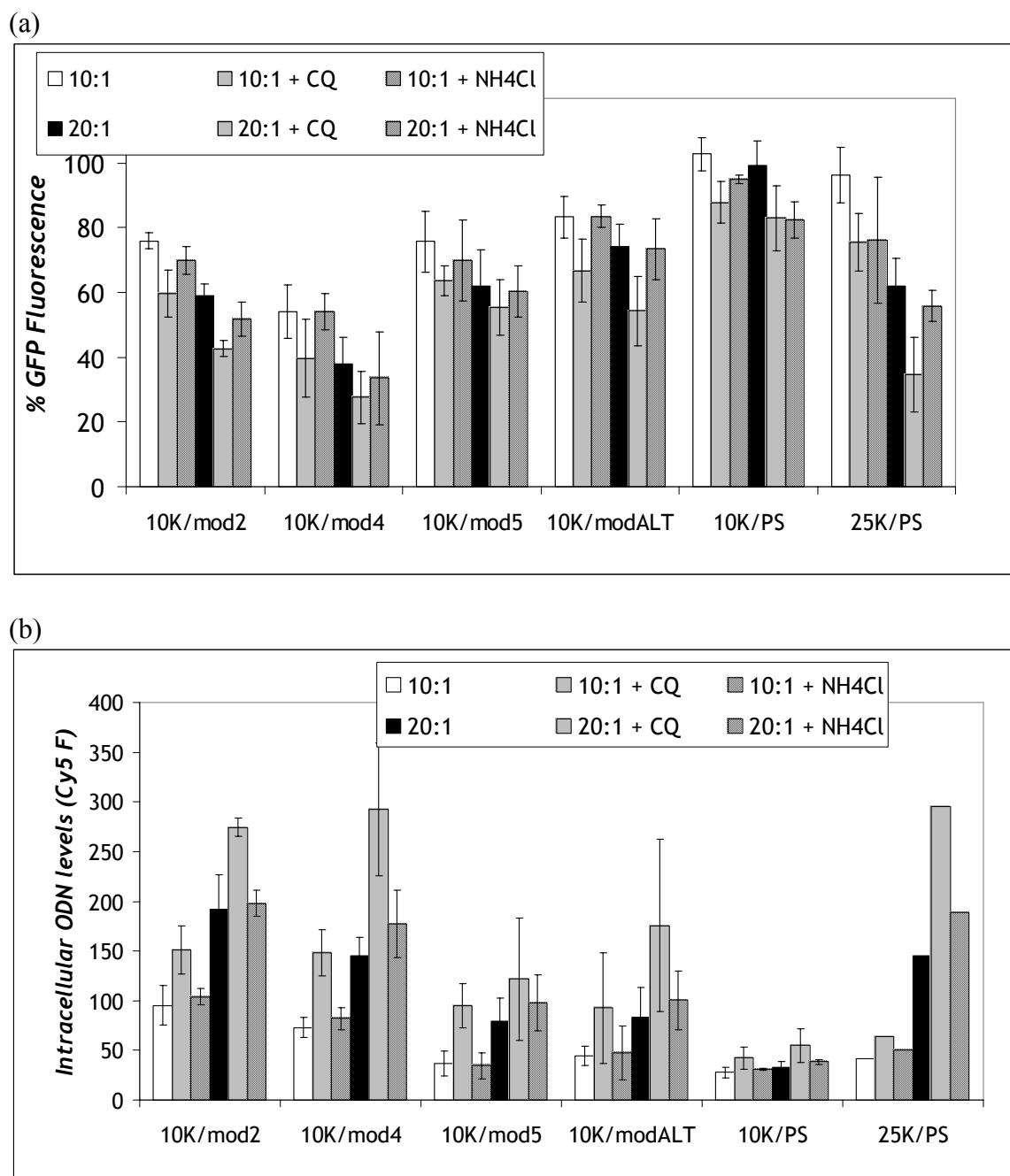


Figure 4.5 Effects of chloroquine and ammonium chloride on antisense down-regulation and intracellular ON levels

CHO-d1EGFP cells were treated with PEI/ON complexes prepared with 10K or 25K PEI and various ON chemistries at 10:1 and 20:1 charge ratio for 4 hours at a 300nM ON concentration in the presence of 100 μ M chloroquine (CQ) or 10mM ammonium chloride (NH₄Cl) and subsequently analyzed for GFP down-regulation and intracellular ON levels at 8 h from introduction of complexes. To measure intracellular ON levels, Cy5 end tagged ONs were utilized.

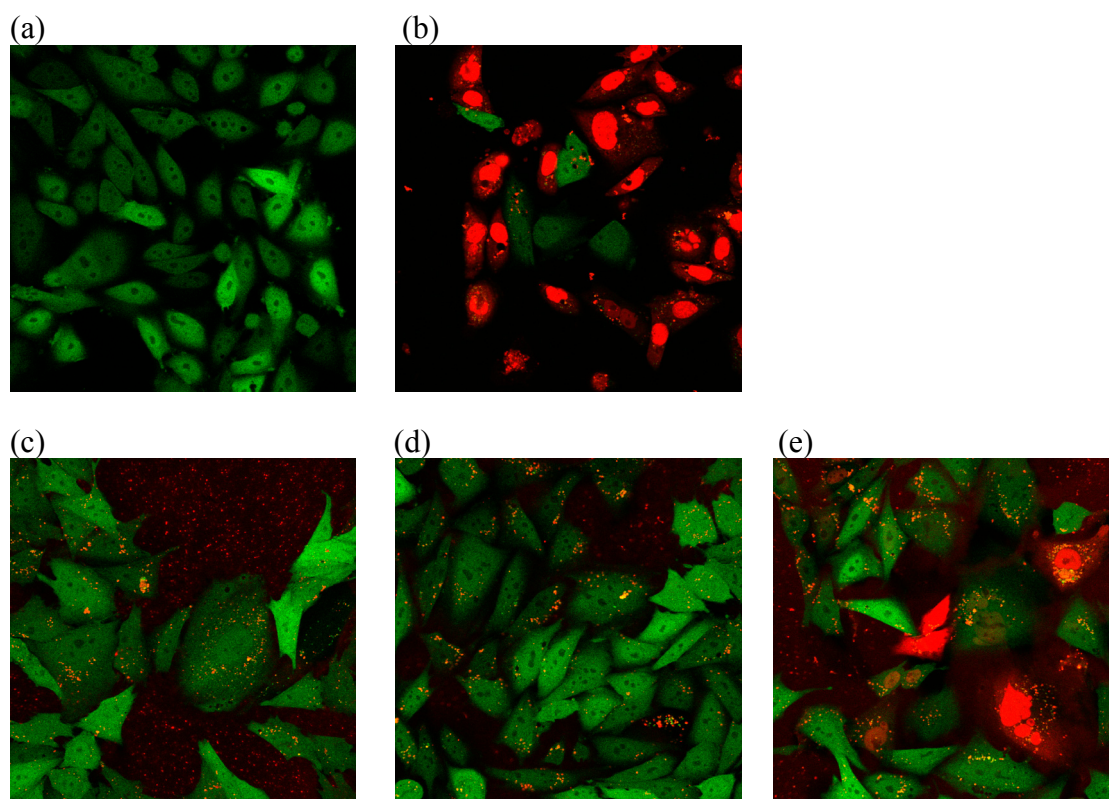


Figure 4.6 Confocal microscopy of d1EGFP cells treated with PEI/ON complexes

CHO-d1EGFP cells were treated with PEI/Cy-PS complexes or Lipofectamine/Cy-PS complexes at a 300nM ON concentration for 4 hours in the presence or absence of chloroquine (CQ) and visualized at 24 h from the introduction of the complexes.

(a) d1EGFP CHO cells (untreated) (b) Lipo/Cy-PS (2.5:1 w/w) (c) PEI 25K/Cy-PS (10:1) (d) PEI 25K/Cy-PS (10:1) + 100 μ M CQ (e) PEI 25K/Cy-PS (20:1) + 100 μ M CQ

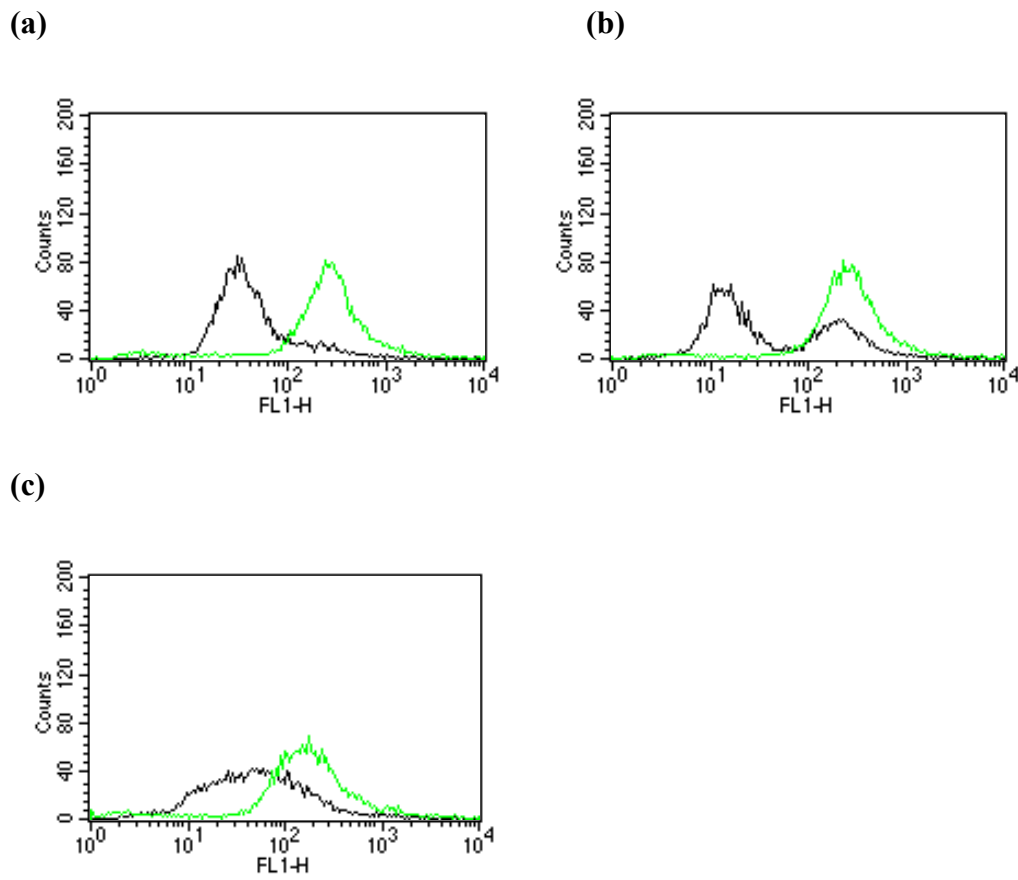


Figure 5.1 Heterogeneity in GFP down-regulation in cell populations

(a) GFP is down-regulated in the entire cell population. (b) Fraction of cells remain completely unaffected (c) A varied distribution of response over the entire cell population

References

1. Gewirtz AM, Sokol DL, Ratajczak MZA. 1998. Nucleic acid therapeutics: state of the art and future prospects. *Blood* 92: 712-36
2. Stephenson ML, Zamecnik PC. 1978. Inhibition of Rous sarcoma viral RNA translation by a specific oligodeoxyribonucleotide. *Proc Natl Acad Sci U S A* 75: 285-8
3. Opalinska JB, Gewirtz AMA. 2002. Nucleic-acid therapeutics: basic principles and recent applications. *Nat Rev Drug Discov* 1: 503-14
4. Merdan T, Kopecek J, Kissel TA. 2002. Prospects for cationic polymers in gene and oligonucleotide therapy against cancer. *Adv Drug Deliv Rev* 54: 715-58
5. Anderson KP, Fox MC, Brown-Driver V, Martin MJ, Azad RF. 1996. Inhibition of human cytomegalovirus immediate-early gene expression by an antisense oligonucleotide complementary to immediate-early RNA. *Antimicrob Agents Chemother* 40: 2004-11
6. Lee LK, Roth CM. 2003. Antisense technology in molecular and cellular bioengineering. *Curr Opin Biotechnol* 14: 505-11
7. Milner N, Mir KU, Southern EM. 1997. Selecting effective antisense reagents on combinatorial oligonucleotide arrays. *Nat Biotechnol* 15: 537-41
8. Walton SP, Stephanopoulos GN, Yarmush ML, Roth CM. 2002. Thermodynamic and kinetic characterization of antisense oligodeoxynucleotide binding to a structured mRNA. *Biophys J* 82: 366-77
9. Crooke ST. 1999. Molecular mechanisms of action of antisense drugs. *Biochim Biophys Acta* 1489: 31-44
10. Dias N, Stein CA. 2002. Antisense oligonucleotides: basic concepts and mechanisms. *Mol Cancer Ther* 1: 347-55
11. Lebedeva I, Stein CA. 2001. Antisense oligonucleotides: promise and reality. *Annu Rev Pharmacol Toxicol* 41: 403-19
12. Lebedeva I, Benimetskaya L, Stein CA, Vilenchik M. 2000. Cellular delivery of antisense oligonucleotides. *Eur J Pharm Biopharm* 50: 101-19
13. Felgner PL, Barenholz Y, Behr JP, Cheng SH, Cullis P, et al. 1997. Nomenclature for synthetic gene delivery systems. *Hum Gene Ther* 8: 511-2
14. Balicki D, Reisfeld RA, Pertl U, Beutler E, Lode HN. 2000. Histone H2A-mediated transient cytokine gene delivery induces efficient antitumor responses in murine neuroblastoma. *Proc Natl Acad Sci U S A* 97: 11500-4
15. Mao HQ, Roy K, Troung-Le VL, Janes KA, Lin KY, et al. 2001. Chitosan-DNA nanoparticles as gene carriers: synthesis, characterization and transfection efficiency. *J Control Release* 70: 399-421
16. Ferrari ME, Rusalov D, Enas J, Wheeler CJ. 2002. Synergy between cationic lipid and co-lipid determines the macroscopic structure and transfection activity of lipoplexes. *Nucleic Acids Res* 30: 1808-16
17. Wyman TB, Nicol F, Zelphati O, Scaria PV, Plank C, Szoka FC, Jr. 1997. Design, synthesis, and characterization of a cationic peptide that binds to nucleic acids and permeabilizes bilayers. *Biochemistry* 36: 3008-17

18. Andreadis ST, Roth CM, Le Doux JM, Morgan JR, Yarmush ML. 1999. Large-scale processing of recombinant retroviruses for gene therapy. *Biotechnol Prog* 15: 1-11
19. Davis HE, Morgan JR, Yarmush ML. 2002. Polybrene increases retrovirus gene transfer efficiency by enhancing receptor-independent virus adsorption on target cell membranes. *Biophys Chem* 97: 159-72
20. Escriou V, Carriere M, Scherman D, Wils P. 2003. NLS bioconjugates for targeting therapeutic genes to the nucleus. *Adv Drug Deliv Rev* 55: 295-306
21. Roth CM, Sundaram S. 2004. Engineering synthetic vectors for improved DNA delivery: insights from intracellular pathways. *Annu Rev Biomed Eng* 6: 397-426
22. Nishikawa M, Huang L. 2001. Nonviral vectors in the new millennium: delivery barriers in gene transfer. *Hum Gene Ther* 12: 861-70
23. Lechardeur D, Lukacs GL. 2002. Intracellular barriers to non-viral gene transfer. *Curr Gene Ther* 2: 183-94
24. Godbey WT, Wu KK, Mikos AG. 1999. Tracking the intracellular path of poly(ethylenimine)/DNA complexes for gene delivery. *Proc Natl Acad Sci U S A* 96: 5177-81
25. Sonawane ND, Szoka FC, Jr., Verkman AS. 2003. Chloride accumulation and swelling in endosomes enhances DNA transfer by polyamine-DNA polyplexes. *J Biol Chem*
26. Thomas M, Klibanov AM. 2002. Enhancing polyethylenimine's delivery of plasmid DNA into mammalian cells. *Proc Natl Acad Sci U S A* 99: 14640-5
27. Gebhart CL, Kabanov AV. 2001. Evaluation of polyplexes as gene transfer agents. *J Control Release* 73: 401-16
28. Jones NA, Hill IR, Stolnik S, Bignotti F, Davis SS, Garnett MC. 2000. Polymer chemical structure is a key determinant of physicochemical and colloidal properties of polymer-DNA complexes for gene delivery. *Biochim Biophys Acta* 1517: 1-18
29. Almofti MR, Harashima H, Shinohara Y, Almofti A, Li W, Kiwada H. 2003. Lipoplex size determines lipofection efficiency with or without serum. *Mol Membr Biol* 20: 35-43
30. Bennis JM, Choi JS, Mahato RI, Park JS, Kim SW. 2000. pH-sensitive cationic polymer gene delivery vehicle: N-Ac-poly(L-histidine)-graft-poly(L-lysine) comb shaped polymer. *Bioconjug Chem* 11: 637-45
31. Zhdanov RI, Podobed OV, Vlassov VV. 2002. Cationic lipid-DNA complexes-lipoplexes-for gene transfer and therapy. *Bioelectrochemistry* 58: 53-64
32. Lobo BA, Vetro JA, Suich DM, Zuckermann RN, Middaugh CR. 2003. Structure/function analysis of peptoid/lipitoid:DNA complexes. *J Pharm Sci* 92: 1905-18
33. Banks GA, Roselli RJ, Chen R, Giorgio TD. 2003. A model for the analysis of nonviral gene therapy. *Gene Ther* 10: 1766-75
34. Leopold PL. 2000. Fluorescence methods reveal intracellular trafficking of gene transfer vectors: the light toward the end of the tunnel. *Mol Ther* 1: 302-3
35. James MB, Giorgio TD. 2000. Nuclear-associated plasmid, but not cell-associated plasmid, is correlated with transgene expression in cultured mammalian cells. *Mol Ther* 1: 339-46

36. Tachibana R, Harashima H, Ide N, Ukitsu S, Ohta Y, et al. 2002. Quantitative analysis of correlation between number of nuclear plasmids and gene expression activity after transfection with cationic liposomes. *Pharm Res* 19: 377-81
37. Tewary HK, Iversen PL. 1997. Qualitative and quantitative measurements of oligonucleotides in gene therapy: Part I. In vitro models. *J Pharm Biomed Anal* 15: 857-73
38. Wagner E, Plank C, Zatloukal K, Cotten M, Birnstiel ML. 1992. Influenza virus hemagglutinin HA-2 N-terminal fusogenic peptides augment gene transfer by transferrin-polylysine-DNA complexes: toward a synthetic virus-like gene-transfer vehicle. *Proc Natl Acad Sci U S A* 89: 7934-8
39. Zuber G, Dauty E, Nothisen M, Belguise P, Behr JP. 2001. Towards synthetic viruses. *Adv Drug Deliv Rev* 52: 245-53
40. Plank C, Oberhauser B, Mechtler K, Koch C, Wagner E. 1994. The influence of endosome-disruptive peptides on gene transfer using synthetic virus-like gene transfer systems. *J Biol Chem* 269: 12918-24
41. Xu L, Frederik P, Pirollo KF, Tang WH, Rait A, et al. 2002. Self-assembly of a virus-mimicking nanostructure system for efficient tumor-targeted gene delivery. *Hum Gene Ther* 13: 469-81
42. Remy JS, Kichler A, Mordvinov V, Schuber F, Behr JP. 1995. Targeted gene transfer into hepatoma cells with lipopolyamine-condensed DNA particles presenting galactose ligands: a stage toward artificial viruses. *Proc Natl Acad Sci U S A* 92: 1744-8
43. Pitard B, Aguerre O, Airiau M, Lachages AM, Boukhnikachvili T, et al. 1997. Virus-sized self-assembling lamellar complexes between plasmid DNA and cationic micelles promote gene transfer. *Proc Natl Acad Sci U S A* 94: 14412-7
44. Tan W, Wang K, Drake TJ. 2004. Molecular beacons. *Curr Opin Chem Biol* 8: 547-53
45. Bratu DP, Cha BJ, Mhlanga MM, Kramer FR, Tyagi S. 2003. Visualizing the distribution and transport of mRNAs in living cells. *Proc Natl Acad Sci U S A* 100: 13308-13
46. Lorenz P, Baker BF, Bennett CF, Spector DL. 1998. Phosphorothioate antisense oligonucleotides induce the formation of nuclear bodies. *Mol Biol Cell* 9: 1007-23
47. Meidan VM, Glezer J, Amariglio N, Cohen JS, Barenholz Y. 2001. Oligonucleotide lipoplexes: the influence of oligonucleotide composition on complexation. *Biochimica Et Biophysica Acta-General Subjects* 1568: 177-82
48. De Smedt SC, Demeester J, Hennink WE. 2000. Cationic polymer based gene delivery systems. *Pharm Res* 17: 113-26
49. Bieber T, Meissner W, Kostin S, Niemann A, Elsassner HP. 2002. Intracellular route and transcriptional competence of polyethylenimine-DNA complexes. *J Control Release* 82: 441-54
50. Zhang ZY, Smith BD. 2000. High-generation polycationic dendrimers are unusually effective at disrupting anionic vesicles: membrane bending model. *Bioconjug Chem* 11: 805-14
51. Simoes S, Pires P, Duzgunes N, Pedrosa de Lima MC. 1999. Cationic liposomes as gene transfer vectors: barriers to successful application in gene therapy. *Curr Opin Mol Ther* 1: 147-57

52. Hope MJ, Mui B, Ansell S, Ahkong QF. 1998. Cationic lipids, phosphatidylethanolamine and the intracellular delivery of polymeric, nucleic acid-based drugs (review). *Mol Membr Biol* 15: 1-14
53. Islam A, Handley SL, Thompson KS, Akhtar S. 2000. Studies on uptake, sub-cellular trafficking and efflux of antisense oligodeoxynucleotides in glioma cells using self-assembling cationic lipoplexes as delivery systems. *J Drug Target* 7: 373-82
54. Ogris M, Brunner S, Schuller S, Kircheis R, Wagner E. 1999. PEGylated DNA/transferrin-PEI complexes: reduced interaction with blood components, extended circulation in blood and potential for systemic gene delivery. *Gene Ther* 6: 595-605
55. Oupicky D, Konak C, Dash PR, Seymour LW, Ulbrich K. 1999. Effect of albumin and polyanion on the structure of DNA complexes with polycation containing hydrophilic nonionic block. *Bioconjug Chem* 10: 764-72
56. Oupicky D, Ogris M, Howard KA, Dash PR, Ulbrich K, Seymour LW. 2002. Importance of lateral and steric stabilization of polyelectrolyte gene delivery vectors for extended systemic circulation. *Mol Ther* 5: 463-72
57. Simoes S, Slepishkin V, Pires P, Gaspar R, de Lima MP, Duzgunes N. 1999. Mechanisms of gene transfer mediated by lipoplexes associated with targeting ligands or pH-sensitive peptides. *Gene Ther* 6: 1798-807
58. Nakanishi M, Eguchi A, Akuta T, Nagoshi E, Fujita S, et al. 2003. Basic peptides as functional components of non-viral gene transfer vehicles. *Curr Protein Pept Sci* 4: 141-50
59. Dean DA, Dean BS, Muller S, Smith LC. 1999. Sequence requirements for plasmid nuclear import. *Exp Cell Res* 253: 713-22
60. Henderson BR, Percipalle P. 1997. Interactions between HIV Rev and nuclear import and export factors: the Rev nuclear localisation signal mediates specific binding to human importin-beta. *J Mol Biol* 274: 693-707
61. Chirila TV, Rakoczy PE, Garrett KL, Lou X, Constable IJ. 2002. The use of synthetic polymers for delivery of therapeutic antisense oligodeoxynucleotides. *Biomaterials* 23: 321-42
62. Deshpande MC, Garnett MC, Vamvakaki M, Bailey L, Armes SP, Stolnik S. 2002. Influence of polymer architecture on the structure of complexes formed by PEG-tertiary amine methacrylate copolymers and phosphorothioate oligonucleotide. *Journal of Controlled Release* 81: 185-99
63. Aguilar L, Hemar A, Dautry-Varsat A, Blumenfeld M. 1996. Hairpin, dumbbell, and single-stranded phosphodiester oligonucleotides exhibit identical uptake in T lymphocyte cell lines. *Antisense Nucleic Acid Drug Dev* 6: 157-63
64. Lee IK, Ahn JD, Kim HS, Park JY, Lee KU. 2003. Advantages of the circular dumbbell decoy in gene therapy and studies of gene regulation. *Curr Drug Targets* 4: 619-23
65. Walton SP, Stephanopoulos GN, Yarmush ML, Roth CM. 1999. Prediction of antisense oligonucleotide binding affinity to a structured RNA target. *Biotechnol Bioeng* 65: 1-9

66. Zhang W, Bond JP, Anderson CF, Lohman TM, Record MT, Jr. 1996. Large electrostatic differences in the binding thermodynamics of a cationic peptide to oligomeric and polymeric DNA. *Proc Natl Acad Sci U S A* 93: 2511-6
67. Epstein IR. 1978. Cooperative and non-cooperative binding of large ligands to a finite one-dimensional lattice. A model for ligand-oligonucleotide interactions. *Biophys Chem* 8: 327-39
68. Zhang W, Ni H, Capp MW, Anderson CF, Lohman TM, Record MT, Jr. 1999. The importance of coulombic end effects: experimental characterization of the effects of oligonucleotide flanking charges on the strength and salt dependence of oligocation (L8⁺) binding to single-stranded DNA oligomers. *Biophys J* 76: 1008-17
69. Hawley P, Gibson I. 1996. Interaction of oligodeoxynucleotides with mammalian cells. *Antisense Nucleic Acid Drug Dev* 6: 185-95
70. Mislick KA, Baldeschwieler JD. 1996. Evidence for the role of proteoglycans in cation-mediated gene transfer. *Proc Natl Acad Sci U S A* 93: 12349-54
71. Lucas B, Van Rompaey E, De Smedt SC, Demeester J, Van Oostveldt P. 2002. Dual-color fluorescence fluctuation spectroscopy to study the complexation between poly-L-lysine and oligonucleotides. *Macromolecules* 35: 8152-60
72. Wiethoff CM, Gill ML, Koe GS, Koe JG, Middaugh CR. 2003. A fluorescence study of the structure and accessibility of plasmid DNA condensed with cationic gene delivery vehicles. *J Pharm Sci* 92: 1272-85
73. Tsai JT, Furstoss KJ, Michnick T, Sloane DL, Paul RW. 2002. Quantitative physical characterization of lipid-polycation-DNA lipopolyplexes. *Biotechnol Appl Biochem* 36: 13-20
74. Choi SJ, Szoka FC. 2000. Fluorometric determination of deoxyribonuclease I activity with PicoGreen. *Analytical Biochemistry* 281: 95-7
75. Liu G, Molas M, Grossmann GA, Pasumathy M, Perales JC, et al. 2001. Biological properties of poly-L-lysine-DNA complexes generated by cooperative binding of the polycation. *Journal of Biological Chemistry* 276: 34379-87
76. Bronich TK, Nguyen HK, Eisenberg A, Kabanov AV. 2000. Recognition of DNA topology in reactions between plasmid DNA and cationic copolymers. *Journal of the American Chemical Society* 122: 8339-43
77. Godbey WT, Wu KK, Mikos AG. 1999. Size matters: molecular weight affects the efficiency of poly(ethylenimine) as a gene delivery vehicle. *J Biomed Mater Res* 45: 268-75
78. Belting M, Petersson P. 1999. Intracellular accumulation of secreted proteoglycans inhibits cationic lipid-mediated gene transfer - Co-transfer of glycosaminoglycans to the nucleus. *Journal of Biological Chemistry* 274: 19375-82
79. Mounkes LC, Zhong W, Cipres-Palacin G, Heath TD, Debs RJ. 1998. Proteoglycans mediate cationic Liposome-DNA complex-based gene delivery in vitro and in vivo. *Journal of Biological Chemistry* 273: 26164-70
80. Wolfert MA, Seymour LW. 1996. Atomic force microscopic analysis of the influence of the molecular weight of poly(L)lysine on the size of polyelectrolyte complexes formed with DNA. *Gene Ther* 3: 269-73

81. Kreiss P, Cameron B, Rangara R, Mailhe P, Aguerre-Charriol O, et al. 1999. Plasmid DNA size does not affect the physicochemical properties of lipoplexes but modulates gene transfer efficiency. *Nucleic Acids Research* 27: 3792-8
82. White RE, Wade-Martins R, Hart SL, Frampton J, Huey B, et al. 2003. Functional delivery of large genomic DNA to human cells with a peptide-lipid vector. *J Gene Med* 5: 883-92
83. Dheur S, Dias N, van Aerschot A, Herdewijn P, Bettinger T, et al. 1999. Polyethylenimine but not cationic lipid improves antisense activity of 3'-capped phosphodiester oligonucleotides. *Antisense Nucleic Acid Drug Dev* 9: 515-25
84. Gleave ME, Monia BP. 2005. Antisense therapy for cancer. *Nat Rev Cancer* 5: 468-79
85. Dean NM, Bennett CF. 2003. Antisense oligonucleotide-based therapeutics for cancer. *Oncogene* 22: 9087-96
86. Dallas A, Vlassov AV. 2006. RNAi: a novel antisense technology and its therapeutic potential. *Med Sci Monit* 12: RA67-74
87. Lebedeva I, Benimetskaya L, Stein CA, Vilenchik MA. 2000. Cellular delivery of antisense oligonucleotides. *Eur J Pharm Biopharm* 50: 101-19
88. Shi F, Hoekstra D. 2004. Effective intracellular delivery of oligonucleotides in order to make sense of antisense. *J Control Release* 97: 189-209
89. Lee LK, Williams CL, Devore D, Roth CM. 2006. Poly(propylacrylic acid) enhances cationic lipid-mediated delivery of antisense oligonucleotides. *Biomacromolecules* 7: 1502-8
90. Zatsepin TS, Turner JJ, Oretskaya TS, Gait MJ. 2005. Conjugates of oligonucleotides and analogues with cell penetrating peptides as gene silencing agents. *Curr Pharm Des* 11: 3639-54
91. Oishi M, Hayama T, Akiyama Y, Takae S, Harada A, et al. 2005. Supramolecular assemblies for the cytoplasmic delivery of antisense oligodeoxynucleotide: polyion complex (PIC) micelles based on poly(ethylene glycol)-SS-oligodeoxynucleotide conjugate. *Biomacromolecules* 6: 2449-54
92. Junghans M, Loitsch SM, Steiniger SC, Kreuter J, Zimmer A. 2005. Cationic lipid-protamine-DNA (LPD) complexes for delivery of antisense c-myc oligonucleotides. *Eur J Pharm Biopharm* 60: 287-94
93. Davis ME, Pun SH, Bellocq NC, Reineke TM, Popielarski SR, et al. 2004. Self-assembling nucleic acid delivery vehicles via linear, water-soluble, cyclodextrin-containing polymers. *Curr Med Chem* 11: 179-97
94. Sundaram S, Viriyayuthakorn S, Roth CM. 2005. Oligonucleotide structure influences the interactions between cationic polymers and oligonucleotides. *Biomacromolecules* 6: 2961-8
95. Sirsi SR, Williams JH, Lutz GJ. 2005. Poly(ethylene imine)-poly(ethylene glycol) copolymers facilitate efficient delivery of antisense oligonucleotides to nuclei of mature muscle cells of mdx mice. *Hum Gene Ther* 16: 1307-17
96. Meidan VM, Glezer J, Amariglio N, Cohen JS, Barenholz Y. 2001. Oligonucleotide lipoplexes: the influence of oligonucleotide composition on complexation. *Bba-Gen Subjects* 1568: 177-82

97. Lucas B, Van Rompaey E, Remaut K, Sanders N, De Smedt SC, Demeester J. 2004. On the biological activity of anti-ICAM-1 oligonucleotides complexed to non-viral carriers. *J Control Release* 96: 207-19
98. von Harpe A, Petersen H, Li Y, Kissel T. 2000. Characterization of commercially available and synthesized polyethylenimines for gene delivery. *J Control Release* 69: 309-22
99. Boussif O, Lezoualc'h F, Zanta MA, Mergny MD, Scherman D, et al. 1995. A versatile vector for gene and oligonucleotide transfer into cells in culture and in vivo: polyethylenimine. *Proc Natl Acad Sci U S A* 92: 7297-301
100. Sonawane ND, Szoka FC, Jr., Verkman AS. 2003. Chloride accumulation and swelling in endosomes enhances DNA transfer by polyamine-DNA polyplexes. *J Biol Chem* 278: 44826-31
101. Neu M, Fischer D, Kissel T. 2005. Recent advances in rational gene transfer vector design based on poly(ethylene imine) and its derivatives. *J Gene Med* 7: 992-1009
102. Helin V, Gottikh M, Mishal Z, Subra F, Malvy C, Lavignon M. 1999. Cell cycle-dependent distribution and specific inhibitory effect of vectorized antisense oligonucleotides in cell culture. *Biochem Pharmacol* 58: 95-107
103. Lee LK, Dunham BM, Li Z, Roth CM. 2006. Cellular dynamics of antisense oligonucleotides and short interfering RNAs. *Ann NY Acad Sci* 1082: 47-51
104. Roth CM. 2005. Molecular and cellular barriers limiting the effectiveness of antisense oligonucleotides. *Biophys J* 89: 2286-95
105. Raj A, Peskin CS, Tranchina D, Vargas DY, Tyagi S. 2006. Stochastic mRNA synthesis in mammalian cells. *Plos Biology* 4: 1707-19
106. Bollig F, Winzen R, Kracht M, Ghebremedhin B, Ritter B, et al. 2002. Evidence for general stabilization of mRNAs in response to UV light. *Eur J Biochem* 269: 5830-9
107. Glaunsinger B, Chavez L, Ganem D. 2005. The exonuclease and host shutoff functions of the SOX protein of Kaposi's sarcoma-associated herpesvirus are genetically separable. *J Virol* 79: 7396-401
108. Paschoud S, Dogar AM, Kuntz C, Grisoni-Neupert B, Richman L, Kuhn LC. 2006. Destabilization of interleukin-6 mRNA requires a putative RNA stem-loop structure, an AU-rich element, and the RNA-binding protein AUF1. *Mol Cell Biol* 26: 8228-41
109. Vinogradov SV, Bronich TK, Kabanov AV. 1998. Self-assembly of polyamine-poly(ethylene glycol) copolymers with phosphorothioate oligonucleotides. *Bioconjug Chem* 9: 805-12
110. Brus C, Petersen H, Aigner A, Czubyko F, Kissel T. 2004. Efficiency of polyethylenimines and polyethylenimine-graft-poly(ethylene glycol) block copolymers to protect oligonucleotides against enzymatic degradation. *Eur J Pharm Biopharm* 57: 427-30
111. Forrest ML, Meister GE, Koerber JT, Pack DW. 2004. Partial acetylation of polyethylenimine enhances in vitro gene delivery. *Pharm Res* 21: 365-71
112. von Gersdorff K, Sanders NN, Vandenbroucke R, De Smedt SC, Wagner E, Ogris M. 2006. The internalization route resulting in successful gene expression

- depends on both cell line and polyethylenimine polyplex type. *Mol Ther* 14: 745-53
113. Boletta A, Benigni A, Lutz J, Remuzzi G, Soria MR, Monaco L. 1997. Nonviral gene delivery to the rat kidney with polyethylenimine. *Hum Gene Ther* 8: 1243-51
 114. Gabrielson NP, Pack DW. 2006. Acetylation of polyethylenimine enhances gene delivery via weakened polymer/DNA interactions. *Biomacromolecules* 7: 2427-35
 115. Thomas M, Lu JJ, Ge Q, Zhang C, Chen J, Klibanov AM. 2005. Full deacetylation of polyethylenimine dramatically boosts its gene delivery efficiency and specificity to mouse lung. *Proc Natl Acad Sci U S A* 102: 5679-84
 116. Glodde M, Sirsi SR, Lutz GJ. 2006. Physiochemical properties of low and high molecular weight poly(ethylene glycol)-grafted poly(ethylene imine) copolymers and their complexes with oligonucleotides. *Biomacromolecules* 7: 347-56
 117. Chiu Y-L, Ali A, Chu C, Cao H, Rana TM. 2004. Visualizing a correlation between siRNA localization, cellular uptake, and RNAi in living cells. *Chem Biol* 11: 1165-75
 118. Fischer D, Li Y, Ahlemeyer B, Krieglstein J, Kissel T. 2003. In vitro cytotoxicity testing of polycations: influence of polymer structure on cell viability and hemolysis. *Biomaterials* 24: 1121-31
 119. Kopatz I, Remy JS, Behr JP. 2004. A model for non-viral gene delivery: through syndecan adhesion molecules and powered by actin. *J Gene Med* 6: 769-76
 120. Akinc A, Thomas M, Klibanov AM, Langer R. 2005. Exploring polyethylenimine-mediated DNA transfection and the proton sponge hypothesis. *J Gene Med* 7: 657-63
 121. Okuda T, Niidome T, Aoyagi H. 2004. Cytosolic soluble proteins induce DNA release from DNA--gene carrier complexes. *J Control Release* 98: 325-32
 122. Funhoff AM, van Nostrum CF, Koning GA, Schuurmans-Nieuwenbroek NM, Crommelin DJ, Hennink WE. 2004. Endosomal escape of polymeric gene delivery complexes is not always enhanced by polymers buffering at low pH. *Biomacromolecules* 5: 32-9
 123. Tang MX, Redemann CT, Szoka FC, Jr. 1996. In vitro gene delivery by degraded polyamidoamine dendrimers. *Bioconjug Chem* 7: 703-14
 124. Saenger W. 1984. *Principles of Nucleic Acid Structure Modified nucleosides and nucleotides; nucleoside di- and triphosphates; coenzymes and antibiotics*. New York: Springer-Verlag Inc
 125. Maksimenko AV, Gottikh MB, Helin V, Shabarova ZA, Malvy C. 1999. Physicochemical and biological properties of antisense phosphodiester oligonucleotides with various secondary structures. *Nucleos Nucleot* 18: 2071-91
 126. Ghosh MK, Ghosh K, Cohen JS. 1993. Phosphorothioate-phosphodiester oligonucleotide co-polymers: assessment for antisense application. *Anticancer Drug Des* 8: 15-32
 127. Bartlett DW, Davis ME. 2006. Insights into the kinetics of siRNA-mediated gene silencing from live-cell and live-animal bioluminescent imaging. *Nucleic Acids Res* 34: 322-33
 128. Mathews DH, Disney MD, Childs JL, Schroeder SJ, Zuker M, Turner DH. 2004. Incorporating chemical modification constraints into a dynamic programming

algorithm for prediction of RNA secondary structure. *Proc Natl Acad Sci U S A*
101: 7287-92

CURRICULUM VITAE

Sumati Sundaram

Address: 233 Wayne Street
Highland Park, NJ 08904, USA
E-mail: sumatis@eden.rutgers.edu

Phone: 908-217-9631 (m)
732-445-3047 (w)

ACADEMIC EXPERIENCE

PhD Chemical Engineering (*Jan 2008*)

Rutgers, The State University of NJ, Piscataway, NJ

Thesis title: Interplay of polymer molecular weight and oligonucleotide backbone chemistry in the dynamics of antisense activity

Advisor: Dr. Charles Roth

B. Chem. Engg. Chemical Engineering (*June 2000*)

University Institute of Chemical Technology

(Previously, University Dept. of Chemical Technology (UDCT)),

University of Mumbai, India

TECHNICAL SKILLS

- Formulation of synthetic DNA delivery systems (composed of lipids, polymers, plasmid DNA and/or antisense oligonucleotides)
- Physicochemical characterization of synthetic DNA delivery systems using dynamic light scattering, zeta potential measurements, fluorescence assays, gel electrophoresis
- Mammalian cell culture - CHO (Chinese hamster ovary) cells & HepG2 cells, transfection and selection of mammalian cells, cellular assays, flow cytometry (FACS), fluorescence microscopy
- Bacterial cell culture
- Computational: Matlab, MS Office, EndNote, Fortran, C

LABORATORY MAINTENANCE SKILLS

- Setting up laboratory
- Ordering equipment & supplies for the laboratory, maintenance of laboratory supplies inventory
- Maintenance of laboratory protocol database
- Tissue culture instructor

REFEREED JOURNAL PUBLICATIONS

1. **Sundaram S**, Hwang M, Roth CM. Design of mixed-backbone antisense oligonucleotides for PEI-mediated cellular delivery. (*In preparation for Nucleic Acids Research*)
2. **Sundaram S**, Lee LK, Roth CM. Interplay of polyethyleneimine molecular weight and oligonucleotide backbone chemistry in the dynamics of antisense activity. *Nucleic Acids Research* (Published online - Advance access, June 18, 2007)
3. **Sundaram S**, Viriyayuthakorn S, Roth CM. Oligonucleotide structure influences the interactions between cationic polymers and oligonucleotides. *Biomacromolecules*. 2005 Nov-Dec;6(6):2961-8
4. Roth CM, **Sundaram S** Engineering synthetic vectors for improved DNA delivery: insights from intracellular pathways. *Annu Rev Biomed Eng*. 2004;6:397-426. Review
5. Pai A, Gondkar S, **Sundaram S**, Lali A. Expanded bed adsorption on supermacroporous cross-linked cellulose matrix. *Bioseparation*. 1999;8(1-5):131-8

RESEARCH EXPERIENCE

Graduate Research Assistant, Rutgers University, Piscataway, NJ, USA (2000-Present)

Advisor: Dr. Charles Roth

- Optimized the use of polymer polyethyleneimine for the cellular delivery of antisense oligonucleotides
- Developed assays for the physicochemical analysis of polymer/oligonucleotide complexes
- Detailed study of the effects of oligonucleotide backbone chemistry on the dynamics of antisense activity

Summer Intern, Hindustan Petroleum Corporation Limited (HPCL), Mumbai, India (Summer 1999)

- Rotational position in various departments of the refinery to obtain an understanding of the application of chemical engineering concepts in an industrial setting

Undergraduate Research Assistant, University Institute of Chemical Technology, Mumbai, India (Summer 1998)

Advisor: Dr.Arvind Lali

- Studied hydrodynamics of expanded beds used in chromatography

CONFERENCE PRESENTATIONS

1. **Sundaram S** (Speaker), Lee LK, Hwang ME, Roth CM, "Role of vector in the dynamics of antisense activity", *232nd American Chemical Society National Meeting and Exposition, San Francisco, CA*, September 2006.
2. Lee LK, **Sundaram S**, Roth CM (Speaker), "Biophysical Characterization of Antisense Delivery Systems", *1st Annual Methods in Bioengineering Conference, Boston, MA*, July 2006.
3. **Sundaram S** (Speaker), Lee LK, Roth CM, "Role of vector in the dynamics of antisense activity", *19th Annual Meeting of Mid-Atlantic Biochemical Engineering Consortium, Raleigh, NC*, June 2006.
4. **Sundaram S** (Speaker), Lee LK, Roth CM, "Role of vector in the dynamics of antisense activity", *32nd Northeast Bioengineering Conference, Easton, PA*, April 2006.
5. **Sundaram S** (Speaker), Lee LK, Roth CM, "Quantitative evaluation of the role of vector in the dynamics of antisense effects", *American Institute of Chemical Engineers (AIChE) Annual Meeting, Cincinnati, OH*, November 2005.
6. **Sundaram S** (Speaker), Lee LK, Oddo, J, Viriyayuthakorn S, Roth CM, "The role of vector in the dynamics of antisense activity", *Biomedical Engineering Society (BMES) Annual Meeting, Baltimore, MD*, October 2005.
7. **Sundaram S** (Speaker), Viriyayuthakorn S, Roth CM, "Implications of Oligonucleotide Structure for the Design of Polymeric Oligonucleotide Delivery Vectors", *Mid-Atlantic Biochemical Engineering Conference, Piscataway, NJ*, April 2005.
8. **Sundaram S** (Speaker), Shah N, Roth CM, "Implications of oligonucleotide structure for the design of polymeric oligonucleotide delivery vectors", *American Institute of Chemical Engineers (AIChE) Annual Meeting, Austin, TX*, November 2004.
9. **Sundaram S** (Speaker), Shah N, Roth CM, "Implications of oligonucleotide structure for the design of polymeric oligonucleotide delivery vectors", *Biomedical Engineering Society (BMES) Annual Meeting, Philadelphia, PA*, October 2004.
10. Viriyayuthakorn S (Speaker), **Sundaram S**, Roth CM, "Implications of Oligonucleotide Structure for the Design of Polymeric Oligonucleotide Delivery Vectors", *Biomedical Engineering Society (BMES) Annual Meeting, Philadelphia, PA*, October 2004.
11. **Sundaram S** (Speaker), Shah N, Roth CM, "Effect of Oligonucleotide Structure on Oligoplex Properties", *American Institute of Chemical Engineers (AIChE) Annual Meeting, San Francisco, CA*, November 2003.
12. Shah N (Speaker), **Sundaram S**, Roth CM, "Study of Oligoplex Uptake in HepG2 Cells: Effect of Oligonucleotide Structure", *Biomedical Engineering Society (BMES) Annual Meeting, Nashville, TN*, October 2003.
13. **Sundaram S**, Roth CM, "Effect of Oligonucleotide Structure on Behavior of Oligoplexes", *29th Northeast Bioengineering Conference, Newark, NJ*, March 2003.

TEACHING EXPERIENCE

- *Teaching assistant*, Spring 2001, Chemical engineering thermodynamics
- *Teaching assistant*, Spring 2002, Chemical engineering analysis I
- *Academic Tutor* (Algebra and Pre-Calculus), Summer 2003, Learning Resource Center Tutor Project, Livingston Campus
- *Guest lecturer*, Spring 2005, Molecular and cellular bioengineering
- Mentored undergraduate students in the research laboratory (2001-Present)

Name of student

- Neha Shah
- Sandra Viriyayuthakorn
- Mark Hwang

Current Placement

- PhD candidate, Univ. Minnesota
- Scientist, Celgene, NJ
- MD/PhD candidate, UIUC

AWARDS

- Represented Rutgers at the 19th Annual Meeting of Mid-Atlantic Biochemical Engineering Consortium, Raleigh, NC, June 2006.
- Graduate research and teaching assistantships, Rutgers University, 2000-Present.
- Was placed 1st for the paper presented on “Osmotic distillation” at Technical symposium-Technokrec’99 held at Karnataka Regional Engineering College, Suratkal, India.
- Review paper on “Electronic Nose” was selected for Technical festival of D.K.T.E society’s Textile and Engineering Institute, Ichalkaranji, India.
- Was placed 12th of ~3,00,000 students in the Bombay Merit list for securing 92.67% in the Higher Secondary Certificate Examination held in March 1996.
- Was placed 19th of ~3,00,000 students in the Bombay Merit list for securing 92.14% in the Secondary School Certificate Examination held in March 1994.

PROFESSIONAL AFFILIATIONS

- American Institute of Chemical Engineers (AIChE)
- American Chemical Society (ACS)
- Biomedical Engineering Society (BMES)

ADDITIONAL INTERESTS

- Outdoors & travel (mainly hiking)
- The culinary arts
- Graphics and design
- Voluntary work

REFERENCES

1. Dr. Charles M. Roth, PhD

Associate Professor
Dept of Biomedical Engineering
Rutgers University
599 Taylor Road, Piscataway, NJ 08904
Email: cmroth@rci.rutgers.edu
Phone: 732-445-4500 X 6205

2. Dr. Prabhas Moghe, PhD

Professor
Dept of Biomedical Engineering
Rutgers University
599 Taylor Road, Piscataway, NJ 08904
Email: moghe@rci.rutgers.edu
Phone: 732-445-4500 X 6315

3. Dr. Henrik Pedersen, PhD

Professor & Chair
Dept of Chemical & Biochemical Engineering
Rutgers University
98, Brett Road, Piscataway, NJ 08854
Email: hpederse@sol.rutgers.edu
Phone: 732-445-2568